MECHANISMS UNDERLYING VASCULAR AND RESPIRATORY COMPLICATIONS ASSOCIATED WITH DIABETES

By

ALLISON CAMPOLO

Bachelor of Arts in Biology
University of Texas at Dallas
Richardson, Texas
2012

Master of Science in International Agriculture
Oklahoma State University
Stillwater, Oklahoma
2016

Submitted to the Faculty of the
Graduate College of the
Oklahoma State University
in partial fulfillment of
the requirements for
the Degree of
DOCTOR OF PHILOSOPHY
July, 2019

MECHANISMS UNDERLYING VASCULAR AND RESPIRATORY COMPLICATIONS ASSOCIATED WITH DIABETES

Dissertation Approved:

Dr. Véronique Anne Lacombe

Dissertation Adviser

Dr. Martin Furr

Dr. Lin Liu

Dr. Myron Hinsdale

Dr. Brenda Smith

ACKNOWLEDGEMENTS

I would firstly like to thank my husband, Alex. This undertaking would not have been possible without his unyielding love and support of my every whim, idea, and attempt, his picking up the pieces of every disappointment, and sharing in every success. I am incredibly lucky, and grateful, to have such a partner in life.

I would like to extend an equal amount of gratitude to my advisor, Dr. Veronique Lacombe, for her guidance and dedication to this effort. Both to me personally, as a trainee, and to this project, which would not have been possible without her vision and inquisitiveness for this immensely unique and exciting area of research. I am vastly grateful for the time and effort she has put into my training in order to help make me a well-rounded scientist going forward.

My family deserves a huge amount of credit for this accomplishment. My mom and dad, Shirley and Carter Thompson, and my sister, Arianne, and her husband, Ewan, are all responsible for the person I am today. They have encouraged me every step of the way to be curious, to embrace the notion that nothing is impossible, and to strive for excellence in every endeavor. Most importantly, they have always shown me that anything that I apply myself to is achievable, which is an absolutely invaluable lesson.

I would like to thank my committee, Dr. Myron Hinsdale, Dr. Lin Liu, Dr. Martin Furr, and Dr. Brenda Smith, for their guidance and help with all of the projects disclosed here.

I am extremely grateful to my kung fu instructors, Dr. Sifu Henry Su and Master Johnny Lee, for giving me the mental fortitude and perspective necessary to appreciate and hopefully excel at this undertaking.

I would finally like to thank my lab mates along the way for all of their assistance and team work to make these endeavors successful – Dr. Zahra Maria, Dr. Mego Terhuja, Shanell Shoop, Ellen Jackson, Alia Houser, Dominic Martin, Samantha Lazarowicz, Delanie Beevers, Matthew Frantz, Matthew Rochowski, Domonique Jette, Erin McCarty, and Kristyn Maxwell. I would also like to thank Jill Murray and my office mates for their unending camaraderie and help in all things throughout this journey.

This body of work is dedicated to my Uncle Sanford, who embodied the pursuit of knowledge, love of the world, and belief in what is possible.

Name: ALLISON CAMPOLO

Date of Degree: JULY, 2019

Title of Study: MECHANISMS UNDERLYING VASCULAR AND RESPIRATORY COMPLICATIONS ASSOCIATED WITH DIABETES

Major Field: VETERINARY BIOMEDICAL SCIENCE

Abstract: Diabetes and metabolic syndrome has risen to epidemic proportions in both humans and veterinary species. Diabetes is characterized by a lack of insulin production (type 1) or action (type 2), with subsequent alterations in glucose transport and utilization in insulin-sensitive tissue. Importantly, diabetes is well known to cause multi-organ failure (including cardiovascular dysfunction). Additionally, diabetes has recently been shown to increase the risk of respiratory infection in diabetic patients. Thus, we here sought to describe the mechanisms underlying glucose dysregulation-derived organ dysfunction in several tissues (e.g., insulin-sensitive tissues, lamellae, and lung). While equine metabolic syndrome is well-known to be associated with endocrinopathic laminitis, the underlying cause of laminitic pathogenesis remains unknown. We determined that horses with laminitis induced by a 48-hour euglycemic hyperinsulinemic clamp had a significant upregulation of the insulin signaling pathway in the heart. Thus, horses with endocrinopathic laminitis were not insulin resistant. After proteomic analysis, we subsequently found an upregulation of heat shock protein 90, alpha-2-macroglobulin, and fibrinogen beta, and a downregulation of cadherin-13, vinculin, and talin-1 in lamellae of hyperinsulinemic horses. Separately, the regulation of glucose homeostasis in the lung, and how it may be affected during diabetes or during influenza infection, is under-investigated. We determined the protein and mRNA quantities of seven glucose transporter (GLUT) isoforms in the lung of healthy and diabetic mice. After infecting diabetic mice with H1N1 Influenza A (A/PR/8/34), infected and diabetic mice displayed an increased amount of glucose in BALF over control and non-infected counterparts. Insulin or metformin rescued these metabolic alterations in both non-infected and infected diabetic mice. While diabetes significantly altered protein expression of some GLUTs in the total lysate from the whole lung, influenza alone increased the cell-surface expression of insulin-sensitive GLUT4. Thus, overall, it can be concluded that alterations in glucose and insulin metabolism result in substantial alterations in the regulation of glucose transport in the lamellae of hyperinsulinemic horses, as well as in the lung of (type 1 and type 2) diabetic mice infected with influenza. Together, these findings underscore that glucose and insulin dysregulation contribute to multiple organ dysfunction during diabetes and metabolic syndrome.

TABLE OF CONTENTS

Chapter Page

LIST OF TABLES

LIST OF FIGURES

Figure Page

Figure Page

Figure Page

Figure Page

CHAPTER I

INTRODUCTION

Diabetes mellitus is a serious metabolic disorder affecting more than 30 million people in the United States[2] and 422 million people worldwide.[3] It is presently the 7th leading cause of death in the US[1] and in the world,[2] and if current trends continue, a full 10% of the worldwide population is expected to be afflicted with some form of diabetes by the year 2030.[4] Diabetes is defined by hyperglycemia, which is caused by either a lack of insulin production (type 1) or a lack of insulin action (type 2). Importantly, primarily due to vascular dysfunction, diabetes is well-documented to lead to multiple organ dysfunction including stroke, blindness, heart failure, kidney failure, and peripheral neuropathy leading to limb amputation.[2] Similarly, domestic animals in Western countries have followed alongside their human counterparts and are now experiencing burgeoning rates of obesity and metabolic disease.[5] From this knowledge, two major gaps of knowledge are addressed in this study: 1) how metabolic syndrome and the ensuing metabolic derangements lead to laminitis in horses, and 2) how diabetes affects glucose homeostasis in the lungs, particularly in concert with diabetic patients concurrently afflicted with viral respiratory infection.

Hypothesis 1: Hyperinsulinemia during equine metabolic syndrome will lead to laminitis through metabolic pathways.

Specific Aim 1: To test the hypothesis that the downstream insulin signaling and glucose transport pathways will be altered during hyperinsulinemia-induced laminitis.

Specific Aim 2: To test the hypothesis that insulin-induced laminitis will cause a significant differential expression of proteins in the inflammatory and metabolic pathways, and additional novel cellular pathways.

Hypothesis 2: Impaired glucose metabolism during diabetes will alter the glucose transporter expression in the lung and increase viral replication, thereby increasing the severity and mortality of diabetes-involved influenza infection.

Specific Aim 1: To test the hypothesis that diabetes will alter the glucose transporter activity in the lung, and that insulin or metformin treatment will rescue these alterations.

Specific Aim 2: To test the hypothesis that insulin or metformin treatment during diabetic influenza infection will rescue pulmonary glucose homeostasis and thus prevent alterations to viral replication in the lung of diabetic animals.

CHAPTER II

REVIEW OF THE LITERATURE

2.1 Diabetes

Diabetes is defined by a sustained hyperglycemic state above what is considered normal (79-100 mg/dL, fasting, in most mammals).[6] This is either caused by a lack of insulin production from pancreatic beta islet cells (type 1 diabetes) or a lack of insulin action at the site of the cellular insulin receptor (type 2 diabetes). Diabetes is currently the 7th leading cause of death both in the United States and worldwide.[7,8] Importantly, the prevalence of diabetes has been steadily rising over the last decades. In the United States, 1 in 3 adults is now predicted to have either diabetes or pre-diabetes (a normoglycemic, hyperinsulinemic state preceding true diabetes),[9] and worldwide almost 10% of the global population is estimated to be afflicted with diabetes or glucose intolerance.[10]

This serious metabolic disorder is now known to cause multiple organ dysfunction and failure, including nephropathy, retinopathy, neuropathy, loss of bone density, and cardiomyopathy.[2] Recently, diabetes (both type 1 and type 2) has also been identified as a significant and independent risk factor for the development of severe respiratory infections.[11-13] While hyperglycemia-involved respiratory infections are still being described, the majority of diabetic organ dysfunction results from vascular complications, as diabetic patients are a two-fold excess risk for micro- and macro-vascular disease versus their non-diabetic counterparts.[14] To be sure, diabetes has recently been identified as a substantial risk factor in the development of significant cardiac disease, including cardiomyopathy, stroke, heart failure, and arrhythmia.[15, 16] Due to vascular dysfunction, diabetic patients generally develop fewer collateral vessels in response to ischemia than non-diabetic patients.[15] Thus, in addition to atherosclerotic disease and hypertension, diabetic patients have a 2-3-fold increased risk of developing

heart failure following a myocardial infarction.[15] Endothelial cells generally regulate vascular function and structure within any organ.[17] Importantly, nitric oxide (NO) is synthesized by endothelial NO synthase (eNOS).[17] Normally, NO promotes vasodilation by activating guanylyl cyclase on neighboring vascular smooth muscle cells.[17] Additionally, NO prevents vessels from endogenous injury by preventing platelet and leukocyte interaction, and inhibiting vascular smooth muscle cell proliferation and migration.[17] However, hyperglycemia has been shown to decrease endothelium-derived NO[18] and reduce endothelium-dependent vasodilation.[19] This is largely due to the hyperglycemic upregulation of reactive oxygen species which then inactivate NO,[20] but hyperglycemia has also been shown to increased synthesis of prostanoids, endothelin, and cyclooxygenase-2, which cause vasoconstriction.[21, 22] Finally, blood flow is negatively impacted by the increase of plasma coagulation factors and lesion-based coagulants, while endogenous anticoagulants are decreased.[17] Thus, platelet activation and aggregation combined with a tendency for coagulation becomes a significant risk during hyperglycemia.[17]

Together, the combined result of hyperglycemia-induced vascular disease can make a significant contribution to multi-organ dysfunction and failure in either type of diabetes. Despite these common symptoms, type 1 and type 2 diabetes have quite different disease pathophysiologies due to the different causalities of the disease.

2.1.1 Type 1 Diabetes

Type 1 diabetes mellitus is an autoimmune disorder wherein the body destroys the pancreatic beta-islet cells, which are predominately responsible for the production of

insulin, while leaving the alpha, delta, and gamma islet cells relatively intact.[23] Because of this, type 1 diabetes is often referred to juvenile diabetes, since it most often presents at a young age, or insulin-dependent diabetes, since insulin therapy is required for survival.[23] There is currently no way to prevent the onset of type 1 diabetes, nor is there a known cure. However, automated glucometers and insulin pumps have recently progressed to allow for regular insulin delivery without the need for constant subcutaneous injections throughout the day. Type 1 diabetes constitutes 5-10% of all known diabetes cases.[23] Nevertheless, while the disease is much less prevalent than type 2 diabetes, it is not curable, and if left untreated or poorly managed, the severe hyperglycemia (>350mg/dL if untreated) is far more damaging than that found during type 2 diabetes.

The onset of type 1 diabetes can be diagnosed by the appearance of autoantibodies before any symptoms manifest.[24] The autoantibodies include autoantibodies to islet cells, insulin, glutamic acid decarboxylase, the phosphatase-related IA-2 molecule, and zinc transporters.[25] However, many type 1 diabetics are instead diagnosed (via the pronounced hyperglycemia) after the onset of diabetic ketoacidosis, polyuria polydipsia, unexplained weight loss, or a combination of these.[24] Diabetic ketoacidosis is a high concentration of ketone bodies, or ketosis, to such an extreme degree that the pH of the blood is decreased.[24] This is the result of a lack of glucose uptake (due to the lack of insulin) resulting in gluconeogenesis (thereby exacerbating the hyperglycemia) and the utilization of fatty acids by the liver to support ketosis.[24] The polyuria is caused by the exceptionally high concentration of the glucose in the blood

leading to osmotic diuresis via water passively following the high glucose concentrations being excreted in the urine. This in turn naturally causes the associated polydipsia.[24]

The destruction of the pancreatic beta islet cells is thought to be T-cell mediated, via both CD4+ and CD8+ T cells.[26] As the destruction of the beta islet cells occurs, the beta islet cells release autoantigens.[26] The macrophages then process these and present them on their surface, which is identified by the helper T cells.[26] The helper T cells then activate both the cytotoxic T cells and the B cells, which also activate the natural killer cells.[26] Together, these immune forces complete the destruction of the pancreatic beta islet cells.[26] Additionally, the process of the beta cell destruction can be highly inflammatory. Before the onset of diabetic ketoacidosis, mild persistent hyperglycemia may be evident. This alone can trigger endoplasmic reticulum (ER) stress and oxidative stress in pancreatic beta islet cells.[26] This may cause a damaging positive feedback loop as ER stress itself is prone to cause damage to beta cell proteins, generating peptides which may be presented by MHC to attract further autoimmune response.[26] Additionally, T cells may upregulate inflammatory cytokines and interferons such as IL-1β, IFN-γ, and TNF-α, which further promote beta cell apoptosis.[26]

2.1.2 Type 2 Diabetes

Type 2 diabetes comprises the other 90-95% of diabetic cases. It is a somewhat more complex disease than type 1 diabetes in its pathogenic mechanisms, although the cause is generally more simple: this is a disease which almost always results from overnutrition, which results in high secretions of insulin from the pancreatic beta islet cells in order to compensate for the constant high levels of glucose.[27] Insulin resistance, a

decrease in insulin-stimulated glucose uptake, is associated with ageing, obesity, and a sedentary lifestyle.[27] While pancreatic islets respond to this challenge by increasing their cell mass and insulin secretion, the eventual failure of the functional expansion of beta islet cells to compensate adequately for the degree of insulin resistance leads to the type 2 diabetic condition. Even at the beginning stages of this disease, the constant hyperglycemia (a fasting blood glucose level of 126 mg/dL or higher on at least two separate tests) can lead to glucotoxicity, lipotoxicity, oxidative stress, ER stress, and amyloid deposition.[27] Together, all of these mechanisms form a non-linear but multifactorial positive feedback loop which results in pronounced, chronic insulin resistance and hyperglycemia.

In the case of glucotoxicity, hyperglycemia itself has been shown to impair insulin secretion, via beta cell exhaustion, and to induce pancreatic beta islet cell death, via full glucose toxicity, which causes irreversible damage to cellular components of insulin production.[28] Similarly, lipotoxicity occurs as long-chain free fatty acids increase in the plasma during insulin resistance.[29] Saturated fatty acids in particular tend to be quite toxic, as they have been associated with impairing beta cell secretory function, inducing beta cell apoptosis, and, in a circular pattern, further inducing insulin resistance.[30, 31] Beta cells also undergo significant NO-mediated ER stress due to the high output of insulin, and ER stress-mediated apoptosis in beta cells can be a further additive to insulin resistance.[32] Additionally, islet amyloid deposits are associated with the islets of type 2 diabetic patients, and are associated with beta cell failure.[33] Finally, oxidative stress is an important part of the type 2 diabetic condition, as hyperglycemia – and

several of the other concurrent cell stressors – lead to the generation of reactive oxygen species.

Together, these etiologies make type 2 diabetes a highly inflammatory disease. Following excessive levels of circulating glucose and free fatty acids, the pancreatic islets and insulin-sensitive tissues (striated muscle, adipose tissue, liver) produce inflammatory cytokines and chemokines, particularly as mast cells, macrophages, and T cells are recruited to the adipose tissue.[27] These circulating pro-inflammatory mediators include IL-1β, TNF-α, CCL2, CCL2, CXCL8.[27] Further, the hypoxic response occurring in expanding adipose tissue, as well as the activated NF-kB and JNK pathways, may further promote inflammation and insulin resistance.[27] Together, these pro-inflammatory cytokines and chemokines, combined with the stress of endothelial dysfunction in the vessels, can lead to significant organ damage and failure.

2.2 Regulation of Glucose Transport

The glucose transporters (GLUTs) are a family of membrane proteins which facilitate the transport of glucose across the cellular plasma membrane. Because glucose is an essential source of metabolism and ATP production in virtually all life forms, and because glucose is a relatively large molecule which requires a membrane transporter to facilitate transport, the GLUT family is highly conserved and is present in all phyla. The glucose transporter isoforms, of which there are currently 14 known, are organized into three classes based on sequence similarities. Here, the relevant investigations regarding the glucose transporters, including their discovery, structure, and pathophysiological functions currently known, are discussed. The class I glucose transporters discussed here include GLUT1, GLUT2, GLUT3, and GLUT4. A brief overview of the class II glucose transporters includes GLUT5, GLUT7, GLUT9, and GLUT11. This class III glucose transporter review includes discussion on GLUT6, GLUT8, GLUT10, GLUT12, and GLUT13. While there are a number of varying reviews regarding the glucose transporters as a whole, the class III GLUT isoforms frequently receive less attention than the other classes. However, this is a budding group of glucose transporters which have recently been identified as significant in disease pathophysiology and potentially critical in stimulated and unstimulated glucose transport. Finally, some glucose transporters such as the class II glucose transporters (GLUT-5, -7, -9, and -11) and some of the class III glucose transporters (GLUT-6, -13) were not part of this study due to their high specificity for certain species, tissues, or molecules, such as fructose.[34-39]

As discussed later in this review, there are two basic mechanisms regulating glucose uptake into the cell: mediated glucose uptake (via insulin, calcium, AMPK, or

neuregulin) and basal glucose uptake. Mediated glucose uptake via the insulin-signaling pathway (dependent on production of insulin by the pancreatic beta islet cells and functional insulin receptors) functions primarily through the activation of PI3K, AKT, and AS160 (AKT substrate of 160 kilodaltons) in order to stimulate the trafficking of the intracellular GLUT vesicle to the cell membrane. This pathway may also be activated through the binding of insulin-like growth factor 1 to its receptor. Additionally, as this pathway shares several major proteins with other significant signaling cascades, including inflammatory signaling, the ultimate functioning of insulin-mediated GLUT trafficking may be altered downstream by several possible effectors. Basal glucose uptake is mediated predominantly by any particular GLUT isoform's affinity for glucose. For instance, GLUT1 and GLUT3 are considered high affinity (low Km) GLUT isoforms, while GLUT2 has a high Km and thus a low affinity. Additionally, each GLUT isoform has specific roles depending on their expression in certain organs (or, in the case of some GLUTs, their role is ubiquitous basal glucose uptake, such as for GLUT1, due to expression in nearly all of the organs).

Finally, once inside the cell, glucose can be utilized in several different ways. Firstly, glucose may be used in glycolysis, which is an oxygen-independent pathway. Glycolysis breaks down a glucose molecule into two pyruvate molecules while releasing ATP and NADH. Oppositely, the process of gluconeogenesis produces glucose via the reverse process of glycolysis. Glycogenesis is the process of converting glucose into glycogen, a polysaccharide, for stored energy. When needed, molecules of glucose can be cleaved from branched glycogen and can enter glycolysis via glycogenolysis.

2.2.1 Glucose Transporters

2.2.1.a Class I Glucose Transporters

GLUT1

GLUT1 is the major basal glucose transporter, primarily found on the cell surface, and does not rely on trafficking mechanisms in order to transport glucose into the cell.[40]

GLUT1 is formed by 492 amino acid residues and includes one site of N-linked glycosylation, with no other known post-translational modifications.[40, 41] In contains 12 transmembrane segments.[40, 41]

GLUT1 is predominately a glucose transporter, but it is also able to transport mannose, galactose, glucosamine, and reduced ascorbate.[40] It was first described as being expressed in human erythrocytes,[41] but is also described as an important part of glucose transport across the blood brain barrier.[42] Along these lines, GLUT1 protein has been found in brain endothelial cells,[42] brain astrocytes,[43] skeletal muscle,[44] cardiac muscle,[45] adipose tissue,[46] lamellar tissue,[44] as well as most organs and tumors.[40]

GLUT1 deficiency syndrome is an autosomal dominant genetic disease caused by a haplodeficiency of the *slc2a1* gene.[47] Symptoms of this disease include seizures, developmental delay, and ataxia, beginning in infancy.[47] These symptoms are ameliorated with a ketogenic diet but not cured.[47] Total GLUT1 knockout in mice is embryonic lethal.[48] Mouse models of GLUT1 and GLUT3 knockout in platelets abolishes platelet glucose uptake and decreased thrombosis and platelet activation.[49]

GLUT2

GLUT2 is a basal glucose transporter, not relying on trafficking mechanisms or signaling cascades in order to transport glucose into the cell. It is the major glucose transporter of hepatocytes, kidney proximal convoluted tubules, and pancreatic beta islet cells,[40] but has also been described in the intestine, brown adipose tissue, skeletal muscle, the lung, and the nervous system.[50, 51]

GLUT2 has a 55% amino acid sequence identity with GLUT1, and has similar structure and orientation in the plasma membrane.[52]

GLUT2 is known to have the highest Km value (15-20mM) and thus the lowest affinity for glucose, which allows it have a rate of glucose entry which is proportional to blood glucose levels.[53] GLUT2 can also transport mannose, galactose, and fructose, and has a high affinity (~0.8mM) for glucosamine.[50]

While GLUT2 is widely known to be the predominant glucose transporter of the liver, pancreas, and intestine, GLUT2 knockouts of these organs do not prove lethal.[54, 55] Indeed, intestine-specific knockouts do not result in impaired intestinal glucose uptake,[54] and liver-specific knockouts did not impact glucose output. However, GLUT2 knockouts did result in suppressed glucose-stimulate insulin secretion from beta cells[56] and suppression of glucose uptake in the liver.[57] Interestingly, GLUT2 knockouts in the brain or the nervous system led to delayed initiation of feeding after fasting, loss of glucagon secretion during hyper- and hypoglycemia, impaired thermoregulation, and impaired stimulation of parasympathetic activity and inhibition of sympathetic activity by glucose.[55] Whole-body GLUT2 knockout mice demonstrate a diabetic phenotype and die

two to three weeks after birth due to a defect in glucose-stimulated insulin secretion.[54] However, when these whole-body GLUT2 knockout mice are then rescued by re-expressing either GLUT1 or GLUT2 in the pancreatic beta cells, specifically, they survive and breed.[54] In humans, a mutation of the *SLC2A2* gene causes Fanconi Bickel syndrome, resulting in accumulations of glycogen in the liver and kidneys.[58]

GLUT3

GLUT3 is considered a neuron-specific glucose transporter due to its high expression in the brain, but it's also highly expressed in the testis, placenta, preimplantation embryos, and several tumor types.[53] It is highly conserved among mammals, fish, and birds.[59, 60]

GLUT3 consists of 481 amino acids, and weighs 52.5 kilo Daltons. Similar to the other facilitative glucose transporters, it consists of 12 membrane spanning segments.[53]

Along with GLUT1, GLUT3 has a relatively low Km value (5mM), allowing for a high affinity for glucose and a constant uptake of available glucose from the blood, regardless of blood glucose concentration. GLUT3 is required for proper brain organogenesis and embryonic growth.[60]

Homozygous loss of GLUT3 is embryonic lethal.[53] GLUT3 dysregulation has been implicated in the development of dyslexia.[53] Heterozygous GLUT3 knockout mice have demonstrated enhanced cerebrocortical activity, but otherwise have normal coordination, reflexes, motor skills, anxiety, learning, and memory.[53] Additionally, heterozygous GLUT3 knockout mice possessed normal body weight, blood glucose, insulin, food intake, and food choices.[53] However, one group reported a potential increase in fat mass of adult male mice with a heterozygous GLUT knockout, while female mice remained

normal.[53] In heterozygous GLUT3 knockout mice, some groups have reported an increase of GLUT1 and GLUT8 protein, potentially as a compensatory mechanism.[53]

GLUT4

Together, GLUT1 and GLUT4 represent the most studied glucose transporter isoforms, which is representative of their ubiquitous nature and their importance to normal glucose homeostasis. While GLUT1 is the predominant basal glucose transporter, GLUT4 is the predominant insulin-stimulated isoform, and its trafficking to the cell surface from its intracellular vesicle is the rate-limiting step of insulin-mediated glucose uptake.[53] GLUT4 is most relied upon in the insulin-sensitive tissues: the heart, skeletal muscle, and adipose tissue.[53] GLUT4 is also expressed in the brain[61] and, recently, GLUT4 has also been described in the trachea and lung in humans.[62] GLUT4 has been demonstrated to be highly conserved among mammals and fish,[63] and can be expressed in yeast experimentally. However, GLUT4 has been noted as absent in birds.[59]

GLUT4 is has 65% sequence identity with GLUT1 and, similar to GLUT1, GLUT4 possesses an affinity for glucose of a Km around 5mM.[53, 64] It is also able to transport dehydroascorbic acid and glucosamine.[53] GLUT4 is unique among glucose transporters for its well-investigated system of insulin-stimulated GLUT vesicle trafficking which is required for insulin-mediated glucose uptake into the cell. The end of this pathway ultimately results in the phosphorylation of AS160 (AKT substrate of 160 kilodaltons), which then activates Rab10, and ultimately allows for the translocation of GLUT4 to the cell surface.[65] While insulin has been shown to be the most effective and predominant initiator of the signaling cascade which leads to GLUT4 translocation, calcium,[66]

AMPK,[66] and neuregulin[67] have also been demonstrated to be able to phosphorylate AS160 and stimulate GLUT4 trafficking.

Major alterations to total protein and cell surface protein expression of GLUT4 in the insulin-sensitive tissues are evident during type 1 and type 2 diabetes.[16, 68-72] The lack of insulin production or insulin action result in the inaction of the insulin signaling pathway, which is the primary source of signaling required for the translocation to the cell surface. However, it has been shown that upregulating contraction via exercise can ameliorate GLUT4 alterations in the diabetic state.[73] Surprisingly, homozygous GLUT4 knockout mice do not show a diabetic phenotype, although they are small, possess significant cardiac hypertrophy, and have a maximum life span of 5 to 7 months.[74] Additionally, while these mice maintain normal blood glucose levels, they also possess significantly increased postprandial insulin concentrations, and had a decreased level of lactate and free fatty acids in both fasting and fed states.[74] The relatively normal phenotype of total GLUT knockout mice may be due to the compensatory upregulation of other GLUT isoforms.[74] Mice which only have one allele of GLUT4 knocked out are phenotypically normal and are fertile despite the fact that they have substantially reduced GLUT-mediated glucose uptake and less GLUT4 protein in the insulin-sensitive tissues.[74]

2.2.1.b Class II Glucose Transporters

GLUT5

GLUT5 is a facilitative fructose transporter, with no ability to transport glucose or galactose.[34] Active GLUT5 protein is largely located in the small intestine and the kidney, but GLUT5 has also been described in the adipose tissue, skeletal muscle, and

brain.[34] GLUT5 has also been consistently found in the testes and sperm, though its role in sperm metabolism remains unclear.[34] GLUT5 seems to be well-conserved, having been described in humans, rats, rabbits, chickens, horses, and cattle.[34] Interestingly, patients with type 2 diabetes exhibit an increase of GLUT5 mRNA and protein in skeletal muscle, while other muscle-specific GLUT isoforms did not change.[34] Conversely, in obese *fa/fa* rats, GLUT5 protein expression in the adipose tissue is significantly decreased.[34] In general, GLUT5 expression and activity have been shown to be decreased during inflammatory diseases, including in the intestine.[34] GLUT5 has also been highly expressed in some cancers, despite not being highly expressed in the healthy tissue, such as breast cancer. This would indicate that neoplastic cells use fructose to enhance glycolysis, but this area of research requires further investigation.[34]

GLUT7

GLUT7 is considered to be the closest isoform to GLUT5 in structure and function,[75] and has previously been suggested to transport both glucose and fructose with low capacity. However, studies indicate that GLUT7 does not transport either, and in fact the substrate which it is responsible for transporting has yet to be identified.[75] GLUT7 is expressed in the small intestine and colon, with modest amounts also expressed in testis and prostate.[75] GLUT7 protein expression in the jejunum and ileum does increase alongside an increase in dietary carbohydrates, so has been hypothesized to be involved in the regulation of other GLUT isoforms.[75]

GLUT9

GLUT9 is fairly unique among the GLUT isoform family for itself having two splice variants with different expression patterns.[75] However, both variants are predominantly located in the intestine (specifically the jejunum and ileum), kidney, and placenta.[75] Current research indicates that GLUT9 is a high affinity urate transporter, and, similar to GLUT7, no studies have confirmed that GLUT9 is able to transport either fructose or glucose.[75] Enterocyte-specific GLUT9 knockout mice develop hyperuricemia, hyperuricosuria, and metabolic syndrome, possibly because of impaired enterocyte urate clearance.[75] Total GLUT9 knockout leads again to hyperuricemia and hyperuricosuria, but also to early-onset nephropathy and renal insufficiency.[37]

GLUT11

GLUT11 is another close relative of GLUT5 in terms of sequence homology and, similar to GLUT9, possesses three different variants: GLUT11A, GLUT11B, and GLUT11C.[76] GLUT11 has been shown to transport both fructose and glucose.[76] GLUT11 is absent from the rodent genome, but the variants have been found in human tissues.[76] For example, GLUT11A is noted to be present in the heart, skeletal muscle, and kidneys, GLUT11B in the placenta, adipose tissue, and kidneys, and GLUT11C in the adipose tissue, heart, skeletal muscle, and pancreas.[76]

2.2.1.c Class III Glucose Transporters

GLUT6

GLUT6 (formally known as GLUT9)[77] is one of the least studied glucose transporters. GLUT6 has been found in the spleen,[78] leukocytes,[78] the brain,[78] the endometrium,[79] peripheral blood leukocytes,[80] and vascular smooth muscle cells.[81] It has been found humans, rats,[77] cows,[82] and zebrafish.[83] The GLUT6 gene (SLCA26) is composed of 507 amino acids[78] and 10 exons, and is located on chromosome 9 in humans.[80] It contains a dileucine internalization motif at the 5th and 6th amino acids, as well as a monosaccharide binding site from 286-292.[80] GLUT6 has a molecular weight of 48kDa.[80]

In mouse model which had GLUT6 knocked out using a CRISPR-Cas9 mediated deletion, whole-body glucose metabolism, development, and growth were all unaltered. This was true in male and female mice fed either a chow or western diet.[84] Based on this study, GLUT6 does not appear to be a major regulator of metabolic physiology. GLUT6 also does not seem to be stimulated by insulin.[77] GLUT6 mRNA has was decreased in zebrafish in a fed state versus a fasted state.[83]

GLUT6 is not widely expressed in normal tissues, but it has been found to be upregulated in several cancers. GLUT6 has been implicated as a potential player in cancer development, and based on the recent study by Byrne et al, GLUT6 inhibition may have minimal effect on normal physiology while targeting cancer growth.[84] In gastric cancer, GLUT6 protein was found in significant quantity in cancerous samples, but the amount of protein did not correlate with prognosis.[85] There is also a significantly increased amount of GLUT6 protein in the endometrium of obese postmenopausal endometrial cancer

patients.[79] Additionally, along with GLUT10, GLUT6 has been implicated in vascular disease: white adipose tissue in patients with an abdominal aortic aneurysm possessed significantly more GLUT6 mRNA and protein compared to patients without an abdominal aortic aneurysm.[86]

GLUT8

Glucose transporter 8 is a novel class III glucose transporter which has been demonstrated to be important in cellular glucose and fructose uptake from the blood stream in some tissues. This transporter has been established to possess some tissue specificity in terms of location and function, and has been described in a wide variety of species. As this glucose transporter isoform continues to be defined, it begins to emerge as a potentially major player in diabetes research and metabolism overall. Importantly, this isoform may be a novel target for metabolic disease therapy in the future. Here, the relevant investigations and identifications of glucose transporter 8, including its discovery, structure, and pathophysiological functions currently known, are discussed.

GLUT8 has been described in multiple tissues since its discovery, including the brain,[87] testes,[88] spermatozoa,[88] placenta,[89] liver,[90] kidney,[91] intestine,[92] adipose tissue,[77] skeletal muscle,[93] and most recently, the heart,[68, 94] and the lungs.[95] Also, it is important to note that GLUT8 has been described in a wide variety of species including yeast,[96] rats,[97] mice,[68] chickens,[98] horses,[99] cows,[100] boars,[101] and humans.[93] Thus, it appears to be fairly ubiquitous, it is found in high quantities in both basal and insulin-sensitive tissues, and is widely conserved among species.

Both mouse and human GLUT8 contains 12 membrane-spanning helices[93] and a cytoplasmic N-51 terminal dileucine motif.[102] GLUT8 has been reported as anywhere between 42 kDa[93] to 55 kDa[102] in weight. GLUT8 helices have been reported to contain several highly conserved motifs which may be essential for transport activity, such as, "GRK in loop 2, PETPR in loop 6, QQLSGVN in helix 7, DRAGRR in loop 8, GWGPIPW in helix 10, and PETKG in the C-55 terminal tail."[93]

Insulin-sensitive glucose transporters such as GLUT4 are well known for the insulin-mediated translocation from its intracellular vesicle to the cell surface to facilitate the transport of glucose from the blood to the intracellular environment.[103] The potential translocation of GLUT8 in a similar fashion has been widely debated in various tissues and remains as a subject of scrutinization as this novel transporter continues to be evaluated fully. Importantly, GLUT8 has been demonstrated to not participate in the same particular vesicular recycling process at GLUT4, but it does appear to localize to an endosomal compartment.[102] GLUT8 has been shown to translocate to the endoplasmic reticulum during glucose administration in the rat hippocampus.[104] It has been described as associating with a specific intracellular compartment in hippocampal neurons,[105] which could indicate a similar translocation technique to GLUT4, and it has been described as being insulin-sensitive in cardiac tissue.[68] It has also been speculated to be responsive to calcium signaling, similar to GLUT4, in the myocardium.[106] And again, while some groups have specifically described GLUT8 as being an intracellular glucose transporter during hippocampal neurogenesis,[107] GLUT8 has conversely been described as being specifically localized to the cell surface in hepatocytes[108] and in the acrosomal

region of spermatozoa,[88] so it is possible that GLUT8 possesses different mechanistic operations in different tissues.

However, while many have been able to speculate or define the cellular location of GLUT8 in various cell types under differing glucose conditions, the mechanistic intracellular regulation of this glucose transporter remains largely unknown. The other glucose transporters continue to be investigated of course, but much more is known about their expression and transport mechanisms. For instance, GLUT4 is heavily reliant on the PI3K/AKT (phosphoinositide 3-kinase/protein kinase B) pathway resultant from insulin signaling,[109, 110] but can also be stimulated in this same fashion by calcium[111] and by AMPK (5' adenosine monophosphate-activated protein kinase).[112] GLUT1 does not need to translocate to function, but it has been demonstrated that glycogen synthase kinase beta (GSK3B) regulates the overall protein expression of GLUT1.[113] Conversely, while the expression of GLUT8 has been correlated with the expression or phosphorylation of staple proteins in the insulin signaling pathway such as PI3K and AKT,[68, 114] to our knowledge a true mechanistic investigation of the regulatory processes of this transporter has yet to be undertaken. However, it has been demonstrated in some cell lines that endocytosis may be the primary regulatory step for this isoform, and in order for GLUT8 to be recruited to its appropriate endocytic machinery beta2-adaptin must interact with GLUT8's dileucine motif.[115]

GLUT8 has been shown to be an important facilitator of both glucose[87, 88, 91, 93, 99, 116-118] and fructose[97, 108, 119] transport into the cell from the blood.

Whole-body GLUT8 knockout mice have been shown to be viable and maintained normal development, although they possessed "mild alterations" in the brain, heart, and sperm cells.[120] Similarly, other groups have determined that an inactivation of the glut8 gene demonstrated that GLUT8 was not required for embryonic development and did not affect postnatal development, glucose homeostasis, or stress responses.[107] This same group also determined that GLUT8-deficient mice possessed an increased proliferation of hippocampal cells, but no alterations in memory acquisition or memory retention, and that this knockout did increase the duration of the P wave in the heart without altering the size or morphology. Interestingly, when Schmidt et al. investigated the importance of GLUT8 to neuronal cells, they found that GLUT8 knockout mice had increased physical activity, reduced risk assessments, altered grooming, and increased arousal.[118] Furthermore, GLUT8 protein levels have also been demonstrated to increase in motor neurons after injury, and it has been specifically implicated in the potential increase of glucose transport in motor neuron regeneration.[116] GLUT8 has been shown to be present in significant quantities in cardiac tissue, both in the atria and in the ventricle, and may play a significant role in glucose uptake in the heart.[68, 106]

Due to the known detrimental effects of type 1 (insulin-dependent) diabetes on sperm,[121] Gawlik et al. specifically investigated the effects of a GLUT8 knockout in terms of male reproductive cells.[122] They found that without glut8, sperm were less motile, possessed reduced ATP levels, and had lesser mitochondrial membrane potential, even though overall spermatozoa survival rate was not decreased.[122] In female reproduction, GLUT8 has also been implicated as an important player in the lactating mammary gland and it may be regulated by lactogenic hormones in this tissue in particular.[100]

It has also been established that some translocational glucose transporters can use AMPK activation to translocate from their intracellular vesicles to the cell surface.[123] This same finding has recently been replicated to indicate that GLUT8 is similarly activated by AMPK in equine striated muscle.[99] Also, while exercise has been shown to improve GLUT4 translocation in skeletal muscle in both diabetic and healthy subjects, GLUT8 protein expression is still being investigated in this area. Interestingly, Seki et al. found that while females are more sensitive to exercise and thus have a more pronounced post-exercise overall GLUT response than males do, GLUT8 mRNA is not altered in either gender after exercise.[124]

GLUT8-deficient hepatocytes demonstrate reduced fructose uptake, and GLUT8-deficient mice exhibit reduced fructose-induced accumulation of triglycerides and cholesterol.[108] Along these lines, DeBosch et al. recently made the very striking claim that by potentially altering PPARγ-dependent hepatic fatty acid metabolism, a "GLUT8 blockade prevents fructose-induced metabolic dysregulation".[119] Thus, blocking the ability of GLUT8 to transport fructose may be a beneficial target for patients with type 2 diabetes and other metabolic diseases which are heavily involved with hepatic fatty acid metabolism.

GLUT8 has also been demonstrated as affecting cellular functions which are not directly related to glucose or fructose transport. It has been recently implicated in having a significant role in autophagy.[125] Trehalose is a disaccharide which has been postulated to induce cellular autophagy,[126] and Mayer et al. provided a body of work to demonstrate that GLUT8 is a trehalose transporter in mammals, and that GLUT8 is thus required for both trehalose-induced autophagy and for signal transduction.[125]

However, what remains largely unknown in terms of functionality is the degree to which GLUT8 is able to compensate for other predominate GLUT isoforms when those isoforms are nonfunctional. For instance, it is well established that GLUT4 is the predominate isoform in adipose tissue and striated muscles.[127] However, while GLUT4 is crucial for normal growth, GLUT4 knockout mice are certainly compatible with life and are only mildly hyperglycemic.[128] This would suggest that, given the amount of GLUT8 protein which has been reported in many of the tissues which utilize the most glucose in the body, GLUT8 may be able to play a compensatory role in rescuing glucose transport. To our knowledge, the results of experiments involving the quantification of active GLUT8 protein in various tissues after other predominate GLUT isoforms are functionally muted has yet to be reported.

The glucose transporters in general have repeatedly found to be altered during disease states, particularly during metabolic diseases such as diabetes.[68-70, 91, 129, 130] However, it is important to note that under experimental conditions, muting the functionality of a GLUT isoform does not necessarily lead to metabolic dysfunction, and conversely in vivo metabolic dysfunction does not necessarily mean there is an alteration in the expression or functionality of a particular GLUT isoform. For instance, despite what some teams have found in regards to the alteration of male reproductive cells when GLUT8 expression is experimentally knocked out,[93, 122] Gomez et al. found that the expression of GLUT8 is not altered in the testes or the sperm of diabetic rats when compared to their non-diabetic counterparts.[131]

Insulin sensitive glucose transporters rely predominately on the insulin signaling pathway to translocate from their intracellular vesicle to the cell surface in order to facilitate the

diffusion of glucose into the cell.[132] Due to this reliance, the protein expression of insulin sensitive glucose transporters in insulin sensitive tissues has been repeatedly reported to be decreased during diabetes.[68] In some insulin-sensitive tissues, GLUT8 appears to mirror the alterations of GLUT4 in the diabetic myocardium.[68]

Finally, it has been reported that GLUT8 is negatively regulated by hypoxia in mammary cells, and that this regulation occurs through a HIF-1α-independent pathway.[133]

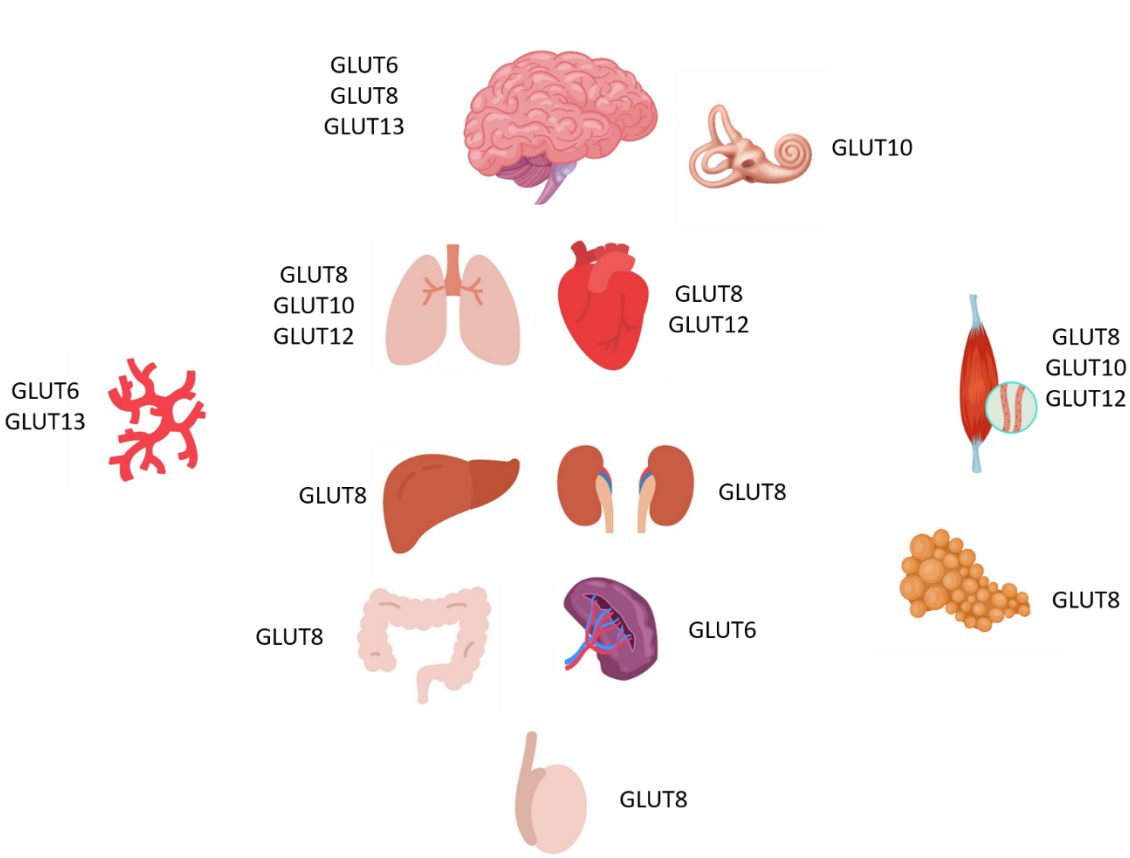

Figure 1: Organs in which class III GLUT protein has been found.

GLUT10

GLUT10 is one of the least investigated class III glucose transporters, and indeed one of the least investigated glucose transporter isoforms in general. GLUT10 mRNA and cDNA has been found in multiple tissues including white adipose tissue,[134] oocytes,[135] tcochlea,[136] small intestine,[134] liver,[137] pancreas,[137] placenta,[137] brain,[137] heart,[134] skeletal muscle,[138] and lungs,[51] across multiple species, including humans,[134] mice,[134] frogs,[135] and zebra fish.[139] GLUT10 protein has been identified in skeletal muscle,[138] cochlea,[136] and lung.[62, 95] *In vitro*, GLUT10 has also been characterized in multiple cell lines including human airway epithelial cells,[62] human anaplastic thyroid carcinoma, poorly differentiated papillary thyroid carcinoma, and follicular thyroid carcinoma, but not in medullary thyroid carcinoma cell lines.[140]

In humans, GLUT10 is located in the chromosomal region 20q12-13,[137, 141] which is a region that has specifically been associated with type 2 diabetes.[141, 142] As reported by Dawson et al, "The GLUT10 gene is located between D20S888 and D20S891 and is encoded by 5 exons spanning 26.8 kb of genomic DNA. The human GLUT10 cDNA encodes a 541 amino acid protein that shares between 31 and 35% amino acid identity with human GLUT1–8".[137] However, this specific length can vary modestly between species as Chiarelli et al reported that the GLUT10 gene (*slc2a10*) encodes a 513 amino acid protein in zebra fish (*Danio rerio*).[139] GLUT10 also maintains 12 transmembrane domains in all reported animals, a hallmark structure of the GLUT family overall.[139, 141]

GLUT10 seems to be reasonably well conserved among mammals, and is fairly similar in structure to the other glucose transporters. Mammalian glucose transporters contain

characteristic sequence motifs such as "VP^{497}ETKG in the cytoplasmic C-terminus, G^{73}R[K,R] between TMD2 and TMD3 (PROSITE PS00216), VD^{92}RAGRR between TMD8 and TMD9 (PROSITE PS00216), Q^{242}QLTG in TMD7, and tryptophan residues W^{430} (TMD10) and W^{454} (TMD11), that correspond to tryptophan residues previously implicated in GLUT1 cytochalasin B binding and hexose transport".[137] However, GLUT10 does not contain the SUGARTRANSPORT2 pattern (PS00217), while the other known human glucose transporters do possess this sequence.[137]

GLUT10 is a d-glucose membrane transporter, with transport kinetics of 0.28mM for 2-deoxy-D-glucose.[80] GLUT10 has been identified as the mitochondrial L-dehydroascorbic acid transporter, and in this respect GLUT10 then protects cells from oxidative injury.[143] Along the same lines, *glut10* gene deletion causes a large proportion of genes involved in mitochondrial function to be altered.[144]

GLUT10 has been reported in multiple tissues in zebra fish, suggesting a wide role in this species.[139] Similar to GLUT12, when GLUT10 is knocked down in zebra fish embryos a wavy notochord develops, along with cardiovascular abnormalities alongside a reduced heart rate and blood flow, and incomplete irregular vascular patterning.[144]

Alongside GLUT2, GLUT10 has been implicated as an important basal transporter for glucose between the airway and the bronchial epithelium in both humans and rodents.[95, 145, 146]

GLUT10 has also been specifically demonstrated as localizing to the endoplasmic reticulum.[147]

Interestingly, GLUT10 protein increases in skeletal muscle 2- to 5-fold after chronic muscle loading.[138]

In mice, GLUT10 protein has been found to localize in the cuticular plate of the outer and inner cochlear hair cells, as well as in the ampullary crest of the vestibular system.[136] Based on these findings, Chen et al determined that GLUT10 may be a contributing factor to glucose transport between the endolymph and the hair cells across the cuticular plate.[136]

A link between GLUT10 and type 2 diabetes has been established.[137, 141] A deficiency of GLUT10 has been linked to an upregulation of the TGF pathway in the arterial wall,[144] which has also specifically been observed in Loeys-Dietz syndrome.[148] Loeys-Dietz syndrome is characterized by aortic aneurysms with arterial tortuosity, and arterial tortuosity syndrome itself has also been associated with a loss-of-function mutation of the GLUT10 gene, *SLC2A10*.[149]

2.2.2.c GLUT12

GLUT 12, considered as second insulin sensitive glucose transport system, was identified in MCF-7 breast cancer cells.[150, 151 1] GLUT12 transports 2-deoxy-glucose glucose, fructose and galactose across intracellular organelle membranes. It has been shown that GLUT12 could work as a proton coupled symporter.[151, 152] In addition, GLUT12 was found to have higher affinity for D-glucose than D-fructose, D-galactose and L-glucose.[153, 154]

It is reported that GLUT12 expresses 29 % amino acid homology to GLUT4[150, 155] and 40 % amino acid identity to GLUT10. This novel glucose transporter protein is encoded

by SLC2A12 and has a molecular weight of molecular weight between 67 kDa[156] and 76kDa.[150] This class of glucose transporters are found expressed in heart,[151, 153] skeletal muscle,[150, 155-157] prostate,[152, 158] adipose tissue,[70, 150, 159] and placenta,[89, 150, 153, 160, 161] thus playing important role in blood glucose metabolism.[160] GLUT12 is found to localize intracellularly at Golgi complex and plasma membrane when ectopically expressed in Chinese Hamster Ovary cells.[40, 162]

The novel and second insulin-sensitive isoform, GLUT 12, contains slc2a12 encoded proteins.[163] It is conserved in human, chicken, cow, horse, rhesus monkey, chimpanzee, dog, mouse, rat, zebrafish, rice and *A. thaliana.*[156, 164] Orthologs are found in 177 organisms in total.[164] The GLUT-12 cDNA encodes 617 amino acids essential for sugar transport. It also possesses dileucine motifs in the NH_2 which influence its subcellular targeting and COOH termini at regions similar to the FQQI and LL targeting motifs in GLUT4.[150, 165, 166] Compared to other members of the family, the cytoplasmic NH2 and COOH termini of GLUT12 have been reported to be longer describing them as the largest glucose transporter.[150] The dileucine motif and adaptor protein (AP) complexes promote protein trafficking to the plasma membrane or different organelles.[167, 168] GLUT12 contains a potential phosphorylation site at Ser11, adjacent to the NH2-terminal di-leucine.[150] The amino acid upstream of NH-2 terminal play an important role in regulating intracellular sorting.[94] GLUT12 localizes in an intracellular compartment and in the plasma membrane when expressed endogenously or overexpressed and this translocation requires PI3-K stimulation.[169]

Primarily functions as basal GLUT located at cell surface in the heart.[156] Unstimulated (that is, lacking stimulation from either insulin or calcium), cell surface GLUT12

contributes to majority of the myocardial GLUT12 protein.[156] In skeletal and adipose tissue, its function and regulations are different compared to the heart. In horses, GLUT12 has the highest expression in the omental adipose tissue[159] as well as higher protein concentration in visceral compared to subcutaneous adipose tissues depots.[70] Over-expression of GLUT12 in transgenic mice has shown to improve glucose homeostasis in insulin-sensitive peripheral tissues on stimulation with insulin.[157] Expression of GLUT12 during rat fetal development showed apical localization in lactating rat mammary epithelial cells which suggested requirement of GLUT12 for glucose metabolism during lactation.[170] It is also found to be expressed in fetal chondrocytes, kidney tubules, and lung bronchioles during gestational period which suggest its importance in transporting hexoses to developing tissues.[135, 170] The presence of GLUT12 and insulin receptors in the syncytiotrophoblast during first trimester indicate insulin regulates glucose uptake by the placenta via GLUT12.[171] This could be a pathway for the regulation glucose supply to fetus in first trimester.[161, 171] GLUT12 thus functions as a second glucose transporter than as basal non-translocatable cell-surface associated GLUT, with some tissue-specific differences emerging in recent research.

During cardiac ischemic and chronic heart failure, a compensatory correlation between GLUT4 and GLUT12 occurs with four-fold increase protein expression of GLUT12 in left ventricle.[156] This combination of enhanced glucose uptake and oxidation is a result of increased ATP demand.[172] This same trend of an increase of total GLUT12 protein has been demonstrated in skeletal muscle and cardiac muscle during type 1 diabetes.[156] Pujol-Gimenez et al. demonstrated GLUT12 is one of the main glucose transporters involved in glycolytic metabolism of cancer cells mediated via a p53-mediated mechanism.[173] In

zebrafish, a GLUT12 knockout alters the development of embryonic heart and results in abnormal valve formation.[174] In addition, embryos deficient in GLUT12 served poor glycemic controls.[174] Recent studies show high level of expression of GLUT12 in frontal cortex, thus implicating its role Alzheimer's disease.[175] GLUT12 also localizes in distal tubules and collecting ducts of rat kidney and is upregulated in diabetic nephropathy and hypertension,[176] further implicating its role in glucose transport.

GLUT12 is a novel, potentially insulin-sensitive Class III glucose transporter. Under physiological insulin-stimulation, GLUT12 does not translocate to the cell surface. Rather, it seems to occur during the diabetic condition as a compensatory mechanism for GLUT4 downregulation. GLUT12 functions as a basal cell-surface GLUT in the heart, where reduction in glucose uptake leads to heart failure. GLUT12 alterations are also linked to development of degenerative brain disorders and cancer. In addition, GLUT12 is an important transporter of hexoses critical during early development stages. Further studies on this GLUT member will help explain its role in metabolic related disorders and its function on different species.

GLUT13

GLUT13 (*slc2a13*) is unique for being a H+/myo-inositol co-transporter (sometimes abbreviated as HMIT or GLUT13/HMIT) that is stimulated by a decrease in the extracellular pH.[177] It is not able to transport 2-deoxy-D-glucose.[177] This isoform is predominately expressed in the brain, with the highest concentrations being in vascular smooth muscle cells,[81] PC12 cells,[178] the hippocampus, hypothalamus, cerebellum, and brainstem.[177] It has been identified in frogs, mice, and in humans.[177, 178] In humans, this

transporter is composed of 648 amino acids and is located on chromosome 12.[80] Like many of the other class III GLUT isoforms, GLUT13 is a predominately intracellular protein.[178] However, it may translocate to the cell surface after stimulation from cell depolarization, activation of protein kinase C, or increased intracellular calcium concentrations.[178] These are similar translocation stimuli as has been found in GLUT4 and GLUT12. [111, 156]

Overall, the class III glucose transporters are a currently under-investigated portion of the proteins contributing to metabolism and glucose homeostasis. While GLUT6 and GLUT13 are the least studied of this class, GLUT8, GLUT10, and GLUT12 are emerging as potentially significant participants not only in healthy glucose metabolism, but also in several disease pathophysiologies.

GLUT8 is a novel class III isoform of a glucose transporter. This GLUT has been demonstrated not to be crucial to viability and compatibility with life, but does seem to play important roles in organs such as the liver, the heart, the testes, and the sperm. It would appear that this GLUT is insulin-sensitive in some tissues, but not in all, and could participate in compensatory mechanisms when other predominant GLUTs in a tissue are downregulated. Due to these potentially insulin-sensitive and compensatory mechanisms, this GLUT isoform appears as a potentially important therapeutic target during metabolic disease. As the GLUT8 isoform continues to be fully investigated, light will surely be shed on some of these important and currently unknown specifics.

While GLUT10 has received scarce attention in comparison to other GLUTs, it has recently been identified as a key player in several tissues. Most importantly, GLUT10 has been implicated as a critical actor during disease, particularly type 2 diabetes, arterial tortuosity, and aortic aneurysms. Overall, investigations regarding this GLUT isoform have predominately involved the mRNA and cDNA expression, while protein expression of GLUT10 is largely unexplored in most tissues, during both healthy and diseased states.

GLUT12 is the second novel glucose transporter of the Class III transporters which has the potential to be insulin-sensitive. However, reports vary in regards to its insulin-sensitivity during a healthy condition, or whether this mechanism is only true as a compensatory manner during metabolic disease. It appears that the majority of the cellular GLUT12 protein is already located at the cell-surface during basal conditions, so it is possible that it's difficult to detect upregulations during stimulations. This glucose transporter has been implicated in several disease pathophysiologies, including diabetes mellitus, brain aging, and cancer.

While this review has attempted to exhaustively identify the functions and alterations of these class III glucose transporters in healthy and diseased states, there is surely a wealth of information yet to be determined about this critical membrane transport family. This is particularly true in regards to how these transporters might be targeted in novel therapeutic therapies for a wide range of diseases in the future.

2.2.2 Insulin Signaling Pathway

The severity of diabetes is largely governed by the function of glucose uptake into insulin-sensitive tissues, which, for the purposes of glucose uptake and whole-body

glucose homeostasis, include the skeletal muscle, the heart, and the adipose tissue. This insulin-mediated glucose uptake is dependent on the insulin signaling pathway. This pathway begins with either insulin or insulin-like growth factor 1 to bind to the insulin receptor or the insulin-like growth factor receptor on the cell surface.[179] These receptors then phosphorylate the insulin receptor substrates and activate PI3K.[179] Following this, PI3K can activate PIP3, which activates PDK-1, which results in the phosphorylation of AKT at the serine 473 and threonine 308 sites.[179] Once phosphorylated, AKT participates in several signaling cascades. Relevant to glucose metabolism, the phosphorylation of AKT leads to the inhibition of glycogen synthase kinase beta, preventing glycogen synthesis.[179] Additionally, the phosphorylation of AKT leads to the phosphorylation of the AKT substrate of 160 kilodaltons (AS160) which activates Rab GTPase.[103] This final step, the activation of Rab GTPase, allows for the translocation of insulin-mediated glucose transporters, such as GLUT4, from their intracellular vesicles to the cell surface.[103] In this same pathway, protein kinase C-ζ can also be activated by PIP3 and can go on to directly participate in GLUT4 translocation.[180]

However, outside of this classical insulin-mediated stimulation of GLUT4 trafficking, other mechanisms have been described to also stimulate the GLUT4 translocation. Firstly, calcium signaling, particularly through muscle contraction and exercise, has been shown to stimulate both intracellular AMPK and calcium/calmodulin-dependent protein kinase type II.[181] Both of these mechanisms stimulate GLUT4 translocation. Additionally, neuregulin has been shown to work through the ErbB 2/4 receptors to stimulate protein kinase C-ζ, which is then followed by GLUT4 translocation.[181]

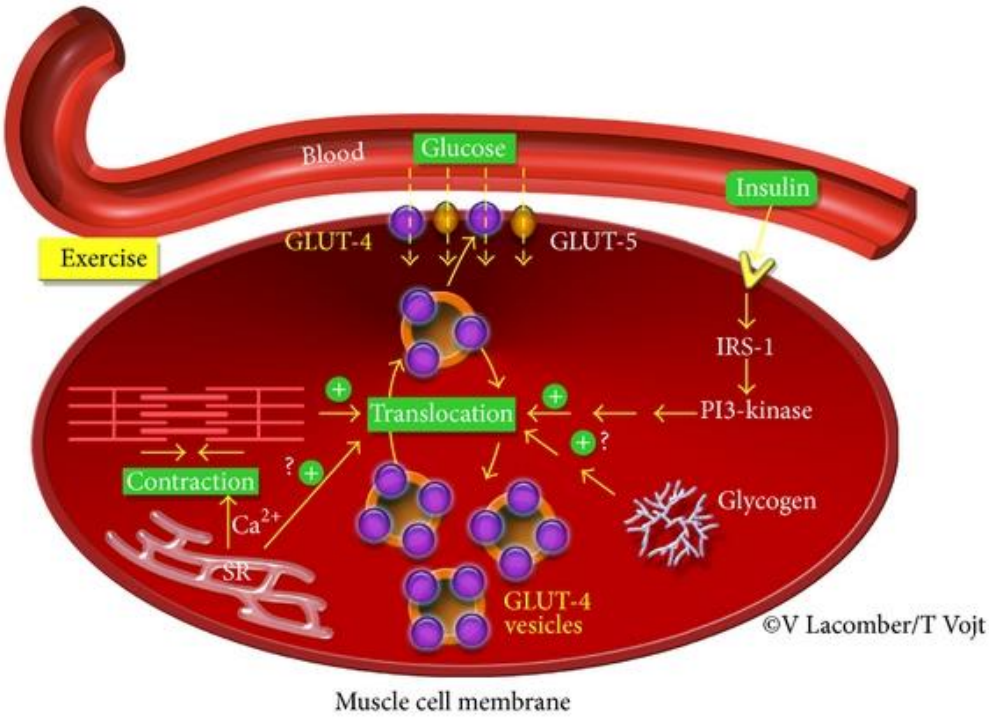

Figure 2: Regulation of glucose transport in striated muscle. GLUT4 translocation to the cell surface is mediated by both insulin-dependent and -independent pathways. GLUT: glucose transporter; PI 3-kinase: phosphatidylinositide 3-kinase; IRS: insulin receptor substrate; Ca^{2+}: calcium; SR: sarcoplasmic reticulum.[1]

2.3 Equine Metabolic Syndrome

First described in 2002, equine metabolic syndrome (EMS) is a relatively recent constellation of symptoms, including obesity, insulin resistance, and laminitis.[182, 183] Obesity alone does not constitute a diagnosis of EMS – there must be an accompaniment of hyperinsulinemia and/or insulin resistance.[182, 184] However, as we show here, we now know that insulin resistance is not required for the onset of EMS-associated (endocrinopathic) laminitis.

Alongside their human counterparts, the incidence of metabolic syndrome and obesity in horses has been steadily rising. Recent studies find that 32% of surveyed horses in the United States are over condition, and 19% are clinically obese, which is a much higher prevalence than previously thought.[185] Accordingly, the frequency of laminitis is estimated to be as high as 34%.[186] Importantly, there is still no known cure for laminitis after its onset,[99] and though research has outlined firm recommendations for avoiding the inception of this condition, there is still a vast knowledge base yet to be elucidated regarding both its cure and its prevention.

While some progress has been made in the endeavor of understanding the metabolic and inflammatory pathways,[99, 130, 186] epithelial cell signaling,[187] the stability of lamellar integrins,[188, 189] and many other biological mechanisms contributing to endocrinopathic laminitis in a top-down approach, the mechanisms for the observed changes occurring during the laminitic episode remain unknown. However, to our knowledge, a wide-scale, bottom-up approach has not been undertaken in the investigation of biochemical derangements underlying endocrinopathic laminitis which would help identify novel therapeutic targets for treating the laminitic condition. Additionally, it is not clear if the alterations in glucose metabolism (in insulin-sensitive tissues and in the lamellar tissue) rely substantially on post transcriptional modification.

2.2.1 Endocrinopathic Laminitis

Endocrinopathic laminitis (EL), the most common form of laminitis,[190] refers specifically to laminitis (rotation of the coffin bone within the hoof, also called founder) which results

from hormonal imbalances, as opposed to mechanical, septic, or supporting-limb laminitis.[191] Within EL there are two categories of hormonal imbalances which are associated with rotation of the coffin bone: glucocorticoid dysregulation (including Equine Cushing's Syndrome), and insulin dysregulation (including EMS). Here, we specifically investigate EL associated with insulin dysregulation and EMS.[192]

Presently there are no known treatments or cures for EL, although there are several preventative strategies.[190, 193] The disease pathophysiology of EL is still being described, but is more well elucidated than the biochemical alterations leading up to it. For instance, we now know that EL is accompanied by significant vascular alterations,[194] swelling and abnormal keratinization of epidermal cells,[195] increased mitotic activity and apoptosis,[195] increases in circulating inflammatory markers,[196] and inflammation in the lamellar tissue itself.[197] And, certainly, there are substantial histological changes in the laminitic hoof, including basement membrane separation, lamellar lengthening and attenuation, and rounding of basal cell nuclei.[198]

Considering the insulin implications, lamellar glucose metabolism has been investigated by our group and by others. Glucose uptake in the hoof, like other non-insulin-sensitive tissues, has been determined to rely on GLUT1 as the predominant glucose transporter.[199] However, during insulin-induced laminitis, GLUT1 was unchanged in the lamellae, while novel class III isoforms, GLUT8 and GLUT12, were increased.[44] However, while these GLUT isoforms have been investigated in terms of protein expression in the lamellae, the mRNA expression and the potential description of posttranscriptional modifications regulating these glucose transport mechanisms are largely unknown.

2.4 Hyperglycemia-involved Respiratory Infections

While both influenza and diabetes have topped the mortality charts for decades, it has only recently become clear that hyperglycemia is an independent risk factor for the development and higher severity of respiratory infections, including influenza infection.[200, 201] This phenomenon is thought to occur due to the hyperglycemic state, which predisposes patients to a higher-than-normal glucose concentration in the airway, leading to an increased risk of pulmonary infections.[146, 202] Although the lung is a major organ of glucose utilization, the role and regulation of glucose homeostasis in the healthy vs. diabetic lung have received little attention.

Despite common perception, the lung is a highly active metabolic organ. As gluconeogenesis does not occur in the lung it relies on glucose present in the circulation.[203] We now know that a steady concentration of glucose exists in the airway surface liquid, which is generally in concert with the level of glucose in the blood, with the blood glucose being roughly 12 times higher than that of the airway.[204] However, how glucose is transported from the vessels to the airway is still under debate. Current hypotheses stipulate that glucose passively diffuses from the blood across the pulmonary epithelium via paracellular pathways.[51] Due to this mechanism, the permeability of the pulmonary epithelial tight junctions is of significant importance, and the alteration of these tight junctions during disease states could introduce a large source of glucose variability in the airway.[51]

In general, very little investigation has been done to examine the status of GLUT protein expression in the adult lung of any mammal, even under healthy conditions.[51, 205] While

some studies have been undertaken to determine the GLUT protein or mRNA present in fetal tissue or in cell culture, and GLUT mRNA in cell culture, fetal, or adult lungs, [51, 205] it is important to note that the protein expression of glucose transporters – and whether they are intracellular or located on the cell surface – is of predominant importance.

The lung is a more complicated organ than the insulin-sensitive tissues in terms of cell type homogeneity and function. While the glucose transport of the lung is still under-studied, some investigations have recently described certain glucose transporter isoforms in certain cell types of the lung. For instance, GLUT-1, -2, and -10 have been found in the ciliated cells of the trachea and the bronchi.[205] GLUT-2 and -10 have been identified in the Clara cells.[205] Sodium glucose linked transporter isoforms have also been found in the submucosal glands and pneumocytes, but no GLUT isoforms have yet been described there.[205] Without identifying which cell type, GLUT4 has been identified in the human respiratory system,[62] and GLUT12 has also been identified in the cow and rat bronchioles.[205] However, despite these recent findings, many questions still remain regarding which of these isoforms are most responsible for pulmonary glucose uptake, what normal and metabolically dysregulated protein expression is for these proteins, and how much GLUT protein of any isoform is expressed on the cell surface during both healthy and diseased states.

Importantly, the Dr. Deborah Baines group at the University of London has undertaken several substantial investigations regarding the effects of pulmonary bacterial infection under hyperglycemic conditions. This group has demonstrated that an increased concentration of blood glucose is directly associated with an increased glucose concentration in the airway,[204] that an increased glucose concentration in the airway leads

to an increase in pulmonary bacterial proliferation,[206] and that rescuing whole-body hyperglycemia leads to a reduced concentration of glucose in the airway and a reduction of pulmonary bacterial proliferation.[207] Additionally, some groups have recently identified susceptibility of type 1 or type 2 diabetic mice to extremely high inoculations of influenza, and while they do not investigate glucose transport in particular, have shown that diabetic mice have a higher mortality than their non-diabetic counterparts.[208, 209]

However, while this work is groundbreaking, large gaps of knowledge still remain surrounding viral infection and diabetes. In particular, it remains to be proven whether the worsened pulmonary infections during the diabetic state are due primarily to hyperglycemia (a type 1 diabetic model) or due to a combination of obesity, inflammation, and insulin resistance (a type 2 diabetic model). Additionally, it is largely unknown what exactly is normal or altered in terms of pulmonary glucose homeostasis during influenza infection. Thus, we seek to answer those questions here.

2.4.1. Viral Pathogenesis

While diabetes may be the 7th leading cause of death in the United States, influenza is the 8th.[210] Of the four subtypes of influenza viruses (A, B, C, and D), influenza A and B can cause significant respiratory infection in humans.[211] However, while influenza B viruses can occasionally cause epidemics, only influenza A virus repeatedly cause epidemics and pandemics, and can be associated with a substantial mortality rate.[211] Influenza is a significant public health concern in the United States, costing $11.2 billion per year,[212]

and resulting in 22.27 million doctor visits, 959,000 hospitalizations, and 79,400 deaths in the 2017-2018 flu season.[213] In that flu season, the influenza A virus predominated.

Influenza A possesses eight separate gene segments, and is subdivided by the antigenic characterization of the hemagglutinin (HA) and neuraminidase (NA) surface glycoproteins that project from the virion.[211] Presently, 16 HA and 9NA subtypes have been described.[211] Additionally, influenza A can infect a wide variety of host species including birds, swine, hoses, humans, and many other mammals.[211] This virus thus possesses a substantial ability to "mix and match" the segmented genome combined with the large array of host species, allowing for significant and relatively expedient antigenic shift, wherein two or more different viruses combine to form a new subtype which possesses a mixture of the surface antigens of the original strains.[211] Not only does this allow for a lack of host response to this new virion, but it may be able to infect new species. Influenza A can also undergo antigenic drift, wherein small changes to the genome occur over time.[211] This may result in a lowered immune response to a virus which the body previously had acquired immunity to.

2.4.2. Viral Interaction with the Host Cell

The viral interaction with the pulmonary host cells is a significant source potential alteration based on the variations in host glucose metabolism. Viral infection of host cells begins when the influenza virion attaches to the host cell via its HA glycoprotein, and is endocytosed into the host cell via clathrin-mediated endocytosis.[214] Once inside the host cell, the encapsulated virion must undergo acidification in order to unencapsulate.[214] The reduction in pH activates the viral M2 ion channel protein, facilitating the flow of protons

into the interior of the endosome, further lowering the pH.[214] This acidification allows it to unencapsulate from the vesicle formed during endocytosis by fusing the viral envelope with the endosome membrane and facilitating the uncoating process.[214] From there, the viral genome is released into the host cell cytoplasm, can enter the nucleus, replicate, and be packaged for export.[214]

The cellular vacuolar-type H^+ ATPase (V-ATPase) pump, located within almost all cellular membranes, including endosomes, intracellular compartments, and the plasma membrane, has been identified as a facilitator of influenza viral entry by maintaining the acidic pH within endosomes which is required for the aforementioned viral release.[202, 215] By coupling ATP hydrolysis to the transport of protons from the cytoplasm into the lumen of an endosome, the V-ATPase pumps acidify the interior of an endosome.[202] Adamson et al has shown that inhibition of the V-ATPase pump inhibits influenza viral infection, and that overexpression of particular subunits of the pumps increase viral replication.[215] Further, the V-ATPase pump is ATP-dependent, and glucose has been shown to stimulate V-ATPase activity in MDCK and A549 cells via activation of ERK and PI3K.[216] Conversely, reduced ATP levels are associated with pump disassembly.[217]

In vitro, Kohio et al demonstrated that when MDCK cells are grown in high levels of glucose (4-6mg/ml) they possess a significantly higher viral titer than cells grown in a normal level of glucose (1-2mg/ml).[202] Furthermore, this same group went on to demonstrate that when cells were treated with glycolytic inhibitors prior to viral infection, viral replication was blunted, indicating a reliance on the host cell access to glucose and a working glucose metabolism in order to replicate.[202] When cells which are bathed with glycolytic inhibitors are then treated directly with exogenous ATP, viral

replication is again increased in accordance with the amount of ATP added.[202] This group then stained the infected cells to understand the acidic or basic staining intensities, and determined that cells grown in high glucose have more acidic compartments than those grown in low glucose.[202] Similarly, cells grown in high glucose, or in low glucose but with ATP added to the media possessed a significant stimulation of the assembly of the V-ATPase pump due to localization of the pump subunits on intracellular compartment membranes.[202] This assembly and localization appears to be dependent on glycolysis.[202]

While this research has been instrumental in identifying the glucose-dependent host cell interactions with the influenza virus, to our knowledge, these interactions have not been identified in non-cancerous human bronchial epithelial cells, or in any manner involving an *in vivo* mammal model.

CHAPTER III

PROLONGED HYPERINSULINEMIA AFFECTS METABOLIC SIGNAL TRANSDUCTION MARKERS IN A TISSUE SPECIFIC MANNER

Allison Campolo, Melody de Laat, Lauren Keith, Kaylynn J. Gruntmeir, and Veronique Lacombe

Published April 1, 2016

Abstract

Insulin dysregulation is common in horses, although the mechanisms of metabolic dysfunction are poorly understood. We hypothesized that expression of proteins involved in the downstream insulin signaling and glucose transport pathways will be altered during prolonged hyperinsulinemia-induced laminitis. Archived tissue samples from horses treated with a prolonged, euglycemic hyperinsulinemic clamp for 48 hours, or a balanced electrolyte solution were used. All treated horses developed marked hyperinsulinemia and clinical laminitis. Protein expression was compared across tissue sites for the insulin (InsR) and insulin-like growth factor-1 (IGF-1R) receptors by Western blotting. Gene expression of key proteins involved in the insulin signaling pathway was evaluated in striated muscle and lamellar samples using real-time reverse transcription PCR with primers selected for insulin receptor substrate-1 (IRS-1), AKT-2, and glycogen synthase kinase beta (GSK-3β). Gene expression of the basal glucose transporter 1 (GLUT-1) and the insulin-sensitive GLUT-4 was evaluated using RT-PCR. Lamellar tissue contained significantly more IGF-1R protein than skeletal muscle, indicating the potential significance of IGF-1R signaling for this tissue. Expression of the selected markers of insulin signaling and glucose transport in skeletal muscle and lamellar tissue were unaffected by marked hyperinsulinemia. This data supports that insulin resistance in the horse is not required for laminitis onset. In contrast, the significant up-regulation of AKT-2, GSK-3β, GLUT-1 and GLUT-4 expression in cardiac tissue suggested that the prolonged hyperinsulinemia induced an increase in insulin sensitivity, as well as a transcriptional activation of glucose transport. Responses to insulin are tissue-specific and extrapolation of data across tissue sites is inappropriate.

Keywords: Insulin signaling; equine metabolic syndrome; insulin; glucose transporter; horse

Introduction

Hyperinsulinemia and insulin dysregulation are becoming as problematic for horses as they are for other species [218, 219]. Unfortunately, data on insulin signaling and the mechanisms of insulin resistance (IR) in this species are scarce [220, 221]. Contrary to other mammals, where cardiovascular risks predominate, the key pathologic outcome of hyperinsulinemia in horses is laminitis, a painful separation of the dermo-epidermal basement membrane situated between the pedal bone and inner hoof wall [222, 223]. However, a mechanistic link between these conditions has not been established. In addition, the cardiovascular consequences of hyperinsulinemia have barely been investigated in the horse, so the existence of insulin-associated cardiovascular pathology cannot be excluded in this species [45].

Insulin is a natural ligand for the insulin receptor (InsR), the insulin-like growth factor-1 receptor (IGF-1R) and a hybrid version of these receptors [224]. Receptor binding affinity varies with the specificity of insulin for each receptor (strongest for InsR), with all receptors able to be bound at supraphysiological insulin concentrations [225, 226]. Ligand-receptor interaction results in phosphorylation of insulin-receptor substrate-1 (IRS-1), which is an activating factor for both the mitogen-activated protein kinase (MAPK) and phosphatidylinositol-3'-kinase (PI3K) intracellular signaling cascades [227-229]. Initiation of MAPK regulates cell differentiation and fate, while PI3K signaling is integral in metabolic regulation [228]. Increased PI3K levels activate the pivotal serine/threonine protein kinase, namely, Akt. This signal transduction cascade promotes glucose transport via GLUT4 translocation from an intracellular inactive pool to the cell surface in insulin-sensitive tissues, including cardiac and skeletal muscle [227, 228]. Impaired insulin signaling during IR has been linked to impaired tyrosine phosphorylation of IRS-1 and inhibition of the

downstream glucose regulatory pathway [219]. Further, the regulation of insulin action by PI3K is thought to be partially mediated through inhibition of glycogen synthase kinase-3 (GSK-3), a protein kinase central to metabolic regulation. Two isoforms of GSK-3 exist, with GSK-3β intrinsic to metabolic regulation [230].

We recently demonstrated that prolonged hyperinsulinemia altered glucose transport in insulin-sensitive tissue and the digital lamellae. However, the underlying pathways modulating glucose transport, including its transcriptional regulation, were not elucidated. We hypothesized that the gene expression of downstream insulin signaling and glucose transport pathways will be altered during hyperinsulinemia-induced laminitis. Therefore, the aims of this study were twofold. Firstly, to compare expression of both the InsR and IGF-1R in striated muscles (cardiac and skeletal) and the lamellae in healthy horses. Secondly, we aimed to quantify gene expression of the downstream metabolic effector proteins; IRS-1, AKT2 and GSK-3β, and glucose transporters (basal GLUT1 and insulin-dependent GLUT4), during both normo- and hyperinsulinemic states.

Materials and Methods

Samples

Healthy Standardbred horses received either a prolonged, euglycemic hyperinsulinemic clamp to induce persistent marked hyperinsulinemia, or a balanced electrolyte solution (normo-insulinemia, n = 4 per group), prior to euthanasia and tissue collection after 46 ± 2.3 hours, as

previously described [198]. Archived samples of cardiac and skeletal muscle and lamellar tissue were obtained for the current study. Serum samples were collected throughout the infusions (every 30 min) to enable retrospective measurement of insulin concentration with a validated immunoassay (Siemens) and confirm hyperinsulinemia (1036 ± 129 μIU/mL) or normo-insulinemia (10 ± 0.9 μIU/mL) in the subjects. All horses maintained normoglycemia throughout the clamp (5.90 ± 0.68 and 5.05 ± 0.56 mmol/L at the end of the 46 hours insulin perfusion in control and treated horses, respectively). All hyperinsulinemic subjects developed laminitis as a consequence of the infusion, while the control group did not [198]. Following the clamp, cardiac (left ventricular) and skeletal (mid-gluteal) muscle and lamellar tissue (dorsal mid-section of left front hoof) was collected from all horses (5 mm^3), immediately frozen in liquid nitrogen and transferred to -80°C until analysed.

Protein extraction and quantification

Crude membrane fractions were extracted from each frozen tissue sample (50 mg) by being pulverised in buffer (210 mM sucrose, 40 mM NaCl, 2 mM EGTA, 30 mM Hepes with a protease inhibitor cocktail) on ice (2 x 15 s) as previously described [221]. Cells were lysed (1.2 M KCl) prior to ultra-centrifugation at 100,000 x *g* for 90 min at 4°C. The pellet was re-suspended in buffer (1 mM EDTA, 10 mM Tris HCl containing 0.33% vol 16% SDS) and centrifuged for a further 45 min at 3,000 x *g* (18°C). Protein concentration was quantitated with the bicinchoninic acid (BCA) protein assay kit (Pierce, IL) in triplicate (intra-assay CV = 1.9%). Absorbance at 562 nm was measured on a microplate reader (BioTek, VT).

Western immunoblotting

The primary antibodies for InsR and IGF-1R were selected based on their protein sequence homology with Equus caballus (> 89%), predicted species reactivity, molecular weight and apparent lack of cross reactivity for the opposing receptor (i.e., IGF-1R when analysing InsR). All antibodies were subject to initial optimisation studies and validated against a positive control (mouse liver). Given that different tissues were loaded on one gel, an internal control for equal protein loading was not included. Protein (25 µg/sample) was resolved on a 12% SDS polyacrylamide gel and then electrophoretically transferred to a polyvinylidene fluoride membrane (Millipore, MA) with subsequent immunoblotting. Membranes were incubated with the primary antibody: InsR; 1:500 (Abcam, MA), IGF-1R; 1:500 (Cell Signaling Technology, MA) at 4°C for 16 h, followed by incubation with an appropriate secondary antibody (1 h at room temperature) conjugated to horseradish peroxidase. Protein content was assessed by enhanced chemiluminescence reaction (KPL, MD) and quantified using a Gel-Pro Analyzer blot scanning and analysis system (Media Cybernetics, MD).

RNA isolation and cDNA synthesis

Frozen samples (50-80 mg) of cardiac and skeletal muscle and lamellae were pulverised in 1mL of Trizol reagent (Invitrogen, CA) according to the manufacturer's instructions. RNA was quantified using Gen5 software with Biotek synergy HT hardware using a take3 plate (BioTek, VT) and DNAse treated using the Ambion DNA-free DNA removal kit (Ambion AM1906M). DNAse-treated RNA was then converted to cDNA using the High Capacity cDNA Reverse

Transcription Kit and random primers (Applied Biosystems, CA, USA) according to manufacturer's recommendations and stored at -80°C until analysis.

Quantitative, real-time-PCR analyses (qRT-PCR)

The qRT-PCR assays for relative quantification of IRS-1, AKT2, GSK-3β, GLUT1 and GLUT4 in the tissue samples were performed using SYBR Green Real Time PCR Master Mix containing AmpliTaq Gold DNA Polymerase, to minimize nonspecific product formation, and dNTPs with dUTP, to reduce carryover contamination (Applied Biosystems, CA). The PCR primer sets for target genes and the house-keeping gene β-actin are shown in Table 1. Primer sequences were identified using NCBI BLAST and custom synthesized by Invitrogen (GenBank accession numbers: β-actin: NM001081838; IRS-1: XM001915475; AKT2: NC009153; GSK-3β: NC009171; GLUT1: DQ139875 and GLUT4: AF531753).

Each PCR reaction (20µl) contained 2x reaction buffer (SYBR Green I dye, Amplitaq Gold DNA Polymerase, dNTPS with dUTP, passive reference, and optimized buffer components), forward and reverse primers (0.5 mM), 0.5 µg of cDNA, and DNase-RNase-free water. The exact primer concentrations and PCR conditions were determined during initial optimisation runs (Table 1). Samples were run in duplicate in a 96-well MicroAmp optical plate (Invitrogen, CA). Quantitative RT-PCR was performed in an ABI 7500 Fast instrument (Applied Biosystems, CA) with the following cycling conditions: 10 min at 95˚C, followed by 40 cycles at 95˚C for 15 sec and 60˚C for 1 minute. No-template controls using water instead of cDNA templates were included for each gene as negative controls. A melting curve was generated to ensure product

purity and the absence of primer dimers. The mRNA expression of the genes of interest was normalized to β-actin and relative gene expression was quantified using the ΔΔCT method [231].

Statistical analyses

Due to non-normally distributed data (Shapiro-Wilk) for the InsR, the comparison of protein content across tissue sites was performed with a one-way ANOVA on ranks. Quantitative RT-PCR data were generated using relative quantification. The difference in CT between the target and reference gene (ΔCT) was determined by subtracting the CT of the target gene from that of β-actin for each horse for each tissue. Relative quantification was analysed using two-tailed Student t-tests. All data are expressed as mean ± se or median (interquartile range) and significance was accepted at $P < 0.05$. Statistical analyses were performed using SigmaPlot v. 12.5.

Results

Given that the distribution of InsR and IGF-1R across major active metabolic tissues has not been reported in horses, we first quantified these proteins in striated muscle and digital lamellae. The presence of the InsR and the IGF-1R receptors was confirmed in all tissues collected from normo-insulinemic horses by Western immunoblotting (Fig. 1). Crude membrane protein extracts of cardiac and skeletal muscle and lamellae expressed the InsR in equal amounts. By comparison, lamellar IGF-1R expression was significantly greater in lamellar tissue than in striated muscles.

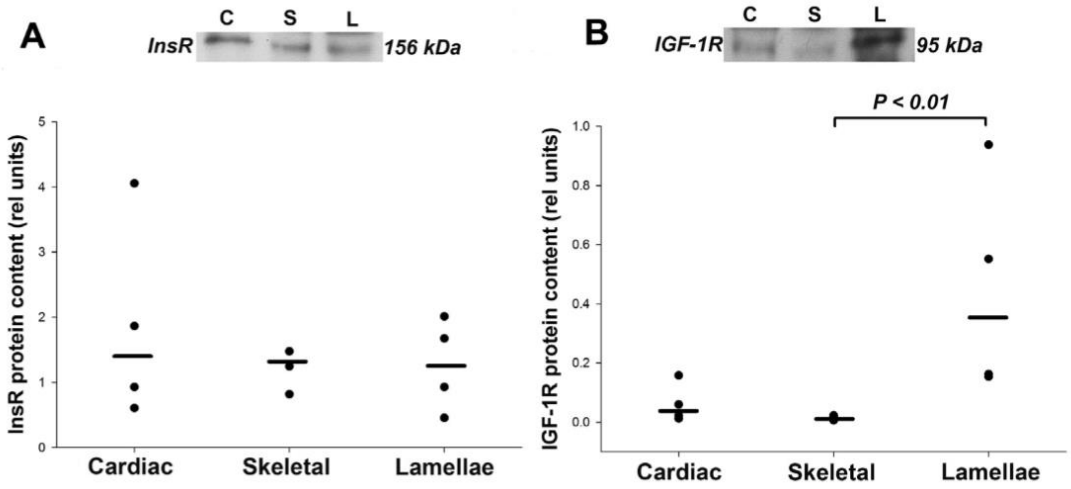

Fig.1. Protein expression of insulin receptor (InsR) and insulin-like growth factor 1 receptor (IGF-1R) was compared in crude membrane fractions of cardiac (C) and skeletal (S) muscle, and lamellae (L) from 4 healthy horses. Results are shown by representative Western blot (above) and scatter plots with median bar (below). (A) InsR protein content did not differ between tissue types. (B) IGF-1R protein expression was less ($P < 0.01$) in skeletal muscle compared with the lamellae.

Gene expression of the downstream signaling proteins and major GLUT isoforms was subsequently examined in all tissues with qRT-PCR. The mRNA expression of three metabolic signal transduction markers of the PI3K pathway (i.e., IRS-1, AKT2 and GSK-3β) did not differ between normo- and hyperinsulinemic horses in skeletal muscle (Fig. 2). In contrast, AKT2 and GSK-3β, but not IRS-1, were increased during hyperinsulinemia in left ventricular cardiac muscle compared to normo-insulinemic horses. The lamellar tissue did not demonstrate a significant difference in mRNA expression of IRS-1, AKT2 and GSK-3β between hyperinsulinemic and control horses. However, a trend for a decrease in mRNA expression of IRS-1($P = 0.085$) and AKT2 ($P = 0.063$) was detected in hyperinsulinemic horses.

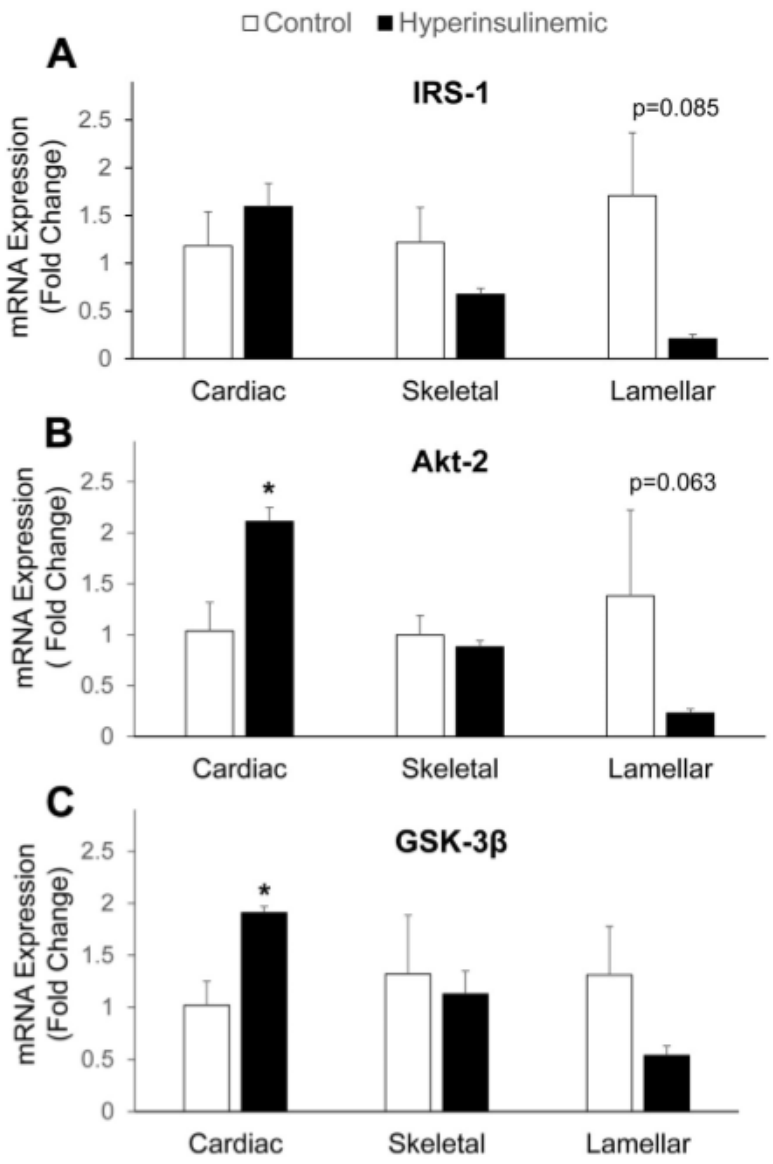

Fig. 2. Mean fold change in messenger RNA (mRNA) expression of insulinsignaling markers (IRS-1, Akt2, and GSK-3b) in striated muscle and lamellar tissue from healthy and hyperinsulinemic horses. (A) IRS-1 expression did not differ between groups in striated muscle but trended (P ¼ 0.085) toward a decrease in lamellar tissue from hyperinsulinemic horses. Akt2 (B) and GSK-3b (C) expressions were increased (*P < 0.05) in cardiac but not in skeletal muscle.

Insulin-independent lamellar tissue showed a trend (P ¼ 0.063) toward decreased Akt2 expression during hyperinsulinemia.

Cardiac muscle mRNA expression of GLUT1, the major basal isoform, and GLUT4, the major insulin-dependent isoform, was increased as a result of hyperinsulinemia compared to normo-insulinemic horses (Fig. 3). Conversely, GLUT1 gene expression showed a trend (P = 0.083) towards being increased in lamellar tissue of hyperinsulinaemic horses, while GLUT4 was unaffected by treatment. Further, skeletal muscle mRNA expression of both GLUTs was also unaffected by prolonged insulin infusion.

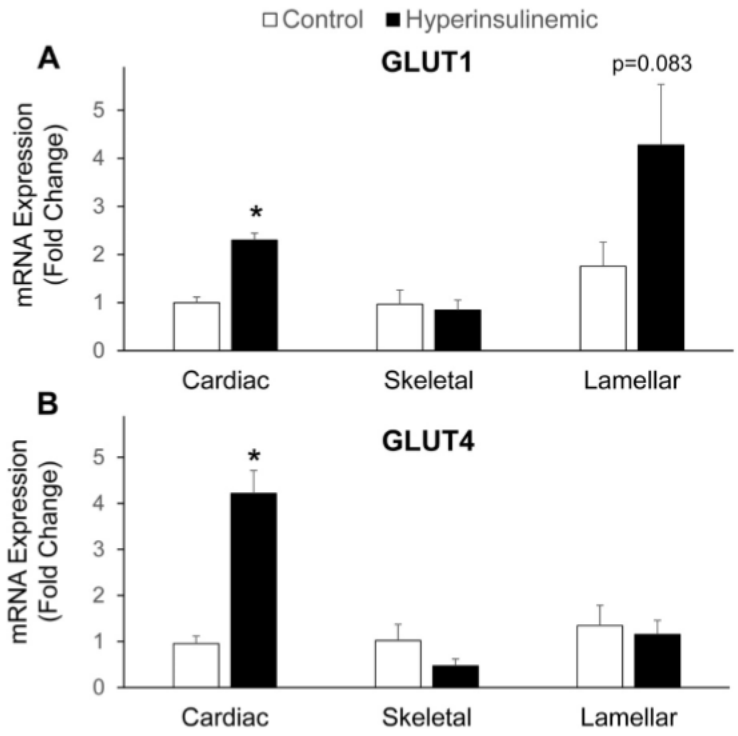

Fig. 3. Mean fold change in messenger RNA (mRNA) expression of glucose transporter (GLUT) 1 (basal isoform) and GLUT4 (insulin-dependent isoform) in striated muscle and lamellar tissue from healthy and hyperinsulinemic horses. Both GLUT1 (A) and GLUT4 (B) expressions were increased (*P < 0.05) incardiac, but notskeletal, muscle ofhyperinsulinemic horses. Insulin-independent lamellar tissue showed a trend (P ¼ 0.083) for an increasein GLUT1, but notGLUT4, expression in hyperinsulinemic horses.

Discussion

Investigations into insulin signaling in the equine species have the power to be instructive for treatment and prevention of both metabolic diseases and their sequelae. Using a unique equine model of prolonged hyperinsulinemia-induced laminitis, this study provided novel insights into metabolic regulation in both insulin-dependent (e.g., striated muscle) and insulin-independent tissues (e.g., lamellae). Interestingly, cardiac muscle responded to marked hyperinsulinemia with increased insulin signaling marker and GLUT expression, a finding in opposition to skeletal muscle, where no changes were seen. Further, while lamellar tissue was also unaffected by the marked hyperinsulinemia, there was a trend for suppression of insulin signaling, which is consistent with previously reported InsR/IGF-1R down-regulation during hyperinsulinemia [232]. The discrepant findings for tissue groups in this study underscore the fact that one should not extrapolate results from one tissue type to another in experimental models and/or disease states.

To our knowledge, this is the first report of comparative protein content of the InsR and IGF-1R, across striated muscle and lamellae in horses. Equal protein expression of the InsR and IGF-1R in striated muscle is consistent with the insulin-dependent nature of these tissues. Lamellae expression of both receptors is consistent with other studies that report the presence of these receptors [233-235]. Interestingly, lamellar tissue expressed significantly more IGF-1R protein than skeletal muscle. This finding supports the hypothesis that IGF-1R activation and signaling may be

significant in this tissue, with potential for being a pathogenic mechanism of insulin-associated laminitis [232, 236].

The heart is not only an insulin-sensitive tissue, but has a substantially greater requirement for energy to sustain the high contractility rate compared to skeletal muscle [237]. During periods of enhanced insulin availability, glucose utilisation by the heart increases, with glucose being the favoured substrate [237]. Accordingly, our data revealed an increase in insulin-sensitive glucose uptake in the cardiac tissue during hyperinsulinemia. The marked increase in circulating insulin lead to an increase in gene expression of AKT2 and GSK-3β, as well as both the basal (GLUT1) and insulin-dependent (GLUT4) glucose transporters. In the heart, insulin is a potent stimulator of AKT2 [238], which in turn activates the translocation of GLUT4 from intracellular inactive pool to cell surface to enhance glucose uptake. The upregulated cardiac (metabolic) insulin signaling and GLUT4 expression in the current study was consistent with these phenomena [237]. In addition, hyperinsulinemia may promote glycogen synthesis in the myocardium by activating GSK-3β gene expression. In addition to the regulation of glycogen synthase, protein translation and negative regulation of cardiac hypertrophy are also functions of GSK-3 [237]. Therefore, given the multi-functional nature of this kinase it may be difficult to interpret the increase in cardiac gene expression of GSK-3β in the current study. Interestingly, studies have shown that the action of GSK-3β, which was unchanged between groups in both striated muscle and lamellar tissue, is tissue specific in humans [239]. Overall, these data suggest that the prolonged, euglycaemia hyperinsulinaemic clamp induced an increase in insulin sensitivity in the heart, as well as a transcriptional activation of glucose transport and utilization.

In contrast, prolonged and marked hyperinsulinemia did not induce a transcriptional activation of the insulin signaling and glucose transport pathways in equine skeletal muscle. Similarly, a previous study has reported that crude membrane protein expression of GLUT4 in skeletal muscle was not affected by marked hyperinsulinemia [44]. In contrast, skeletal muscle GLUT4 translocation was decreased in horses with compensated IR (that had normal circulating insulin concentrations), a finding consistent with mechanisms underlying IR in other species [219, 240]. Collectively, these findings suggest that prolonged euglycemic hyperinsulinemic clamp does not induce peripheral IR. In addition, the current findings support that IR in insulin-sensitive tissues is not a prerequisite for laminitis onset. Regardless, understanding the pathophysiological mechanisms during prolonged hyperinsulinemia could provide novel insight into the understanding of metabolic dysfunction as hyperinsulinemia can precede the development of IR and diabetes in other species [241].

The lamellae, which are principally an epithelial tissue, have been reported to be insulin-independent [199]. However, lamellar tissue is significantly vascularised [242], with vascular endothelial cells a likely reservoir of both InsRs and GLUTs. The current study indicated a trend for down-regulation of AKT2 and GSK-3β during marked hyperinsulinemia in this tissue, which may have occurred as a result of down-regulation of both the InsR and IGF-1R [232]. However, further investigation into whether dampened insulin signaling downstream of IRS-1 and AKT2 affects both the PI3K and MAPK pathways, is required. Investigations of the phosphorylation state of substrates from both pathways, and unravelling their role in mitosis, metabolism and insulin action, could reveal mechanistic insights into the consequences of insulin dysregulation. Failure of GLUT4 gene expression to be affected by prolonged and marked hypersulinemia, suggest that insulin either does not affect the regulation of glucose transport in lamellar tissue, or that it is not a crucial pathway for glucose uptake [243]. Interestingly, GLUT4 gene expression

parallels GLUT4 protein expression in lamellae and striated muscle, which suggests that GLUT4 is transcriptionally regulated. In contrast, GLUT1 gene expression in the current study was not consistent with reported GLUT1 protein expression following prolonged insulin infusion, which may suggest that this basal GLUT is not transcriptionally regulated.

In conclusion, our data support the concept that IR in insulin-sensitive tissues is not a prerequisite for laminitis onset. In addition, responses to insulin are tissue-specific in the horse. Insulin signaling and glucose transporter expression differs between muscle groups and also the digital lamellae during prolonged and marked hyperinsulinemia. Further studies that investigate activation/phosphorylation of both the MAPK and PI3K pathways during insulin dysregulation in horses will aid our understanding of metabolic disease in this domestic species.

Acknowledgements

Technical assistance from Chelsea Clement at Oklahoma State University was greatly appreciated. The involvement of Dr. Melody De Laat, Professors' Christopher Pollitt, Martin Sillence and Catherine McGowan in the study from which the tissue was granted is acknowledged.

CHAPTER IV

DIFFERENTIAL PROTEOMIC EXPRESSION OF EQUINE CARDIAC AND LAMELLAR TISSUE DURING INSULIN-INDUCED LAMINITIS

Abstract

The incidence of Equine Metabolic Syndrome in Western countries has steadily escalated alongside equine obesity rates, and unfortunately the occurrence of endocrinopathic laminitis has risen with them. Despite extensive research, laminitis remains without an effective treatment, and its pathogenesis remains obscure. Endocrinopathic laminitis, similar to the multi-organ dysfunction and peripheral neuropathy found in human with metabolic syndrome, has been shown to at least partially the result of vascular dysfunction. Here, we sought to identify novel proteins and pathways which may be significantly impacting the development of this disease using proteomic analysis. Healthy Standardbred horses (n=4/group) were either given an electrolyte infusion, or a 48-hour euglycemic-hyperinsulinemic clamp. All hyperinsulinemic horses developed laminitis despite being previously healthy. Cardiac and lamellar tissues were analyzed by mass spectrometry (FDR=0.05). We identified 538 and 737 unique proteins in the cardiac and lamellar proteomes, respectively. In the lamellar tissue, we identified 14 proteins which were significantly upregulated and 13 proteins which were significantly downregulated in the hyperinsulinemic group as compared to controls. These results were confirmed via real-time reverse-transcriptase PCR. A STRING analysis of protein-protein interactions identified that these upregulated proteins were primarily involved in coagulation and complement cascades, platelet activity, and ribosomal function. In contrast, the downregulated proteins were involved in focal adhesions, spliceosomes, and cell-cell matrices. No proteins were found to be significantly differentially expressed in the heart of hyperinsulinemic horses compared to controls. These data indicate that while hyperinsulinemia induced, in part, microvascular damage, complement activation, and

ribosomal dysfunction in the lamellae, a similar effect was not seen in the heart. Novel proteins which were found in these significant differentially expressed groups which have not been previously associated with endocrinopathic laminitis include talin-1, vinculin, cadherin-13, fibrinogen, alpha-2-macroglobulin, and heat shock protein 90. Together, these newly identified mechanisms underlying hypersinulinemic endocrinopathic laminitis may contribute to novel therapeutic targets.

Keywords: laminitis, endocrinopathic, proteomic, equine metabolic syndrome, heart, lamellar, vascular

Introduction

Alongside their human counterparts, the incidence of metabolic syndrome and obesity in horses has been steadily rising. Recent studies find that 32% of surveyed horses in the United States are over condition, and 19% are clinically obese, which is a much higher prevalence than previously thought.[185] Accordingly, the frequency of laminitis is estimated to be as high as 34% in populations of horses in Western countries.[186] Importantly, there is still no known cure for laminitis after its onset,[99] and though research has outlined firm recommendations for avoiding the inception of this condition, there is still a vast knowledge base yet to be elucidated regarding both its cure and its prevention.

Similar to peripheral neuropathy in human patients with metabolic syndrome, endocrinopathic laminitis has been linked to vascular dysfunction.[194, 244] While some progress has been made in the endeavor of understanding the metabolic and inflammatory pathways,[99, 130, 186] epithelial cell signaling,[187] the stability of lamellar integrins,[188, 189] and many other biological mechanisms contributing to endocrinopathic laminitis in a top-down approach, the mechanisms for the observed changes occurring during the laminitic episode remain unknown. Here, we find that a modern bottom-up approach of proteomic analyses during insulin-induced laminitis has provided valuable information regarding potential effectors of endocrinopathic laminitis.

Methods

Animal Model

The following experimental protocols were approved by the Oklahoma State University Institutional Animal Care and Use Committee. Healthy Standardbred horses (n = 4/group) received either a prolonged insulin infusion (6 mIU/kg/min) for 46 ± 2.3 h to induce marked hyperinsulinemia (mean serum insulin, 1036 ± 129 μIU/mL) or a balanced electrolyte solution infused at the same rate (mean serum insulin, 10 ± 0.9 μIU/mL) as previously described.[245] Euglycemia (5 ± 1 mM) was maintained during the insulin infusion with a variable rate glucose infusion (mean blood glucose at endpoint, 5.05 ± 0.56 and 5.90 ± 0.68 mM in treated and control horses, respectively). Despite being previously healthy, all hyperinsulinemic horses developed laminitis, whereas the control group did not. Archived samples of cardiac (left ventricular) and lamellar tissue (dorsal midsection of left front hoof) that had been collected and snap frozen on euthanasia (after infusion) were obtained from all horses (5 mm^3) for the present study.

Proteomic Analysis

Tissues were homogenized in tissue lysis buffer (1:500 dilution of RIPA and protease inhibitor cocktail), and protein content was quantified by bicinchoninic assay, as previously described.[68] Samples were then analyzed via an Orbitrap mass spectrometer in triplicate. Proteins were identified through Max Quant and then the LFQ intensity was analyzed by using the Perseus software (Max Planck Institute of Biochemistry).[246]

Protein IDs were verified in UniProt, and protein-protein interactions and KEGG pathways were identified via STRING.

Quantitative real-time polymerase chain reaction analyses (qRT-PCR)

Frozen samples (50–80 mg) were pulverized using Trizol reagent (Invitrogen, CA, USA) according to the manufacturer's instructions and RNA quantified using Gen5 software with Biotek synergy HT hardware on a take3 plate (BioTek, VT, USA). DNAse-treated RNA (Ambion AM1906M) was then converted to complementary DNA using the High Capacity cDNA Reverse Transcription Kit and random primers (Applied Biosystems, CA, USA) according to manufacturer's recommendations and stored at −80°C until analysis. The qRT-PCR assays for relative quantification of IRS-1, Akt2, GSK-3β, GLUT1, and GLUT4 were performed using SYBR Green Real Time PCR Master Mix containing AmpliTaq Gold DNA Polymerase, to minimize nonspecific product formation, and deoxyribose nucleotide triphosphates with deoxyribose uridine triphosphate, to reduce carryover contamination (Applied Biosystems). Primer sequences were identified using the National Center for Biotechnology Information Basic Local Alignment Search Tool and custom synthesized by Invitrogen (GenBank accession numbers: β-actin: NM001081838; IRS-1: XM001915475; Akt2: NC009153; GSK-3β: NC009171; GLUT1: DQ139875; and GLUT4: AF531753). Each PCR reaction (20 μL) contained 2x reaction buffer (SYBR Green I dye, Amplitaq Gold DNA Polymerase, deoxyribose nucleotide triphosphates with deoxyribose uridine triphosphate, passive reference, and optimized buffer components), forward and reverse primers (0.5 mM), 0.5

μg of complementary DNA, and DNase-RNase-free water. Primer concentrations and PCR conditions were determined during initial optimization runs. Samples were run in duplicate in a 96-well MicroAmp optical plate (Invitrogen). qRT-PCR was performed in an ABI 7500 Fast instrument (Applied Biosystems) with the following cycling conditions: 10 min at 95°C, followed by 40 cycles at 95°C for 15 s and 60°C for 1 min. No-template, negative controls were included for each gene. A melting curve was generated to ensure product purity and the absence of primer dimers. The messenger RNA (mRNA) expression of target genes was normalized to β-actin, and relative gene expression was quantified using the ΔΔCT method.[247]

Statistical analyses

The proteomic data was evenly distributed based on histogram visualization after analyzation of LFQ intensity. To determine significance of LFQ intensity, the false discovery rate (FDR<0.05) was used. qRT-PCR data were generated using relative quantification, which was analyzed using 2-tailed Student *t* tests. All data were expressed as mean ± standard error of the mean or median (interquartile range), and significance was accepted at $P < 0.05$.

Results

Experimental design for examining equine metabolic syndrome

Healthy horses were treated with an intravenous electrolyte solution (control) or glucose and insulin infusion (hyperinsulinemic, treated) for 48 hours. Cardiac and lamellar

samples were collected and total lysates were extracted for mass spectrometry or RNA was extracted for real-time reverse transcriptase PCR (**Figure 1**). Mass spectrometry data was analyzed via LFQ intensity. All LFQ data for all tissues were normally distributed.

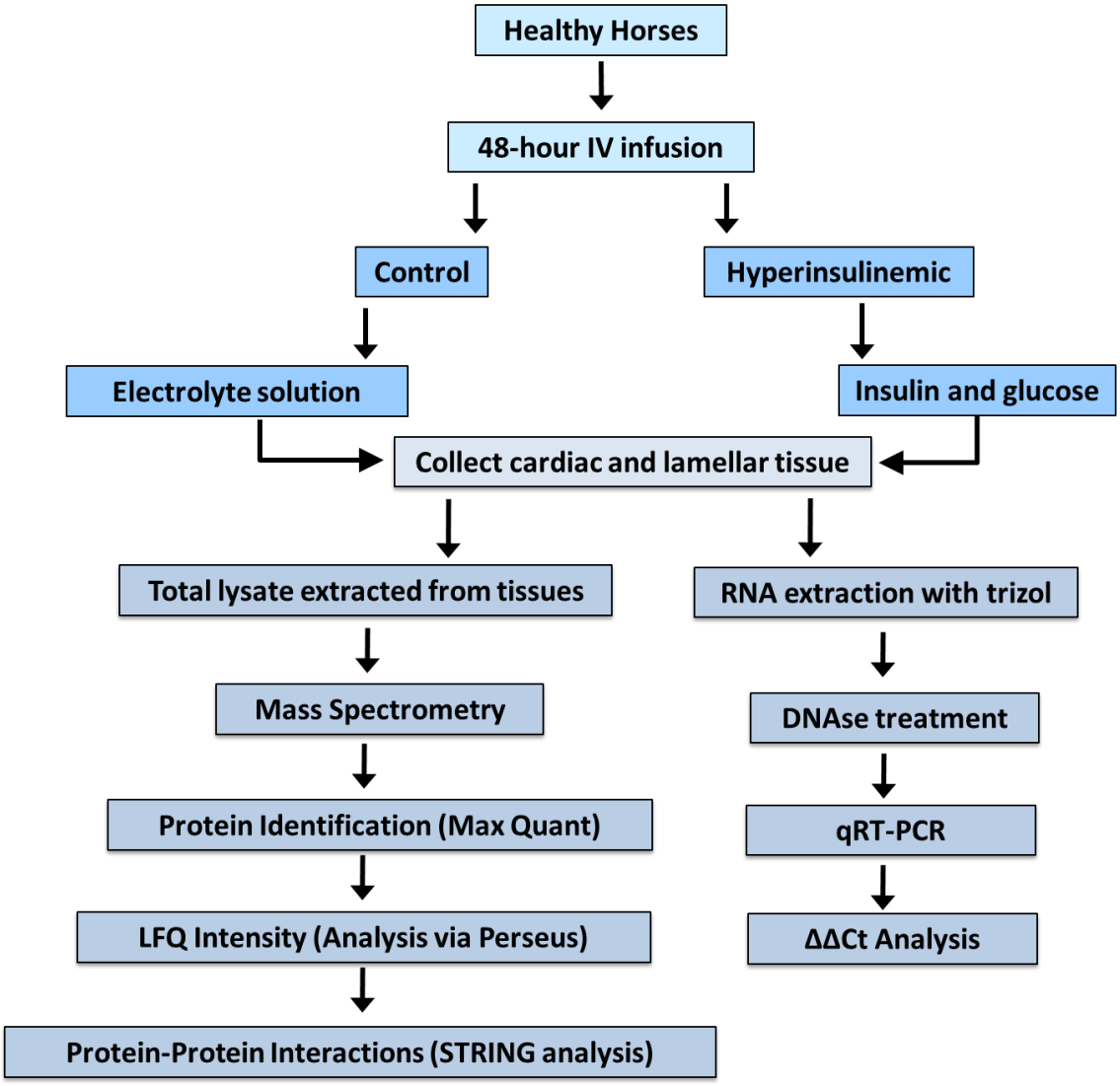

Figure 1. Work flow for proteomic analysis of tissues from hyperinsulinemic horses and real-time reverse-transcriptase analysis.

Significantly differentially expressed proteins

We detected 538 and 737 unique proteins in the cardiac and lamellar proteomes, respectively. We did not identify any proteins which were significantly differentially expressed between the control and treatment groups in the cardiac tissue, but we did identify 27 proteins which were significantly differentially expressed between groups in the lamellar tissue (**Figure 2).** We detected 14 proteins which were significantly downregulated in the treatment group (**Table 1**), and 13 proteins which were significantly upregulated in the treatment group (**Table 2**) (FDR<0.05).

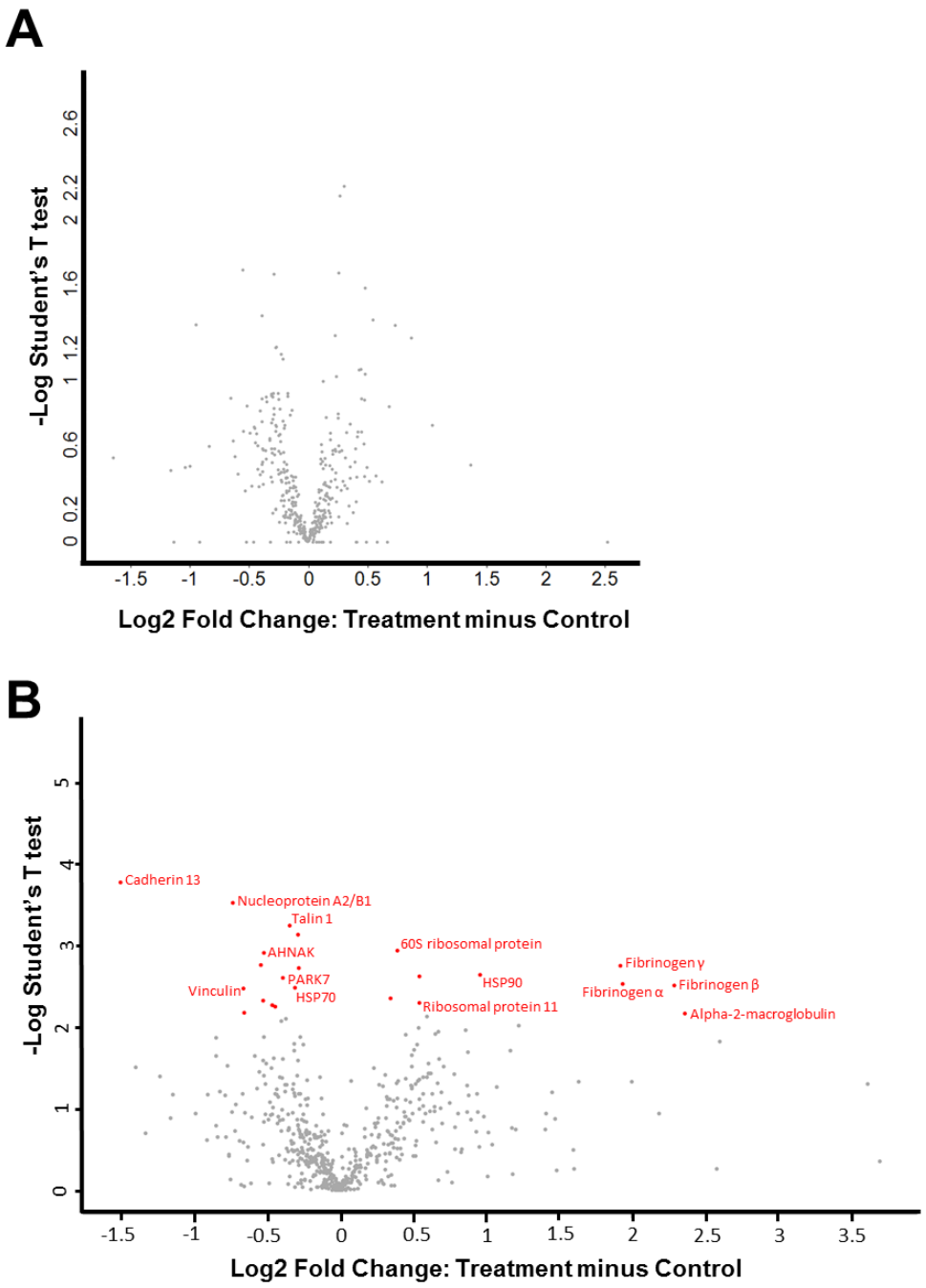

Figure 2. Volcano plots of **(A)** cardiac tissue and **(B)** lamellar tissue of control and hyperinsulinemic horses. Significance was determined using an FDR of 0.05. Significantly differentially expressed proteins are identified in red, and with the corresponding protein ID. n=4/group.

Accession number	Uniprot protein name (Gene name)	P value	Fold Change (Control-Treatment)
F6UGL6	Polypyrimidine tract binding protein 1 (**PTBP1**)	0.002019	1.219790993
F6Q4Q1	Heterogeneous nuclear ribonucleoprotein K (**HNRNPK**)	0.000756	1.221161712
F7DW69	Heat shock 70kDa protein 1A (**HSPA1A**)	0.003238	1.242093026
F6QIZ4	Talin 1 (**TLN1**)	0.001012	1.271566759
F6WPB4	Parkinsonism associated deglycase (**PARK7**)	0.002167	1.312159825
F6S6S0	Uncharacterized protein (**ENSECAG00000005186**)	0.004918	1.379998183
F7AJD4	AHNAK nucleoprotein (**AHNAK**)	0.00295	1.436102875
F6SU04	Calpain 1 (**CAPN1**)	0.004443	1.438021775
F7BFT1	Peroxiredoxin 2 (**PRDX2**)	0.004032	1.441592321
F6WHS3	Heterogeneous nuclear ribonucleoprotein D (**HNRNPD**)	0.002307	1.456644949
F6ZSZ5	Vinculin (**VCL**)	0.002573	1.581565286
F6VYB1	Heterogeneous nuclear protein A2/B1 (**HNRNPA2B1**)	0.000626	1.66432501
F6VN96	Cadherin 13 (**CDH13**)	0.00036	2.839636592

Table 1. Proteins significantly downregulated in lamellar tissue of hyperinsulinemic horses.

Proteins were identified via LFQ intensity and analyzed through Perseus (FDR-0.05). Protein and gene names were derived from Uniprot KB database. Fold change is represented as control minus treatment. n=4/group.

Accession number	Uniprot protein name (Gene name)	P value	Fold Change (Control-Treatment)
H9GZN9	Immunoglobulin heavy constant mu (**IGHM**)	0.006004	0.081751537
F6RI47	Alpha-2-macroglobulin (**A2M**)	0.00102	0.164715248
F6PH38	Fibrinogen beta chain (**FGB**)	0.001653	0.204999056
H9GZU9	Uncharacterized protein (**ENSECAG00000009556**)	0.006159	0.250195495
F6RUZ6	Fibrinogen alpha chain (**FGA**)	0.001893	0.26181576
F6W2Y1	Fibrinogen gamma chain (**FGG**)	0.000808	0.264268296
Q9GKX8	Heat shock protein HSP 90-beta (**HSP90AB1**)	0.000518	0.515382508
F7AWX3	Uncharacterized protein (**ENSECAG00000022567**)	0.00454	0.628735617
F6UUS3	Eukaryotic translation elongation (**EEF2**)	0.005253	0.663524975
F6UB53	Ribosomal protein 11 (**RPL11**)	0.002958	0.687221485
A2Q127	Elongation factor 1-gamma (**EEF1G**)	0.000852	0.687535009
F6STU8	Ribosomal protein 14 (**RPL14**)	0.006072	0.688532874
F6QF58	60S ribosomal protein L6 (**ENSECAG00000017514**)	0.000682	0.762130497
F6UME7	Elongation factor 1-alpha (**EEF1A1**)	0.005522	0.787297942

Table 2. Proteins significantly upregulated in lamellar tissue of hyperinsulinemic horses.

Proteins were identified via LFQ intensity and analyzed through Perseus (FDR-0.05). Protein and gene names were derived from Uniprot KB database. Fold change is represented as control minus treatment. n=4/group.

KEGG pathways and protein-protein interactions

Of the significantly differentially expressed lamellar proteins, those upregulated in the treatment group were primarily involved in coagulation and complement cascades, platelet activation, and ribosomal function. The proteins which were significantly downregulated in the treatment group were predominately involved in focal adhesions and spliceosomes (**Figure 3**).

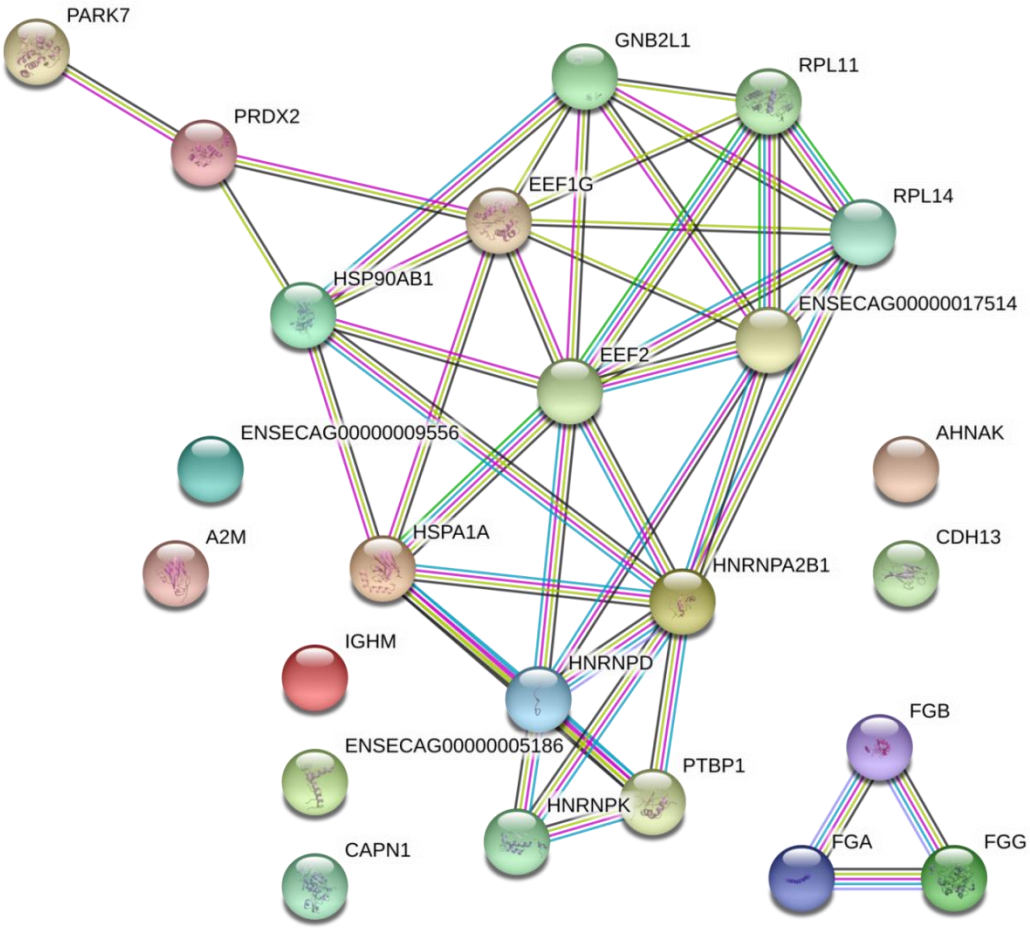

Figure 3: Protein-protein interaction analysis of significantly differentially expressed proteins in the lamellar tissue of hyperinsulinemic horses as compared to controls. Data have been elaborated and graphed using STRING 10.5. Nodes (circles) represent proteins, while edges (lines between nodes) represent protein-protein interactions. Color code for edge interactions: known interactions from: teal – curated databases, magenta – experimentally determined; predicted interactions: green – gene neighborhood, red – gene fusions, blue – gene co-occurrence; other: yellow – textmining, black – co-expression, purple – protein homology. For protein ID lists, reference accession numbers of Tables 1 and 2.

qRT-PCR

Using the proteomic data, we determined that vinculin, talin-1, and cadherin-13 were significantly downregulated in the treatment group as compared to the controls, and that heat shock protein 90, fibrinogen beta, and alpha-2-macroglobulin were significantly upregulated in the treatment group. Given the importance of these proteins in the cell-to-cell matrices and coagulation and complement response, we determined the mRNA of the corresponding genes were also significantly altered in the hyperinsulinemic horses. Using the ΔΔCT method and beta actin as the housekeeping gene, vinculin mRNA was downregulated by 84.5%, talin-1 mRNA was downregulated by 89.02%, and cadherin-13 mRNA was downregulated by 84.66% compared to controls. Similarly, HSP90 mRNA was upregulated by 85.53% (p=0.02918) fibrinogen beta was upregulated by 888.8% (p=0.3655), and alpha-2-macroglobulin was upregulated by 97.32% (p=0.1422) (**Table 3** & **Figure 4**).

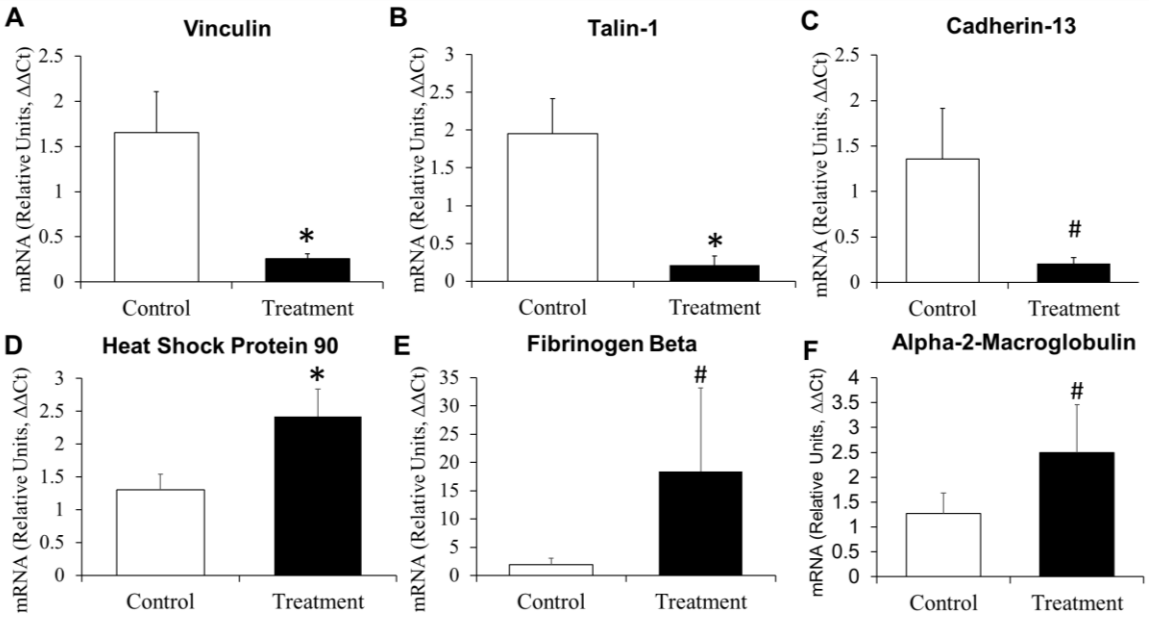

Figure 4. Mean fold change in messenger RNA (mRNA) expression of significantly differentially expressed proteins in lamellar tissue from healthy and hyperinsulinemic horses. (A) Vinculin, **(B)** Talin-1, and **(C)** Cadherin-13 were decreased in hypersinulinemic horses, while **(D)** heat shock protein 90, **(E)** fibrinogen beta, and **(F)** alpha-2-macroglobulin were increased in mRNA expression in hypersinulinemic horses compared to controls. n=4/group; * $p<0.05$ vs control, # $p<0.1$ vs control; statistical test: ΔΔCt method and two-tailed t-test.

Gene Name	Sequence (5'-3')
Beta Actin Forward	ATG ATG ATA TCG CCG CGC TC
Beta Actin Reverse	CCA CCA TCA CGC CCT GG
Vinculin Forward	GTC CAG CAA GCC GGG TAA C
Vinculin Reverse	CCG GCT GAT TGG ATG GCAT T
Cadherin-13 Forward	GCC GCG TGC ATG AAT GAA A
Cadherin-13 Reverse	TGT TAG CAT CAG CAC CTG GG
Talin-1 Forward	ATC GCA GAT ATG CTT CGG GC
Talin-1 Reverse	GGC TTC TGC AGG GTC AGT AG
Heat Shock Protein 90 Forward	CTT GAG TCA CCT CGC GCA
Heat Shock Protein 90 Reverse	CCT CAG GCA TCT TAA CGG GC
Fibrinogen Beta Forward	ATT CAG AAC CGC CAG GAT GG
Fibrinogen Beta Reverse	ATA CTC ACC TGG TAG GCC ACA
Alpha-2-Macroglobulin Forward	ACT CCA GAG GCC AGA TCC AA
Alpha-2-Macroglobulin Reverse	TGT GAG CCA GGT ATT GCC CT

Table 3. Primer Sequences
Primer sequences were designed using NCBI Blast.

Discussion

Equine endocrinopathic laminitis continues to be the most prevalent form of laminitis, presenting a debilitating disease both physically and economically which still presently has no cure.[248, 249] The current study used a wide-ranging proteomic analysis to explore potential mechanisms outside of the common steroid-, inflammation-, and insulin-related pathways explored in the literature thus far. From this analysis, we determined that, in addition to the upregulation of inflammatory markers during insulin-induced laminitis, there was a significant downregulation of key cell-cell matrix and focal adhesion proteins as well as an upregulation of HSP90. These alterations in protein expression were matched by similar alterations in mRNA levels between groups.

Proteomic analysis, the identification and quantification of a complete complement of proteins in a biological system at a point in time, is an investigative tool which has widely been used recently in human and translational medicine. However, proteomic investigation in veterinary medicine is lagging, despite its high potential for advancing veterinary pathology and diagnostics.[250] Indeed, high-throughput proteomics has emerged as the most robust technique for identifying and quantifying protein profiles from biological samples in veterinary species.[250] Most importantly, proteomic analysis allows not only for identification and quantification of specific proteins, but also for the elucidation of protein-protein interactions occurring in a biological system.[251]

Endocrinopathic laminitis is often associated either with pituitary pars intermedia dysfunction, or, more commonly, hyperinsulinemia indicative of insulin resistance.[248] Indeed, it has been previously demonstrated that a 48-hour normoglycemic hyperinsulinemic clamp in an otherwise healthy horse is sufficient to produce Obel grade

2 laminitis in all animals receiving the hyperinsulinemic clamp.[252] We have also previously described novel links to toll-like receptors and pro-inflammatory cytokines,[253, 254] alterations in striated muscle and adipose glucose transport,[70, 255, 256] and the discrepancies between insulin-sensitive tissues and the lamellar tissue[257] during equine insulin resistance and/or endocrinopathic laminitis. However, while these significant mechanisms associated with the pathogenesis of this disease have been described, identifying these mechanisms has not yet lead to substantial advances in treatment or prevention of endocrinopathic laminitis. Thus, we sought to identify new mechanisms outside of the more traditional metabolic or inflammatory pathways which could be potential therapeutic targets in the treatment of endocrinopathic laminitis.

Notably, we reported here that talin-1, vinculin, and cadherin-13, which are critically involved in cell-cell matrices and focal adhesions, are all significantly downregulated in the hyperinsulinemic group as compared to their control counterparts. Of note, these downregulations may be occurring in both the lamellar tissue itself, as well as within the vascular support of the hoof, as these three proteins are significantly involved in vessel structure and homeostasis.[258, 259] Syndecan-1, which is talin-dependent, has been found to couple with the insulin-like growth factor-1 receptor (IGF-1R)[260], which has been previously reported to be significantly higher in protein content in lamellar tissue versus cardiac or skeletal muscle,[257] and to be significantly decreased in insulin-treated horses compared to control counterparts.[261] Given the significant downregulation of talin-1 reported in this study, this finding could be related to the previously reported alterations in lamellar IGF-1R during hyperinsulinemia. Additionally, to our knowledge, vinculin

has not been reported as an underlying mechanism of hyperinsulinemia but is known to be a substrate of protein kinase C,[262] which is part of the insulin signaling pathway. Again, the significant downregulation of this protein could be intimately linked to the insulin dysregulation occurring in the lamellar tissue.

Perhaps most importantly, cadherin-13 (also known as T-cadherin) has been demonstrated to be a regulatory component of insulin signaling endothelial cells, and may in fact be a determinant of the development of endothelial insulin resistance.[263] Additionally, cadherin-13 may also modulate plasma levels of adiponectin in humans,[264] low levels of which is closely linked to a major contributor to human insulin resistance[265] and which has similarly been reported to be significantly lower in horses and ponies prior to the development of clinical laminitis.[266] Interestingly, cadherin-13 has been implicated in vascular disease and atherosclerosis[267] and others have found that cadherin-13 overexpression can promote insulin sensitivity while simultaneously reducing the ability to stimulate the Akt pathway.[268] Finally, independent of its relationship with adiponectin, cadherin-13 appears to be necessary for the release of insulin both *in vitro* and *in vivo*.[269] Taken together, it is not yet clear whether the significant downregulation of cadherin-13 reported in this study during hyperinsulinemia is a result from the hyperinsulinemic infusion or part of the larger laminitic pathogenesis resulting from larger metabolic dysregulation during the clamp. However, to our understanding, the involvement of cadherin-13 or any other focal adhesion proteins have not been previously implicated in the metabolic pathogenesis of endocrinopathic laminitis, and these may be important targets for future investigations.

We also reported here a significant upregulation of several important integrins, namely three fibrinogen isoforms (α, β, and γ) in the treatment group versus the control group. Recent reports indicate the discovery of a potential intimate connection between integrins and IGF-1R. Importantly, it has become apparent that some growth factor signaling cannot occur without specific integrin expression[270] and growth factors such as IGF-1R may act in response to specific action from integrins such as fibrinogen in a ligand-dependent manner.[271] Additionally, IGF-1R inhibition has been reported to reduce fibrinogen binding in platelets of diabetic mice, but not in healthy mice.[272] As fibrinogen is a significant participant in vascular homeostasis and tissue repair,[273] vascular dysfunction has been reported to be associated with the underlying endocrinopathy of this disease.[194] However, despite fibrinogen's well-known role in the extra cellular matrix,[274] and the extra cellular matrix's degradation during laminitis,[275-277] none of the fibrinogen isoforms have been significantly implicated in endocrinopathic laminitis without sepsis prior to this report, to our knowledge.[278] However, fibrinogen has been found to be upregulated in human diabetic patients,[279] and it has been previously postulated that platelet inhibitors could have beneficial therapeutic effect for laminitic horses, which, based on our findings here, may still be a beneficial therapy.[280]

While alpha-2-macroglobulin is a known factor in coagulation, and thus its upregulation in the hyperinsulinemic hoof could be accounted for due to the tissue damage and inflammation inherent in the obel grade 2 laminitis present in the hyperinsulinemic

horses. However, it should be noted that alpha-2-macroglobulin has previously been reported to be increased in human diabetic patients.[281] Similarly, hyperinsulinemia has been described as a hypercoagulable state, in part due to this increased thrombotic activity and the increased presence of alpha-2-macroglobulin.[282] However, to our knowledge, this plasma protein has never before described or implicated in equine metabolic syndrome. As alpha-2-macroglobulin is also capable of binding to growth factors, including insulin, this protein may be a potentially important participant in the equine metabolic syndrome disease physiology.

Finally, we found that heat shock protein 90 (HSP90) was significantly increased in the hyperinsulinemic horses compared to their control counterparts. While, to our knowledge, HSP90 has not been described in laminitic horses, the heat shock response has been found to be damaged during type 2 diabetes in humans,[283] HSP90 is higher in type 2 diabetic humans than in those with only impaired glucose tolerance,[284] and inhibition of HSP90 appears to limit renal and vascular damage in diabetic mice.[285] It is also worth noting that while laminitis is already well-associated with atherosclerotic markers, HSP90 inhibitors may reduce atherosclerosis during diabetes[286] and restore glucocorticoid sensitivity during Cushing's disease.[287] Thus, the upregulation of HSP90 in the lamellar tissue of hyperinsulinemic horses with laminitis may be a significant detrimental contributor to the disease pathogenesis, and may also be a potential target for future therapeutic responses.

In conclusion, we used a proteomic analysis of equine cardiac and lamellar tissue to determine novel effects in the pathogenesis of endocrinopathic laminitis. We determined that during hyperinsulinemia there were significant upregulations of alpha-2-macroglobulin, three fibrinogen isoforms and HSP90, and significant downregulations of several critical cell-cell matrix and focal adhesion participants, including talin-1, vinculin, and cadherin-13 as compared to control horses. These alterations indicate potentially significant vascular dysfunction which has not yet been described to this level of detail in endocrinopathic laminitis. While many of these significantly differentially expressed proteins are described in other species during type 2 diabetes and metabolic syndrome, to our knowledge this is the first time many of them have been reported in relation to endocrinopathic laminitis. Thus, these proteins may represent novel therapeutic targets for hyperinsulinemic horses and the development of laminitis.

Acknowledgements

We would like to thank Dr. Melody de Laat., Dr. Zahra Maria, Matthew Frantz, and Shanell Gray for their excellent technical assistance.

CHAPTER V

DIABETES-INDUCED ALTERATIONS OF REGULATION OF GLUCOSE TRANSPORT IN THE LUNG

Abstract

Diabetes has been identified as a significant and independent risk factor for the development or increased severity of respiratory infection. However, the protein expression of the predominant glucose transporter (GLUT) isoforms in the adult lung in both the healthy and diabetic state remains largely to be identified. We hypothesized that the GLUT isoforms of the lung would be altered during either type 1 or type 2 diabetes, and rescued with insulin or metformin treatment, respectively. Type 1 diabetes was induced via streptozotocin and rescued via subcutaneous semi-osmotic insulin pump for 8 weeks. Type 2 diabetes was induced via high-fat diet for 16 weeks, and both control and type 2 diabetic mice were treated with metformin for the second 8 weeks of the study. Total GLUT protein expression was quantified via Western blotting in homogenized adult whole lung. Pulmonary cell surface GLUT protein was measured using a biotinylated photolabeling assay from homogenized lung samples. Type 1 diabetic mice demonstrated a significant decrease of total GLUT4 and a significant increase of GLUT12 protein in the upper airways. Similarly, in the lower lung, type 1 diabetic mice also demonstrated a significant decrease of total GLUT-1 and -4, and again a significant increase of GLUT12 protein expression. These alterations were rescued following insulin treatment. Type 2 diabetic mice demonstrated a significant decrease of total GLUT-2, -4, -10, and -12 protein in the whole lung. The alterations of GLUT-2, -4, and -10, but not -12, were rescued with metformin treatment. Both type 1 and type 2 diabetic mice demonstrated significant decreases of GLUT-4 and -8 protein at the cell surface of homogenized whole lung, which were rescued with treatment. We conclude that during either type 1 or type 2 diabetes there are significant alterations of GLUT protein in the

adult lung, which were rescued with either insulin or metformin, respectively, and that these alterations in glucose homeostasis during diabetes may contribute to an increased severity of pulmonary infection during diabetes.

Keywords: diabetes, pulmonary, lungs, glucose, GLUT trafficking

Introduction

While diabetes is a relatively recent epidemic, respiratory infections like flu and pneumonia have plagued humans for millennia. However, it has only recently been determined that diabetic patients are three times more likely to die from respiratory infection as their non-diabetic counterparts,[11, 12] and that diabetic patients in particular are considered a high-risk group and should get vaccinated for flu.[288, 289] In order to address this risk factor, therapeutic targets should be identified to assist diabetic patients with concurrent respiratory infection. However, very little is known about the regulation of glucose homeostasis in the lung, and in particular which GLUT isoforms are present and active in the adult whole lung of either humans or rodents. Furthermore, how the regulation of glucose transport might be altered during the diabetic state also has yet to be fully explored.

Recent investigations *in vitro* have identified the mRNA of GLUTs 1-12 and both sodium-glucose linked transporters (SGLTs) in human bronchial epithelial cells, but have only confirmed protein of GLUT1 and GLUT10 in these same cells.[51] To our knowledge, non-cancerous human whole lung tissues have been successfully probed only for

SGLT1[290] and GLUT4 protein.[62] Similarly, non-cancerous adult rodent lung tissue has only been successfully probed for the protein of SGLT1 and SGLT2.[51] Clearly, there is a significant amount of inquiry into the functional GLUT proteins present in the adult mammalian lung.

Based on previous reports,[51, 205] we have hypothesized that GLUT-1, -2, and -10 protein expression will predominate in the lung. However, how the protein expression of pulmonary GLUTs is altered during both type 1 and type 2 diabetes has also never before been described in detail, to our knowledge. Thus, we have here investigated the protein expression of the 7 most predominant GLUTs in mammalian glucose homeostasis (GLUT-1, -2, -3, -4, -8, -10, and -12) in the lung of healthy, type 1 diabetic, and type 2 diabetic mice. Further, while some have previously speculated on the direct effect of insulin stimulation on the lung,[291] to our knowledge it remains unknown whether metabolic therapy such as insulin or metformin (for type 1 and 2 diabetic animals, respectively) will directly affect the protein expression of pulmonary glucose transporter isoforms. Therefore, we have here also explored how these treatment strategies affect both GLUT protein expression and trafficking in the lung.

Research Design and Methods

Type 1 Diabetic Animal Model

The following experimental protocols were approved by the Oklahoma State University Institutional Animal Care and Use Committee. Healthy FVB/N mice (The Jackson

Laboratory, Ellsworth, Maine) received 3 intraperitoneal injections once every 48 hours of either 300mM citrate buffer or streptozotocin (Sigma Aldrich, St. Louis, Missouri) dissolved in citrate buffer (at consecutive doses of 95 mg/kg, 65 mg/kg, and 95 mg/kg) to produce a type 1 diabetic mouse model. Once hyperglycemia was confirmed in type 1 diabetic mice (>250mg/dL), a subset of diabetic mice was given a subcutaneous semi-osmotic insulin pump (Alzet, Cupertino, California) at a dose of 0.5 units of HumulinRU-500 insulin (Eli Lilly, Indianapolis, Indiana) per mouse per day. After 4 weeks, the insulin pumps were replaced. Mice were monitored weekly for blood glucose and weight for a total of 8 weeks. A total of 24 male mice were used in this animal model.

Type 2 Diabetic Animal Model

Healthy C57Bl/6 mice (Charles River, Wilmington, Massachusetts) were fed with either regular chow (AIN-93M Mature Rodent Diet, product #D10012M, Research Diets, New Brunswick, New Jersey) or a high-fat diet (Rodent Diet with 60% kcal from fat, product #D12492, Research Diets, Brunswick, New Jersey) for 16 weeks. A subset of both the healthy mice and the high-fat diet-fed mice received metformin treatment for the second 8 weeks of the study. Metformin was added to their water at a rate of 200 mg/kg/day. A total of 24 male mice were used in this animal model.

Real Time Quantitative PCR (qRT-PCR)

Frozen samples (50–80 mg) were pulverized using Trizol reagent (Invitrogen, CA, USA) according to the manufacturer's instructions and RNA quantified using Gen5 software with Biotek synergy HT hardware on a take3 plate (BioTek, VT, USA). DNAse-treated RNA (Ambion AM1906M) was then converted to complementary DNA using the High Capacity cDNA Reverse Transcription Kit and random primers (Applied Biosystems, CA, USA) according to manufacturer's recommendations and stored at −80°C until analysis. The qRT-PCR assays for relative quantification of murine GLUT-1, -2, -3, -4, -8, -10, -12, and beta actin were performed using SYBR Green Real Time PCR Master Mix containing AmpliTaq Gold DNA Polymerase, to minimize nonspecific product formation, and deoxyribose nucleotide triphosphates with deoxyribose uridine triphosphate, to reduce carryover contamination (Applied Biosystems). Primer sequences were identified using the National Center for Biotechnology Information Basic Local Alignment Search Tool and custom synthesized by Invitrogen. Each PCR reaction (20 μL) contained 2x reaction buffer (SYBR Green I dye, Amplitaq Gold DNA Polymerase, deoxyribose nucleotide triphosphates with deoxyribose uridine triphosphate, passive reference, and optimized buffer components), forward and reverse primers (0.5 mM), 0.5 μg of complementary DNA, and DNase-RNase-free water. Primer concentrations and PCR conditions were determined during initial optimization runs. Samples were run in duplicate in a 96-well MicroAmp optical plate (Invitrogen). qRT-PCR was performed in an ABI 7500 Fast instrument (Applied Biosystems) with the following cycling conditions: 10 min at 95°C, followed by 40 cycles at 95°C for 15 s and 60°C for 1 min. No-template, negative controls were included for each gene. A melting

curve was generated to ensure product purity and the absence of primer dimers. The messenger RNA (mRNA) expression of target genes was normalized to β-actin, and the average cycle threshold was calculated.

Quantification of GLUT translocation to the cell surface

In order to quantify the glucose transporters at the cell surface, lung tissue was finely minced and bathed in a Krebs-Henseleit buffer at 37'C for 30 minutes, as described.[292] For insulin-treated cells, this buffer also contained 0.7nm insulin. Both untreated (basal) and insulin-treated lung homogenates were then photolabeled with the cell surface impermeant biotinylated bis-glucose photolabeling reagent (bio-LC-ATB-BGPA, 300 μM, Toronto Research Chemicals, product #B3956740, Ontario, Canada), of which the hexose group interact specifically interacts with the extracellular binding site of the glucose transporters. This photolabeled reagent cross-linked to the lung homogenates using a Rayonet photochemical reactor (340nm, Southern New England UV), as previously described.[68] Protein extraction was achieved via homogenization and ultracentrifugation (227,000g, 90 minutes at 4'C) to collect the crude membrane protein extract, specifically. Recovery of photolabeled (cell surface, or "labeled") glucose transporters from total lung homogenates was achieved using streptavidin isolation (bound to 6% agarose beads, Thermo Fisher, product #20349, Waltham, Massachusetts) to separate intracellular GLUTs ("unlabeled") from cell-surface GLUTs. The labeled GLUTs were then dissociated from the streptavidin via boiling in Laemmli buffer (Bio-Rad Laboratories, Hercules, California) for 30 minutes prior to Western blotting. Proteins

from the labeled fraction were quantified by densitometry relative to the positive control, as previously described.[68-70, 111, 156, 292, 293]

Western blotting

Crude membrane protein extracts or total lysates were used for Western blotting. For total lysate creation, lung tissue was collected and homogenized in tissue lysis buffer consisting of a 1:500 dilution of RIPA (Thermo Fisher, product #89901, Waltham, Massachusetts) and protease inhibitor cocktail (Sigma Aldrich, product #P8340, St. Louis, Missouri). Protein content was quantified via bicinchoninic assay (Thermo Fisher, product #23227, Waltham, Massachusetts), as previously described.[68]

Equal amounts of protein (30-60µg) were resolved in an 8-12% SDS-polyacrylamide gel and electrophoretically transferred (BioRad) to a polyvinyl-idine fluoride membrane (BioRad), as previously described.[68] After blocking in 5% milk (BioRad), membranes were incubated in primary antibodies overnight on a rocker at 4'C. Primary antibodies were diluted in tween-phosphate buffered saline (TPBS) with 5% milk (polyclonal rabbit anti-mouse GLUT1, 1:500 Abcam product #ab652; polyclonal rabbit anti-mouse GLUT2, 1:1000 polyclonal goat anti-mouse GLUT3, 1:500 Santa Cruz product #sc-7582; Abcam product #ab54460; polyclonal rabbit anti-human GLUT4, 1:750 AbD Serotec, product #4670-1704; polyclonal rabbit anti-human GLUT8, 1:500 Bioss product #bs-4241R; polyclonal rabbit anti-mouse GLUT10, 1:750 Thermo Fisher product #PA1-46137, polyclonal rabbit anti-mouse GLUT12, 1:500 Abcam product #ab75441; mouse

monoclonal β-actin, Santa Cruz product #sc-47778). This was followed by a one-hour incubation at room temperature with an appropriate secondary antibody conjugated to horseradish peroxidase diluted in TPBS with 5% milk (for GLUT-1, -2, -10 and -12, 1:2500 donkey anti-rabbit IgG H&L Abcam product # ab7083; for GLUT3, 1:4000 Santa Cruz product #sc-2020; for GLUT-4 and -8, 1:3000 donkey anti-rabbit IgG HRP-linked GE Healthcare product #NA934; for β-actin, 1:5000 mouse IgG kappa binding protein Santa Cruz product #sc-516102). Primary antibodies were chosen based on their 100% sequence homology with the protein of interest in rodents, and validated against a positive control. Antibody-bound transporter proteins were quantified by enhanced chemiluminescence reaction (Super Signal Max Sensitivity Substrate, product #34095, Thermo Fisher, Waltham, Massachusetts) and autoradiography. Band density and molecular weight were quantified using GelPro Analyzer (Media Cybernetics). The data was expressed relative to appropriate controls. Equal protein loading was confirmed by stripping (Thermo Fisher, product #21063, Waltham, Massachusetts) and reprobing each membrane with β-Actin.

Statistical analyses

Data are presented as mean ± SE. Differences between means were assessed using a statistical software package (Sigmaplot 11.0, Systat Software, Inc, San Jose, California). Two-way repeat measure ANOVA (treatment and time factors) for the *in vivo* measurements, and a one-way analysis of variance (treatment factors) for the *in vitro*

measurements were performed, as appropriate. When a significant difference was identified, post hoc tests were performed using the Student-Newman-Keuls test. Correlation between an independent and dependent variable was determined by regression analysis. Statistical significance was defined as $p<0.05$.

Results

In vivo *results from type 1 and type 2 diabetic mice*

Healthy mice were injected with streptozotocin to induce type 1 diabetes (as indicated by pronounced hyperglycemia, greater >250 mg/dL) and a subset was subsequently treated with a subcutaneous insulin pump to treat hyperglycemia (**Fig 1A**). After STZ injection, untreated diabetic mice maintained a blood glucose level significantly higher than control or treated counterparts ($p<0.01$), and higher than themselves at baseline ($p<0.01$). There were no significant differences in weight between groups in the type 1 diabetic study (**Fig 1B**). Similarly, healthy mice were fed a high-fat diet with 60% kcal from fat to induce type 2 diabetes (indicated by the mild hyperglycemia between 200 and 250 mg/dL, and pronounced hyperinsulinemia, as previously described[294]) (**Fig 1C**). After eating a high-fat diet, untreated diabetic mice maintained a blood glucose level significantly higher than control or treated counterparts ($p<0.05$ for month 1, $p<0.001$ for months 2-4), and higher than themselves at baseline ($p<0.001$). A subset of both control and high-fat diet-fed mice were treated with metformin at a rate of 200 mg/kg/day, which significantly reduced blood glucose concentration of type 2 diabetic mice to a normal level. High-fat

diet-fed mice were significantly heavier than their healthy counterparts, and metformin treatment did not affect weight of either diet group (**Fig 1D**).

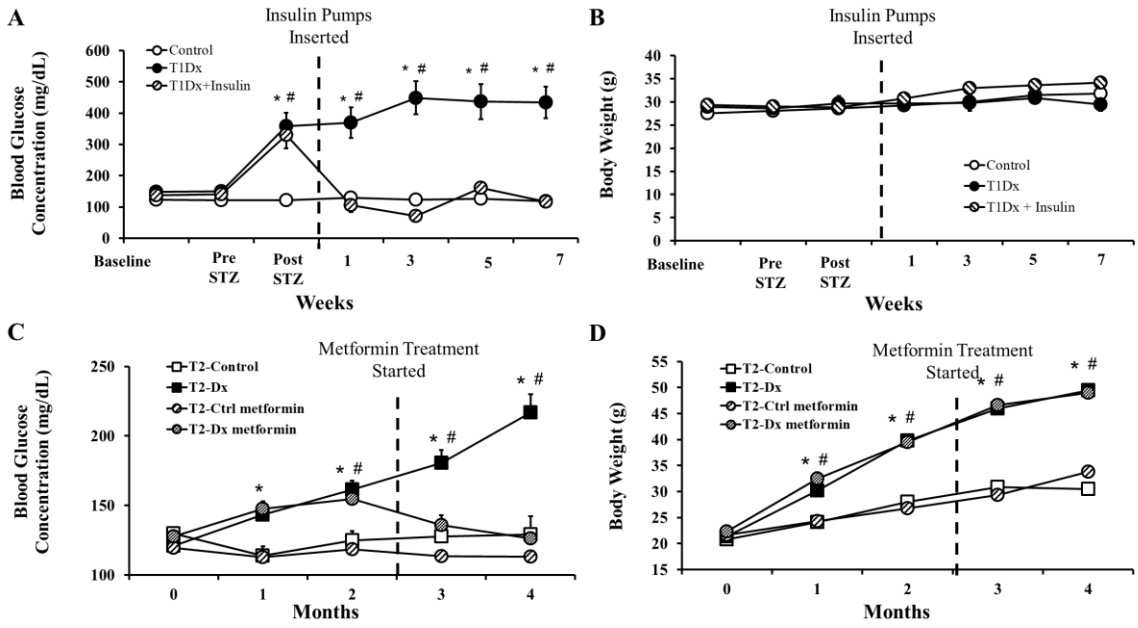

Figure 1. Hyperglycemia was rescued by treatment, without affecting body weight, in both type 1 and type 2 diabetic animals. Mean ± SE of fasted serum blood glucose levels of **(A)** type 1 diabetic (T1Dx) and **(C)** type 2 diabetic (T2Dx) groups. T1Dx were treated with insulin (T1Dx + Ins) while T2Dx animals were treated with metformin. Mean ± SE of body weight of **(B)** type 1 diabetic (T1DX) and **(D)** type 2 diabetic (T2Dx) groups. n=9-12/group. * $p<0.05$ vs control, # $p<0.05$ vs baseline, via two-way repeat measure ANOVA.

Real Time Quantitative PCR (qRT-PCR)

Healthy adult mouse lungs were collected, homogenized, and RNA was extracted using the Trizol method. The average cycle threshold (Ct) value of GLUT-1, -2, -3, -4, -8, -10, and -12 mRNA was normalized to beta actin (**Fig 2**). A lower Ct value indicates a higher expression of mRNA. In the healthy adult mouse lung, GLUT4 was found to be the highest expressed GLUT isoform, followed by GLUT12, then GLUT10. While the protein of GLUTs -1, -2, -4, -8, -10, and -12 were confirmed subsequently through Western blotting (**Fig 3-8**), GLUT3 protein was not found to be present in the adult mouse lung (data not shown).

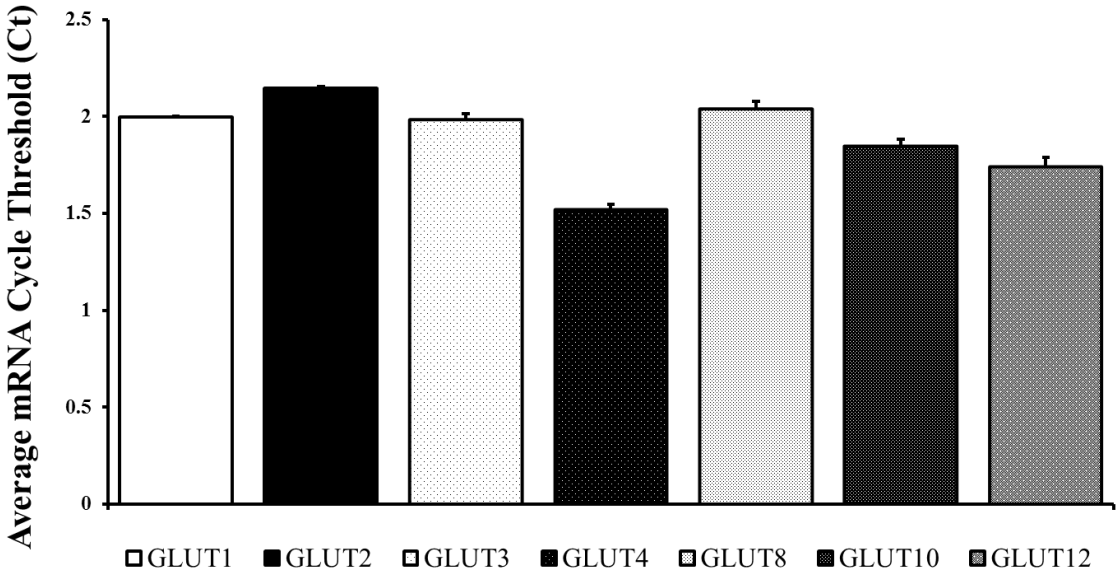

Figure 2. GLUT4 mRNA expression was highest in the adult healthy mouse lung. Mean ± SE of the average cycle threshold (Ct) of GLUTs -1, -2, -3, -4, -8, -10, and -12. All values were normalized to beta actin. A lower Ct value indicates a higher amount of mRNA.

Type 2 diabetic whole lung GLUT protein expression

Mouse whole lung was homogenized and the protein quantity determined via Western blot. Of the 7 glucose transporters which were probed for, protein expression of GLUT-1, -2, -4, -8, -10, -12 was found in adult whole rodent lung (**Fig 3**). GLUT3 protein expression was not found in the lung of any animal investigated. Protein expression of GLUT-2, -4, -10, and -12 was significantly reduced in the whole lung of type 2 diabetic mice ($p=0.032$, $p=0.001$, $p=0.012$, and $p=0.034$, respectively, **Fig 3B, 3C, 3E,** and **3F**). Metformin rescued this alteration only for the protein expression of GLUT-2, -4, and -10.

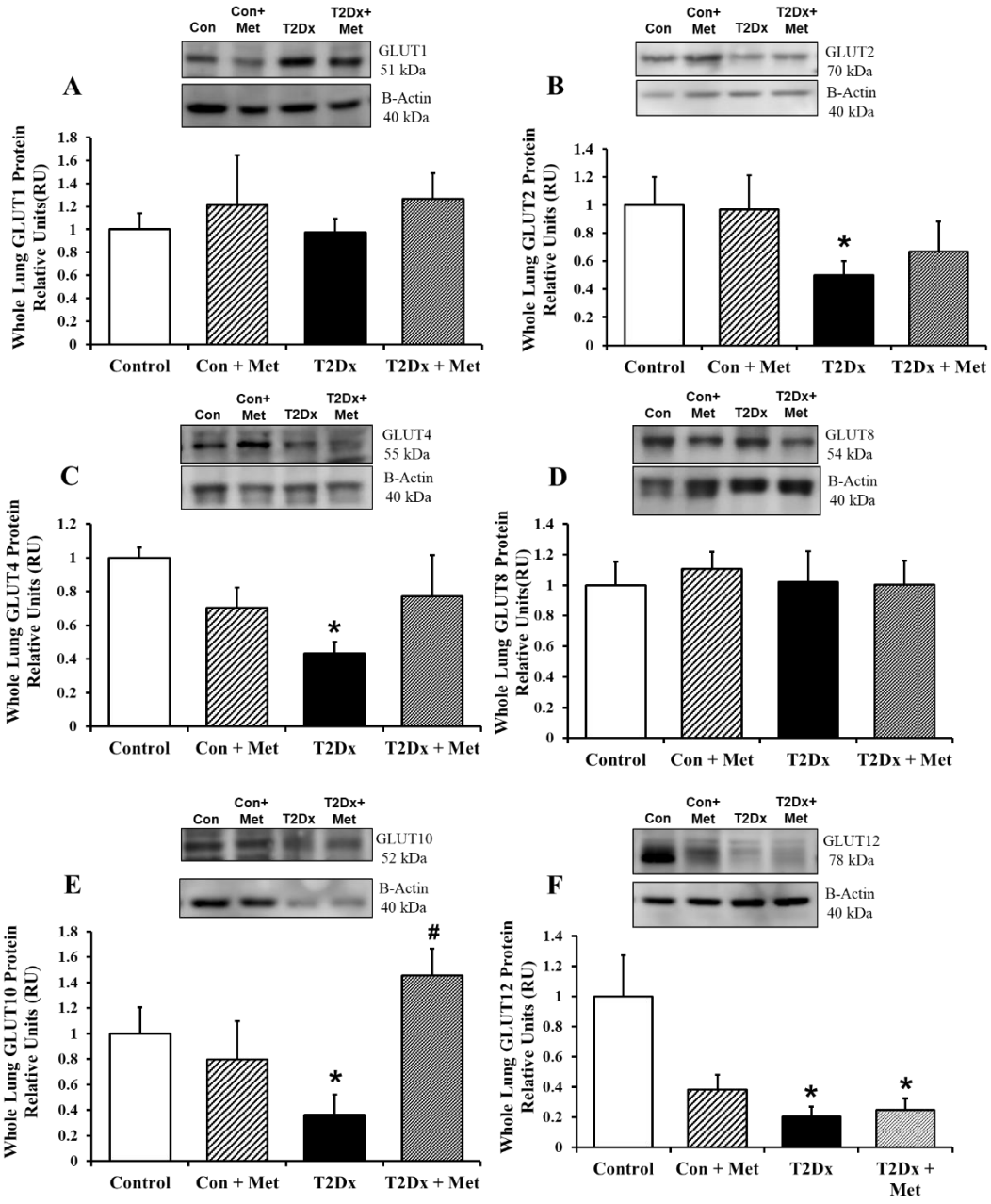

Figure 3. Alterations in glucose transporter (GLUT) protein expression in the adult whole lung during type 2 diabetes were partially rescued by *in vivo* metformin treatment. Total protein expression of **(A)** GLUT1, **(B)** GLUT2, **(C)** GLUT4, **(D)** GLUT8, **(E)** GLUT10, and **(F)** GLUT12 in the adult whole lung of control, type 2 diabetic (T2Dx), and metformin-treated animals. Top panels: representative Western blot from total lysate; loading control: beta actin. Bottom panels: Mean ± SE of total GLUT protein content, normalized to beta actin (values normalized to respective controls, n=3-5/group). * $p<0.05$ vs control, via one-way ANOVA.

Type 2 diabetic cell-surface GLUT protein expression

Mouse whole lung was homogenized and the cell surface glucose transporters were identified via the biotinylated photolabeled technique. To assess glucose transporter trafficking, cell surface glucose transporters (L: labeled) were quantified via Western blot. Both GLUT4, the predominant insulin-sensitive glucose transporter, and GLUT8, a novel insulin-sensitive glucose transporter, were significantly decreased at the cell surface during type 2 diabetes ($p=0.033$ and $p=0.029$ vs. control, respectively, **Fig 4**). Similarly, both of these trafficked glucose transporters were fully rescued with metformin treatment.

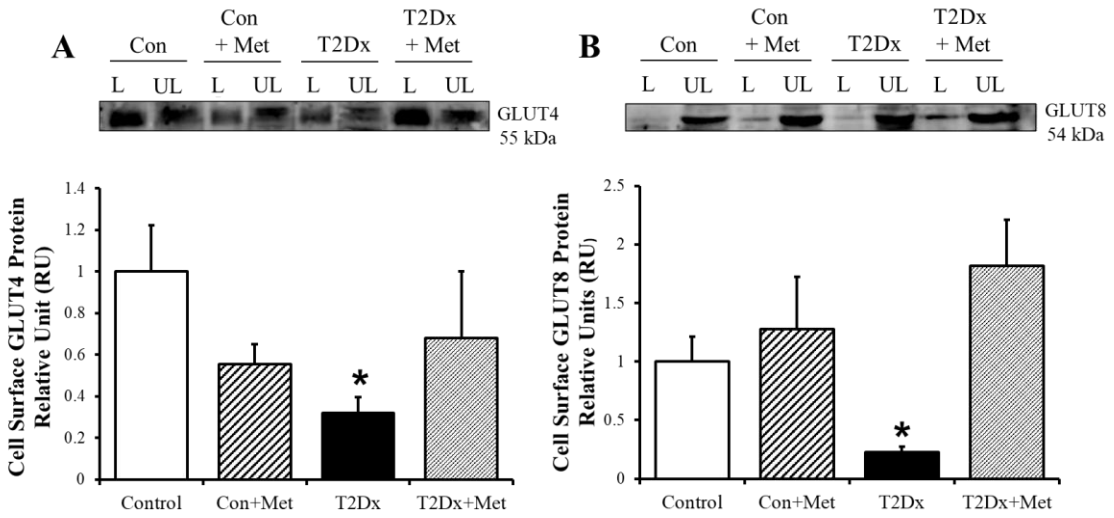

Figure 4: Alterations in glucose transporter (GLUT) protein expression at the pulmonary cell surface during type 2 diabetes were rescued by *in vivo* metformin treatment. Cell-surface protein expression of **(A)** GLUT4, and **(B)** GLUT8 at the cell surface of the adult whole lung of control, type 2 diabetic (T2Dx), and metformin-treated animals. Top panels: representative Western blot. Bottom panels: Mean ± SE of cell-surface GLUT protein content (values normalized to respective controls, n=3-5/group). L: Labeled (cell surface fraction); UL: Unlabeled (intracellular fraction). * $p<0.05$ vs control, via one-way ANOVA.

Type 1 diabetic upper lung GLUT protein expression

In order to determine the difference, generally, between the predominant cells of the upper lung (respiratory epithelial cells of the bronchi and bronchioles) and the lower lung (type 1 and type 2 alveolar cells), the upper and lower lung were separated at collection of the type 1 diabetic animals. The upper mouse lung was homogenized and the protein was quantified via Western blot. In the upper lung total lysate, only GLUT4 was decreased during type 1 diabetes, and only GLUT12 was increased during type 1 diabetes ($p=0.038$ and $p=0.033$ vs. control, respectively, **Fig 5C & 5F**). Insulin treatment fully rescued both of these alterations. Also, while there was no difference in GLUT2 protein expression between the control and type 1 diabetic animals, the insulin-treated animals demonstrated a significant upregulation of GLUT2 ($p=0.039$ vs. control, **Fig 5B**).

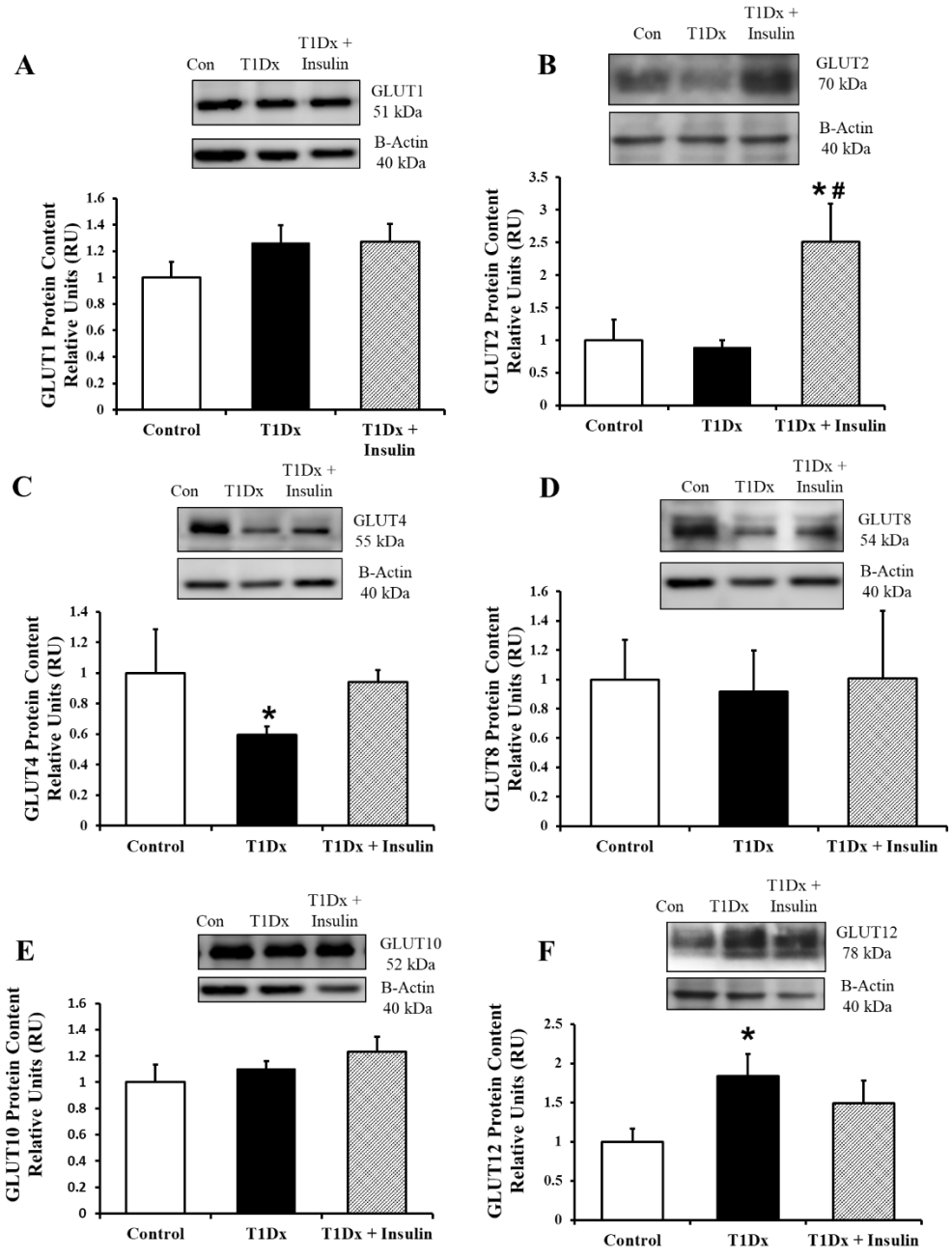

Figure 5. Alterations in glucose transporter (GLUT) protein expression in the adult upper lung during type 1 diabetes were rescued by *in vivo* metformin treatment. Total protein expression of **(A)** GLUT1, **(B)** GLUT2, **(C)** GLUT4, **(D)** GLUT8, **(E)** GLUT10, and **(F)** GLUT12 in the adult whole lung of control, type 1 diabetic (T1Dx), and insulin-treated animals (T1Dx + Insulin). Top panels: representative Western blot from total lysate; loading control: beta actin. Bottom panels: Mean ± SE of total GLUT protein content, normalized to beta actin (values normalized to respective controls, n=3-5/group). * $p<0.05$ vs control, via one-way ANOVA.

You will need to provide some explanations on the discrepancies between GLUT1 and 2 between the upper and lower lungs.

Type 1 diabetic lower lung GLUT protein expression

The lower mouse lung was homogenized and the protein was quantified via Western blot. In the lower lung total lysate, GLUT1 and GLUT4 had a significantly lower amount of protein expression in the type 1 diabetic animals versus their control counterparts ($p=0.014$ and $p=0.048$ vs. control, respectively, **Fig 6A & 6C,** respectively). And similar to the upper lung total lysate, the lower lung also demonstrated a significant upregulation of GLUT12 protein expression in the type 1 diabetic animals ($p=0.0438$ vs. control, **Fig 6F**). All of these alterations were rescued with insulin treatment.

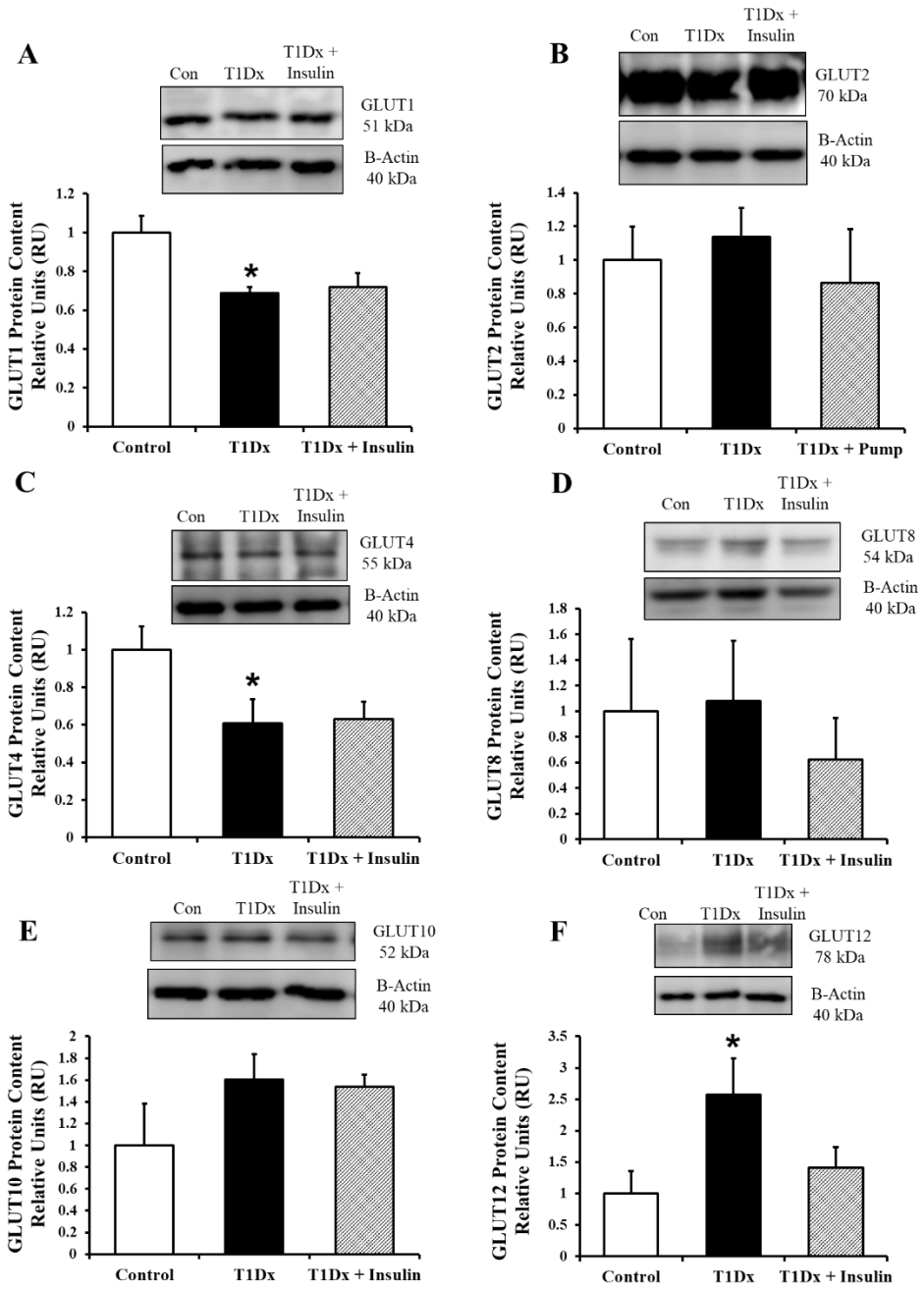

Figure 6. Alterations in glucose transporter (GLUT) protein expression in the adult lower lung during type 1 diabetes were rescued by *in vivo* metformin treatment. Total protein expression of **(A)** GLUT1, **(B)** GLUT2, **(C)** GLUT4, **(D)** GLUT8, **(E)** GLUT10, and **(F)** GLUT12 in the adult whole lung of control, type 1 diabetic (T1Dx), and insulin-treated animals (T1Dx + Insulin). Top panels: representative Western blot

from total lysate; loading control: beta actin. Bottom panels: Mean ± SE of total GLUT protein content, normalized to beta actin (values normalized to respective controls, n=3-5/group). * $p<0.05$ vs control, via one-way ANOVA.

Type 1 diabetic cell surface protein expression

To determine the cell-surface protein expression of insulin-sensitive glucose transporters in type 1 diabetic mice, whole lung homogenates were finely minced and incubated with the biotinylation photolabeled compound. Cell-surface GLUT protein was quantified via Western blot. Both GLUT4 and GLUT8 protein was significantly downregulated at the cell surface in the lung of type 1 diabetic mice compared to control counterparts ($p=0.001$ and $p=0.006$ vs. control, respectively, **Fig 7**). These alterations were rescued with insulin treatment.

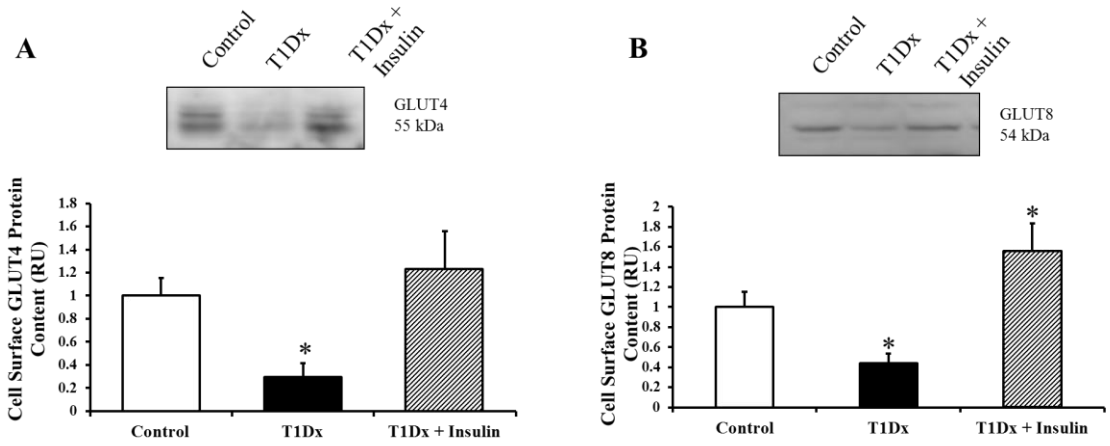

Figure 7: Alterations in glucose transporter (GLUT) protein expression at the pulmonary cell surface during type 1 diabetes were rescued by *in vivo* metformin treatment. Cell-surface protein expression of **(A)** GLUT4, and **(B)** GLUT8 at the cell surface of the adult whole lung of control, type 1 diabetic (T1Dx), and insulin-treated animals (T1Dx + Insulin). Top panels: representative Western blot. Bottom panels: Mean ± SE of cell-surface GLUT protein content (values normalized to respective controls, n=3-5/group). Labeled (cell surface fraction) only in representative blots. * $p<0.05$ vs control, via one-way ANOVA.

Healthy basal- and insulin-stimulated upper and lower lung homogenates

To determine *ex vivo* insulin-stimulated glucose transporter trafficking in the lung, upper and lower lung homogenates from healthy mice were finely minced and incubated for 30 minutes with either just KHB buffer (basal) or KHB buffer plus insulin. Lung homogenates were then incubated with the biotinylation photolabel compound, and cell-surface GLUT protein was quantified via Western blot. The predominant insulin-sensitive glucose transporter, GLUT4, was only detected at the cell surface of the upper lung, and none whatsoever was detected at the cell surface of the lower lung (**Fig 8**). In the upper lung, there was no difference in GLUT4 cell-surface protein expression between basal- and insulin-stimulated lung homogenates.

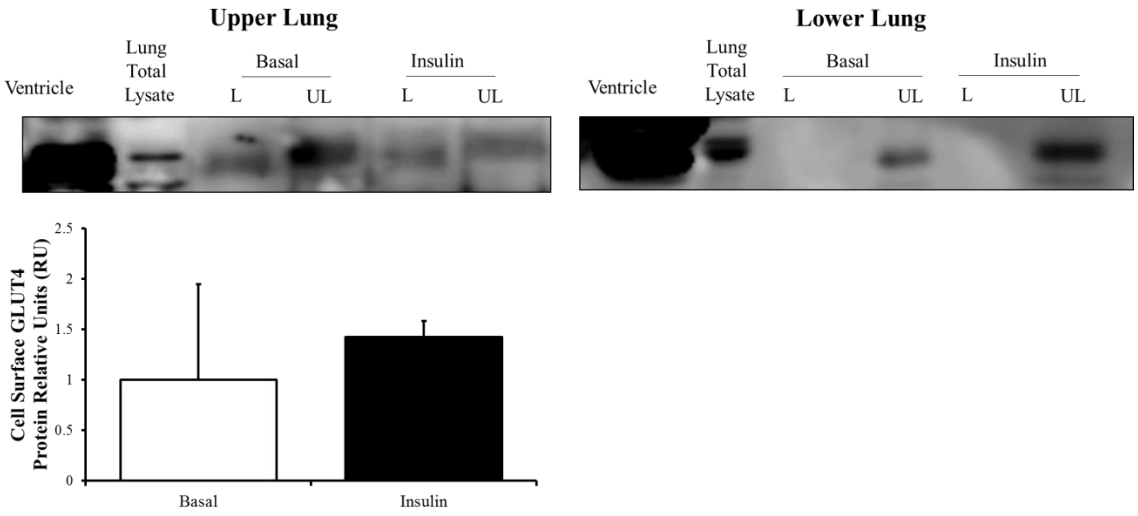

Figure 8: Pulmonary cell surface GLUT4 protein expression is not significantly altered after insulin treatment *ex vivo*. Cell-surface protein expression of GLUT4 in the **(A)** upper lung, and **(B)** lower lung at the cell surface of lung homogenates treated with buffer (Basal) or with insulin. No cell surface protein expression of GLUT4 is evident in the lower lung. Top panels: representative Western blot. Bottom panels: Mean ± SE of cell-surface GLUT protein content (values normalized to respective controls, n=3-5/group). L: Labeled (cell surface fraction); UL: Unlabeled (intracellular fraction). no significance, via one-way ANOVA.

Discussion

It has only recently become apparent that diabetic patients are at a significant risk for pulmonary infection,[11, 12, 288] and glucose homeostasis in the lung has so far remained elusive. Recent investigations have identified that there is a relatively constant ratio of glucose in the airway surface liquid to blood glucose (roughly 12.5 times as much glucose in the blood as the airway)[295] and that this glucose diffuses passively into the airway.[51] However, it is theorized that glucose removal from the airway is conducted primarily via the activity of the glucose transporters in the respiratory system.[51] Thus, understanding the specific protein presence and glucose transporter activity of the airway is of crucial importance in order to unravel the complications causing the increased risk of pulmonary infection in diabetic patients.

In order to examine this hyperglycemic risk as exhaustively as possible, we here used both a type 1 diabetic and a type 2 diabetic mouse model. Similarly, in order to prevent the introduction of variables from genetic variants, we did not use transgenic mouse models of diabetes. Instead, streptozotocin has long been a reliable method of inducing severe hyperglycemia[296] (while maintaining normal body weight and insulin sensitivity) with extremely limited, if any, unintentional side effects. Likewise, we also here chose to induce type 2 diabetes via a diet with 60% kilocalories from fat, producing very mild hyperglycemia but pronounced hyperinsulinemia[294] and weight gain. While type 2 diabetes represents over 90% of all those afflicted with some type of diabetes mellitus in the United States[297] and in the world,[298] it is critically important to understand what alterations are due to hyperglycemia alone versus those due to hyperinsulinemia,

inflammation, and obesity. To our knowledge, we are the first to investigate the alterations of glucose homeostasis of the lung as it relates to type 1 diabetes, specifically.

We also chose to treat our diabetic mice in order to determine if diabetic alterations of pulmonary glucose transporters were reversible, and if these common treatments already readily used in human patients were effective. As expected, insulin fully rescued the pronounced hyperglycemia and almost all of the GLUT alterations of the type 1 diabetic mice. Similarly, metformin treatment rescued the mild hyperglycemia of the type 2 diabetic mice, along with the alterations in pulmonary GLUT protein. Metformin treatment did not affect the weight of either the control or the type 2 diabetic mice. One limiting factor of this study is the differing backgrounds of our mice (type 1 diabetic mice were on an FVB/N background while type 2 diabetic mice were on a C57BL/6 background). However, in our experience, and has been published, these strains are extremely similar in terms of insulin secretion from islet cells, blood glucose, and GLUT protein expression in striated muscle,[299] and are thus highly comparable.

In the type 2 diabetic mice, the whole lung was homogenized and the protein was quantified via Western blot. No GLUT3 protein was detected in any of the lung homogenates. There was no change between any groups for GLUT1 and GLUT8 expression in lung total lysate. Type 2 diabetic mice had a significant decrease of GLUT-2, -4, -10, and -12 protein in the whole lung compared to control counterparts. Metformin treatment did not alter the protein expression of any GLUTs in the control mice, but did

rescue the expression of GLUT-2, -4, and -10 in type 2 diabetic mice. However, metformin did not rescue GLUT12 expression in type 2 diabetic mice. As an AMPK agonist, metformin is known to improve GLUT4 translocation in striated muscle[300] and apidocytes.[301] While, to the best of our knowledge, metformin's direct action on non-cancerous pulmonary glucose transporters is unknown, it has been demonstrated that metformin inhibits tumor growth via an MTOR/AMPK-dependent pathway in pulmonary cell culture,[302] in mice,[303] and in human patients.[304] Interestingly, while some groups using rodent models of lung cancer treated with metformin find no pulmonary activation of AMPK in addition to an inhibition of insulin-like growth factor-1 receptor and the insulin receptor in the lung,[303] others report the anti-inflammatory benefit of metformin during pulmonary LPS challenge via increased AMPK phosphorylation.[305] Despite these discrepancies, metformin has not been reported to directly increase the total protein expression of any glucose transporter in any tissue, to our knowledge. Rather, through its effects of increasing GLUT4 translocation to the cell surface in the insulin-sensitive tissues and decreasing gluconeogenesis in the liver, metformin helps reduce blood glucose levels for the entire body in addition to reducing insulin resistance.[306] This would be the most likely explanation for the rescue of pulmonary total GLUT protein demonstrated in our type 2 diabetic mice.

We here also quantified the cell surface expression of glucose transporters in the lungs of type 2 diabetic mice. Since GLUT-1, -2, -3, and -10 are glucose transporters which reside predominately on the cell surface and do not rely on trafficking mechanisms to function, we did not measure the specific expression of these GLUTs at the cell surface. This same

basal cell surface expression has also been recently determined for GLUT12, a novel class III glucose transporter, in striated muscle.[156] However, both GLUT4, the predominant insulin-sensitive glucose transporter, and GLUT8, another novel class III glucose transporter, rely on trafficking from an intracellular pool to the cell surface after stimulation from either insulin or calcium. We measured the cell surface and intracellular fractions of these GLUTs specifically and determined that they were both significantly reduced at the cell surface during type 2 diabetes. Metformin did not alter the cell surface expression of these GLUTs in control mice, but it did rescue the downregulation of cell surface protein content in type 2 diabetic mice. While the importance of GLUT8 in the lung has yet to be determined in full, it is interesting to note that the total lysate protein content of GLUT8 was unchanged between groups despite the significant downregulation of GLUT8 at the cell surface, indicating a potential reliance on GLUT trafficking in the lung.

We performed the same experiments in the type 1 diabetic mice as we did in the type 2 diabetic mice, with the exception that in the type 1 diabetic mice we separated the upper and lower lung in order to estimate prevalence of GLUT protein in either the bronchial epithelial cells (upper lung) or alveolar type I and type II cells (lower lung). In the upper lung, GLUT4 was significantly downregulated in type 1 diabetic animals while GLUT12 was significantly upregulated. This GLUT12 upregulation is a departure from our findings in the type 2 diabetic animals, but has been reported previously in the past in conjunction with a downregulation of GLUT4 and is speculated to be part of a compensatory response.[156] Both of these changes were rescued with insulin treatment.

And while no other GLUTs in the total lysate of the upper lung were altered in type 1 diabetic animals, we were surprised to find a significant upregulation of GLUT2 in the insulin-treated animals as compared to both the control and the untreated diabetic mice. Previous groups have also reported on this same finding in the kidney.[307] In the lower lung of type 1 diabetic mice, GLUT-1 and -4 were significantly downregulated as compared to controls. GLUT12 protein was again significantly upregulated in type 1 diabetic mice. These alterations were completely rescued by insulin treatment, and there were no alterations of GLUT2 protein in the lower lung of any group in the type 1 diabetic study. Thus, the only differences in GLUT protein expression between groups in terms of upper and lower lung appear to be GLUT1 and GLUT2.

Similar to the type 2 diabetic model, we also quantified the protein expression of GLUT-4 and GLUT-8 at the pulmonary cell surface of the type 1 diabetic animals. We again found that both GLUT-4 and GLUT-8 were significantly decreased at the cell surface in diabetic animals, and that this alteration was rescued with insulin treatment. And, again similar to the type 2 diabetic study, we determined that while GLUT4 protein was decreased in both the lung total lysates and at the pulmonary cell surface, GLUT8 protein was only decreased at the cell surface during type 1 diabetes, but remained unchanged in both the upper and lower lung total lysates. This further indicates that GLUT8 may be an active participant in pulmonary glucose homeostasis and may rely on trafficking mechanisms in order to function in the airway.

Finally, we also sought to determine whether lung homogenates could be stimulated *ex vivo* with insulin treatment, as cardiac, skeletal muscle, and adipose tissue are.[68-70, 292, 294] Based on the GLUT4 protein expression at the cell surface, we found no evidence that lung homogenates are directly stimulated with insulin to induce glucose transporter trafficking. Furthermore, we only found evidence of GLUT4 at the cell surface of the upper lung, and no GLUT4 protein at all in the cell surface of the lower lung using our macroscopic dissection technique to differentiate the two predominate morphologies of the lung (more bronchial epithelial cells in the upper lung, and more alveolar type 1 and type 2 cells in the lower lung). These results would indicate that GLUT4 at the cell surface is more predominate in the bronchial epithelial cells than in the alveolar cells. However, we recognize that this dissection technique is only able to generalize in terms of protein expression of specific cell types. In order to more fully investigate these differences, a technique involving immunohistochemistry, immunofluorescence, or cell isolation should be conducted. To our knowledge, we are the first to apply this biotinylation photolabeling technique to the lung and successfully determine the cell surface protein content of any glucose transporters in the airway.

In conclusion, we have quantified the protein expression of seven predominant glucose transporter isoforms in the adult lung of healthy, diabetic, and treated diabetic animals. Of the six isoforms we found in non-cancerous lung tissue (GLUT-1, -2, -4, -8, -10, and -12), all of the isoforms were determined to have some sort of alteration during either type 1 or type 2 diabetes, either in the total cell lysate or at the cell surface of the homogenized lung tissue. Insulin or metformin treatment rescued almost all of the alterations demonstrated during diabetes. However, whether these treatments are affecting GLUT

protein expression in the lung due to a rescue of whole-body glucose homeostasis or due to a specific pulmonary action remains to be determined. Overall, the results from this study indicate that both type 1 and type 2 diabetes significantly alters the GLUT protein expression in the adult lung, and targeting the maintenance of function of the pulmonary glucose transporters may designate a significant treatment avenue for diabetic patients with concurrent respiratory infections.

Acknowledgements

We would like to thank Dr. Zahra Maria and Jill Murray for their excellent technical assistance.

.

CHAPTER VI

INSULIN OR METFORMIN TREATMENT RESCUES ALTERATIONS IN THE LUNG FOLLOWING H1N1 INFLUENZA VIRUS INFECTION IN DIABETIC MICE

ABSTRACT

Hyperglycemia has recently been identified as a significant and independent risk factor in the development and increasing severity of respiratory infections. However, the glucose homeostasis of the lung as it pertains to diabetes-involved viral infections remains largely unexplored. Thus, we here hypothesized that glucose transporters of the lung would be significantly altered during diabetic influenza, and that insulin or metformin treatment would rescue these alterations. To test this hypothesis, we used both a type 1 diabetic model (T1Dx, streptozotocin-induced, for 8 weeks) and a type 2 diabetic model (T2Dx, high-fat diet-induced, for 16 weeks). A subset of T1Dx mice were treated with semi-osmotic subcutaneous insulin pumps and a subset of T2Dx mice were treated with metformin via the drinking water. At the end of the diabetic period, mice were intranasally infected with 250 plaque forming units of H1N1 Influenza A (A/PR/8/34) and sacrificed 3 days post infection. Bronchoalveolar lavage fluid (BALF) was collected to measure BALF protein, cytology, and glucose concentration of the airway surface liquid. Whole lungs were collected for viral titer determined via real-time reverse-transcriptase PCR (qRT-PCR), for mRNA quantification of glucose transporters (GLUTs), and for protein quantification of GLUTs via Western blotting. Infected and non-infected diabetic mice of both diabetic groups possessed significant alterations of GLUT protein expression in the total lysate and at the cell surface, which was rescued with insulin or metformin treatment. Infected control mice demonstrated significantly upregulated cell surface GLUT4 protein compared to non-infected control mice. Infected diabetic mice possessed less cell surface GLUT protein compared to infected control mice, but still a greater quantity than non-infected diabetic mice. Diabetic mice possessed

significantly more glucose in the BALF versus control mice, and infected control and diabetic mice possessed significantly more glucose in the BALF than their non-infected counterparts. These alterations were rescued with insulin treatment. While control and treated mice possessed similar levels of viral titer in the lung, diabetic mice of either group demonstrated an extremely wide range of variability of viral titer. Overall, we here demonstrate for the first time the influenza directly increases GLUT protein expression at the cell surface of the lung and may be responsible for significant alterations in pulmonary glucose homeostasis. These insights may provide substantial targets for novel therapeutic targets for patients afflicted with both diabetes and influenza.

INTRODUCTION

The CDC has recently identified that diabetic patients die from both bacterial and viral respiratory infection at roughly three time the rate than their non-diabetic patients. Interestingly, both hyperglycemia and obesity have been singled out as independent risk factors for the incidence and increased severity of respiratory infection. Despite these recent discoveries, and the large amount metabolic activity undertaken by the lung, the glucose homeostasis mechanisms of the healthy, diabetic, or infected lung remain largely unexplored.

What is known is that diabetic patients have a significantly increased amount of glucose in their airway surface liquid (ASL) versus healthy patients, and that this elevation persists for the duration of the patient's overall hyperglycemia. Furthermore, it is known that glucose in the ASL is increased during other pulmonary diseases such as cystic fibrosis[295] and viral rhinitis,[308] and it is theorized to be elevated during viral respiratory

tract infection such as cold or influenza.[145] However, to our knowledge, specific ASL glucose concentrations during influenza have not been determined before now. Recent investigations have identified the direct correlation between the increased amount of glucose in the airway and more severe bacterial infections, and some studies have indicated that type 1 diabetes may increase the viral titer in type 1 diabetic mice,[202, 209, 309] but to our knowledge no study has quantified alterations in glucose of the airway surface liquid of either type 1 or type 2 diabetic mice, or human patients, during influenza. Importantly, the majority of patients who die from primary viral infections are thought to be infected with secondary bacterial infections, which could greatly exacerbate the severity of the disease.[310] Thus, understanding the regulation of glucose and viral responses in the airway to both type 1 and type 2 diabetic conditions is of critical importance, particularly if a combination of diabetes and influenza has an additive effect on the increase of glucose in the ASL.

Similarly, the majority of patients in the United States and in the world who suffer from diabetes suffer from type 2 diabetes, specifically.[311, 312] However, to our knowledge, only type 1 diabetic models have been used to investigate the pulmonary response to influenza.[209, 309] Therefore, we here undertake an investigation of both type 1 and type 2 diabetic mouse models with influenza infection in order to begin to unravel the questions concerning whether hyperglycemia alone or the complications of insulin resistance and obesity together are more responsible for the severity of diabetic influenza infection.

Finally, understanding the alterations of the glucose transporters (GLUTs) of the lung, which are the rate-limiting step in pulmonary glucose uptake, is of critical importance. While GLUTs of the lung have been under-investigated as a group, we and others have

recently reported the presence of several GLUT isoforms in the lung, both at the mRNA and protein level.[51, 62, 95] We have also recently reported alteration of protein expression of GLUTs in the lung during diabetes, both in the total lysate and at the cell surface, specifically.[95] However, the alteration of these critical proteins in the lung during influenza infection is still unknown.

Thus, we hypothesized that diabetic mice of both groups would possess a significant alteration in ASL glucose concentration and of GLUT protein expression, and that these alterations would be exacerbated by influenza infection. We furthermore hypothesized that these alterations would be rescued by insulin or metformin treatment.

MATERIALS AND METHODS

Type 1 Diabetic Animal Model

The following experimental protocols were approved by the Oklahoma State University Institutional Animal Care and Use Committee. Healthy FVB/N mice (The Jackson Laboratory, Ellsworth, Maine) received 3 intraperitoneal injections once every 48 hours of either 300mM citrate buffer or streptozotocin (Sigma Aldrich, St. Louis, Missouri) dissolved in citrate buffer (at consecutive doses of 95 mg/kg, 65 mg/kg, and 95 mg/kg) to produce a type 1 diabetic mouse model. Once hyperglycemia was confirmed in type 1 diabetic mice (>250mg/dL), a subset of diabetic mice was given a subcutaneous semi-osmotic insulin pump (Alzet, Cupertino, California) at a dose of 0.5 units of HumulinRU-500 insulin (Eli Lilly, Indianapolis, Indiana) per mouse per day. After 4 weeks, the insulin pumps were replaced. Mice were monitored weekly for blood glucose and weight for a total of 8 weeks. A total of 48 male mice were used in this animal model.

Type 2 Diabetic Animal Model

Healthy C57Bl/6 mice (Charles River, Wilmington, Massachusetts) were fed with either regular chow (AIN-93M Mature Rodent Diet, product #D10012M, Research Diets, New Brunswick, New Jersey) or a high-fat diet (Rodent Diet with 60% kcal from fat, product #D12492, Research Diets, Brunswick, New Jersey) for 16 weeks. A subset of both the healthy mice and the high-fat diet-fed mice received metformin treatment for the second 8 weeks of the study. Metformin was added to their water at a rate of 200 mg/kg/day. A total of 48 male mice were used in this animal model.

Viral Infection

Animals infected with influenza were anesthetized with 3% isoflurane and intranasally challenged with a sublethal dose of 250 PFU of H1N1 A/PR/8/34 influenza virus diluted in 50 µl of phosphate-buffered saline. Mice were weighed on day 0, and every 24 hours thereafter. Blood glucose was taken at day 0 and just before sacrifice. Mice were sacrificed 3 days post infection.

Bronchoalveolar Lavage Fluid Analysis

Mice were anesthetized with 3% isoflurane. A cannula was inserted into the trachea and 1 mL of sterilized phosphate buffered saline was perfused into the lungs and collected. This

was performed a total of 3 times to collect a total of 2-3 mL of BAL fluid per mouse. BAL fluid was then kept on ice, cells were counted using a hemocytometer, and 200µL of sample was spun for 10 minutes at 800g using a cytospin centrifuge to affix the cells to a microscope slide. Slides were then stained with Diff Quick for differential cell counts and imaging. A subset of samples underwent red blood cell lysis and differential cell counting before and after lysis. BAL fluid was analyzed spectrophotometrically for glucose content (Amplex Red Glucose Assay Kity, Thermo Fisher product #A22189).

Viral titer

Viral titer was determined via plaque assay by plating BAL fluid on MDCK monolayers and counting the plaque forming units, and confirmed by qRT-PCR of whole lung homogenates as previously described.[257] Viral titer was subsequently confirmed by qRT-PCR analysis by probing for viral hemagglutinin. Sequences for hemagglutinin: forward: GCTGCAGATGCAGACACAAT, reverse: CCCTCAGCTCCTCATAGTCG. Beta actin was used a housekeeping gene: forward:

Quantification of GLUT translocation to the cell surface

In order to quantify the glucose transporters at the cell surface, lung tissue was finely minced and bathed in a Krebs-Henseleit buffer at 37'C for 30 minutes, as described.[292] For insulin-treated cells, this buffer also contained 0.7nm insulin. Both untreated (basal) and insulin-treated lung homogenates were then photolabeled with the cell surface

impermeant biotinylated bis-glucose photolabeling reagent (bio-LC-ATB-BGPA, 300 μM, Toronto Research Chemicals, product #B3956740, Ontario, Canada), of which the hexose group interact specifically interacts with the extracellular binding site of the glucose transporters. This photolabeled reagent cross-linked to the long homogenates using a Rayonet photochemical reactor (340nm, Southern New England UV), as previously described.[68] Protein extraction was achieved via homogenization and ultracentrifugation (227,000g, 90 minutes at 4'C) to collect the crude membrane protein extract, specifically. Recovery of photolabeled (cell surface, or "labeled") glucose transporters from total lung homogenates was achieved using streptavidin isolation (bound to 6% agarose beads, Thermo Fisher, product #20349, Waltham, Massachusetts) to separate intracellular GLUTs ("unlabeled") from cell-surface GLUTs. The labeled GLUTs were then dissociated from the streptavidin via boiling in Laemmli buffer (Bio-Rad Laboratories, Hercules, California) for 30 minutes prior to Western blotting. Proteins from the labeled fraction were quantified by densitometry relative to the positive control, as previously described.[68-70, 111, 156, 292, 293]

Western blotting

Crude membrane protein extracts or total lysates were used for Western blotting. For total lysate creation, lung tissue was collected and homogenized in tissue lysis buffer consisting of a 1:500 dilution of RIPA (Thermo Fisher, product #89901, Waltham, Massachusetts) and protease inhibitor cocktail (Sigma Aldrich, product #P8340, St.

Louis, Missouri). Protein content was quantified via bicinchoninic assay (Thermo Fisher, product #23227, Waltham, Massachusetts), as previously described.[68]

Equal amounts of protein (30-60µg) were resolved in an 8-12% SDS-polyacrylamide gel and electrophoretically transferred (BioRad) to a polyvinyl-idine fluoride membrane (BioRad), as previously described.[68] After blocking in 5% milk (BioRad), membranes were incubated in primary antibodies overnight on a rocker at 4'C. Primary antibodies were diluted in tween-phosphate buffered saline (TPBS) with 5% milk (polyclonal rabbit anti-mouse GLUT1, 1:500 Abcam product #ab652; polyclonal rabbit anti-mouse GLUT2, 1:1000 polyclonal goat anti-mouse GLUT3, 1:500 Santa Cruz product #sc-7582; Abcam product #ab54460; polyclonal rabbit anti-human GLUT4, 1:750 AbD Serotec, product #4670-1704; polyclonal rabbit anti-human GLUT8, 1:500 Bioss product #bs-4241R; polyclonal rabbit anti-mouse GLUT10, 1:750 Thermo Fisher product #PA1-46137, polyclonal rabbit anti-mouse GLUT12, 1:500 Abcam product #ab75441; mouse monoclonal β-actin, Santa Cruz product #sc-47778). This was followed by a one-hour incubation at room temperature with an appropriate secondary antibody conjugated to horseradish peroxidase diluted in TPBS with 5% milk (for GLUT-1, -2, -10 and -12, 1:2500 donkey anti-rabbit IgG H&L Abcam product # ab7083; for GLUT3, 1:4000 Santa Cruz product #sc-2020; for GLUT-4 and -8, 1:3000 donkey anti-rabbit IgG HRP-linked GE Healthcare product #NA934; for β-actin, 1:5000 mouse IgG kappa binding protein Santa Cruz product #sc-516102). Primary antibodies were chosen based on their 100% sequence homology with the protein of interest in rodents, and validated against a positive control. Antibody-bound transporter proteins were quantified by enhanced

chemiluminescence reaction (Super Signal Max Sensitivity Substrate, product #34095, Thermo Fisher, Waltham, Massachusetts) and autoradiography. Band density and molecular weight were quantified using GelPro Analyzer (Media Cybernetics). The data was expressed relative to appropriate controls. Equal protein loading was confirmed by stripping (Thermo Fisher, product #21063, Waltham, Massachusetts) and reprobing each membrane with β-Actin.

Histochemical and immunohistochemical staining

In mice which did not have BAL fluid collected, the left lobe was perfused with paraformaldehyde and stored in formalin for 48 hours or less before sectioning. Tissues were fixed with paraffin wax and sectioned in 4μm slices onto slides, then stored in -20'C until use. A subset of slides were stained with hematoxylin & eosin for structural analysis. For immunohistochemistry, upon rehydration and deparaffinization, slides were incubated at room temperate for three sets of 5 minutes in xylene, 2 sets of 10 minutes in 100% ethanol, 2 sets of 10 minutes in 95% ethanol, and 2 sets of 5 minutes in distilled deionized water. Slides were then washed in 1x TBST for five minutes before one hour of blocking (5% goat serum in TBST) at room temperature. Slides were then incubated overnight in primary antibody at 4'C (GLUT4: BioRad, #4670-1704, Hercules, CA; GLUT10: Thermo Fisher, #PA1 46137, Waltham, MA). The next day, slides were allowed to incubate in primary antibody for 30 minutes at room temperature before incubation for one hour with secondary antibody (GE Healthcare, #NA934, Chicago, IL) at room temperature. For immunohistochemistry, slides were then washed and then

incubated with Nova Red (Vector Laboratories, #SK-4800 Burlingame, CA) for 15 minutes. This was immediately followed by a 10 second incubation with Hematoxylin QS (Vector Laboratories, #H-3404-100 Burlingame, CA), and washing with water for 1-2 minutes. Slides were then dehydrated, and the cover slips mounted.

Immunofluorescent staining

In mice which did not have BAL fluid collected, the left lobe was perfused with paraformaldehyde and stored in formalin for 48 hours or less before sectioning. Tissues were fixed with paraffin wax and sectioned in 4μm slices onto slides, then stored in -20'C until use. Upon rehydration and deparaffinization, slides were incubated at room temperate for three sets of 5 minutes in xylene, 2 sets of 10 minutes in 100% ethanol, 2 sets of 10 minutes in 95% ethanol, and 2 sets of 5 minutes in distilled deionized water. Slides were then washed in 1x TBST for five minutes before one hour of blocking (5% goat serum in TBST) at room temperature. Slides were then incubated overnight in primary antibody at 4'C (GLUT4: Novus Biologicals, #NBP1-49533, Centennial, CO). The next day, slides were allowed to incubate in primary antibody for 30 minutes at room temperature before incubation for thirty minutes with secondary antibody (GE Healthcare, #NA934, Chicago, IL) at room temperature. Following the secondary antibody incubation, slides were washed with TBST wash buffer for three sets of 5 minutes, and cover slips were mounted using fluoroshield mounting medium with DAPI (AbCam, #ab104139, Cambridge, United Kingdom). Immunofluorescent slides were imaged the same day.

Culture and isolation of bacterial pathogens in bronchoalveolar lavage fluid

Immediately upon sacrifice, bronchoalveolar lavage fluid was collected aseptically using sterile phosphate-buffered saline. 10µl of BAL fluid was plated on a blood agar plate (5% sheep's blood) and incubated at 37'C in an open-air container for 72 hours. Colonies were photographed and counted using the Colony Counter application. Identification of bacterial isolates were identified using MALDI-TOF mass spectrometry and 16S rDNA PCR.

Statistical analyses

Data are presented as mean ± SE. Differences between means were assessed using a statistical software package (Sigmaplot 11.0, Systat Software, Inc, San Jose, California). Two-way repeated measure ANOVA (treatment and time factors) for the *in vivo* measurements, and a one-way ANOVA or two-way ANOVA without repetition (treatment factors) for the *in vitro* measurements were performed, as appropriate. When a significant difference was identified, post hoc tests were performed using the Student-Newman-Keuls test. Correlation between an independent and dependent variable was determined by regression analysis. Statistical significance was defined as $p<0.05$.

RESULTS

In vivo *results from type 1 and type 2 diabetic mice*

Healthy mice were injected with streptozotocin to induce type 1 diabetes (as indicated by pronounced hyperglycemia, >250 mg/dL) and a subset was subsequently treated with a subcutaneous insulin pump to treat hyperglycemia (**Fig 1A**). There were no significant differences in weight between groups in the type 1 diabetic study (**Fig 1B**). Similarly, healthy mice were fed a high-fat diet with 60% kcal from fat to induce type 2 diabetes (indicated by the mild hyperglycemia between 200 and 250 mg/dL, and pronounced hyperinsulinemia, as previously described[294]) (**Fig 1C**). A subset of both control and high-fat diet-fed mice were treated with metformin at a rate of 200 mg/kg/day, which significantly reduced the blood glucose of type 2 diabetic mice to a normal level. High-fat diet-fed mice were significantly heavier than their healthy counterparts, and metformin treatment did not affect weight of either diet group (**Fig 1D**).

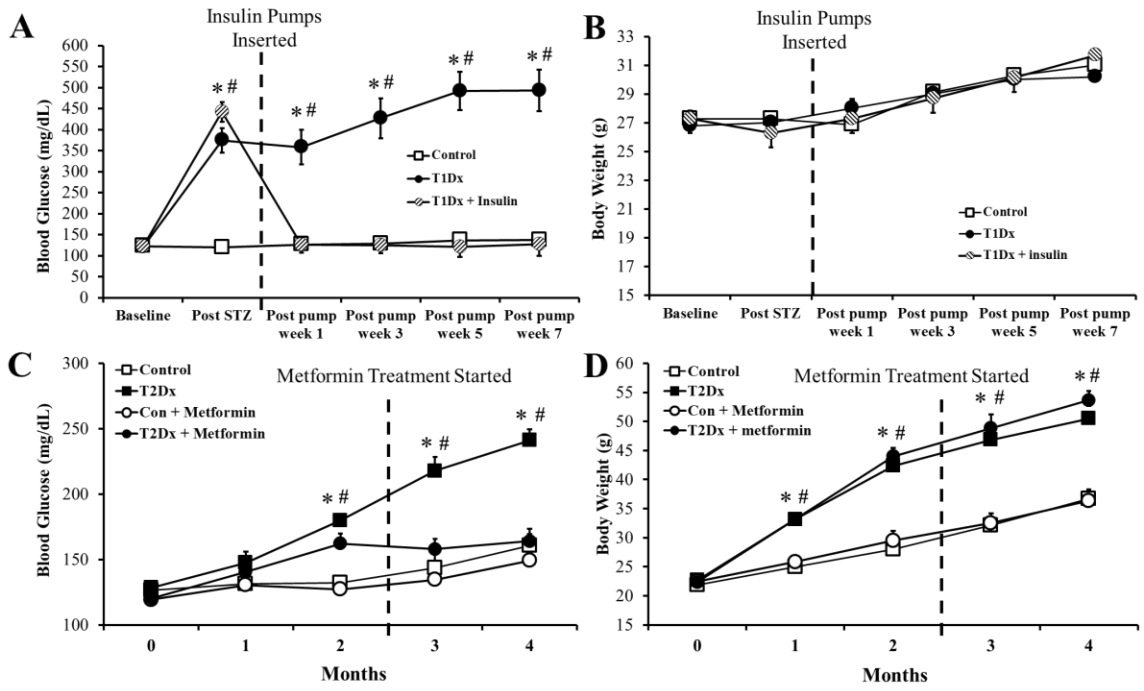

Figure 1. Hyperglycemia was rescued by treatment, without affecting body weight, in both type 1 and type 2 diabetic animals. Mean ± SE of fasted serum blood glucose levels of **(A)** type 1 diabetic (T1Dx) and **(C)** type 2 diabetic (T2Dx) groups. T1Dx were treated with insulin (T1Dx + Ins) while T2Dx animals were treated with metformin. Mean ± SE of body weight of **(B)** type 1 diabetic (T1DX) and **(D)** type 2 diabetic (T2Dx) groups. n=9-12/group. * $p<0.05$ vs control, # $p<0.05$ vs baseline, via two-way repeat measure ANOVA.

In Vivo *results during influenza infection*

Blood glucose was measured on Day 0 and Day 3 after influenza infection via facial puncture (**Figure 2A & 2C**). Body weight was measured every 24 hours, starting at Day 0 and end on Day 3 (**Figure 2B & 2D**). While type 1 diabetic animals had significantly higher blood glucose levels at both day 0 and day 3 than control or insulin-treated animals, there was no difference in blood glucose levels between day 0 and day 3 within any group (**Fig 2A**). Similarly, while type 2 diabetic animals maintained significantly higher blood glucose than control or treated animals at day 0, both type 2 diabetic and type 2 diabetic animals treated with metformin had significantly higher blood glucose levels at day 3 compared to control animals (**Fig 2C**). Within and between groups, there were no differences in body weight during influenza infection in the type 1 diabetic animal model (**Fig 2B**). While treated and untreated type 2 diabetic animals were significantly heavier than either of their control counterparts, there were no differences of body weight within any group of the type 2 diabetic animal model during influenza infection (**Fig 2D**).

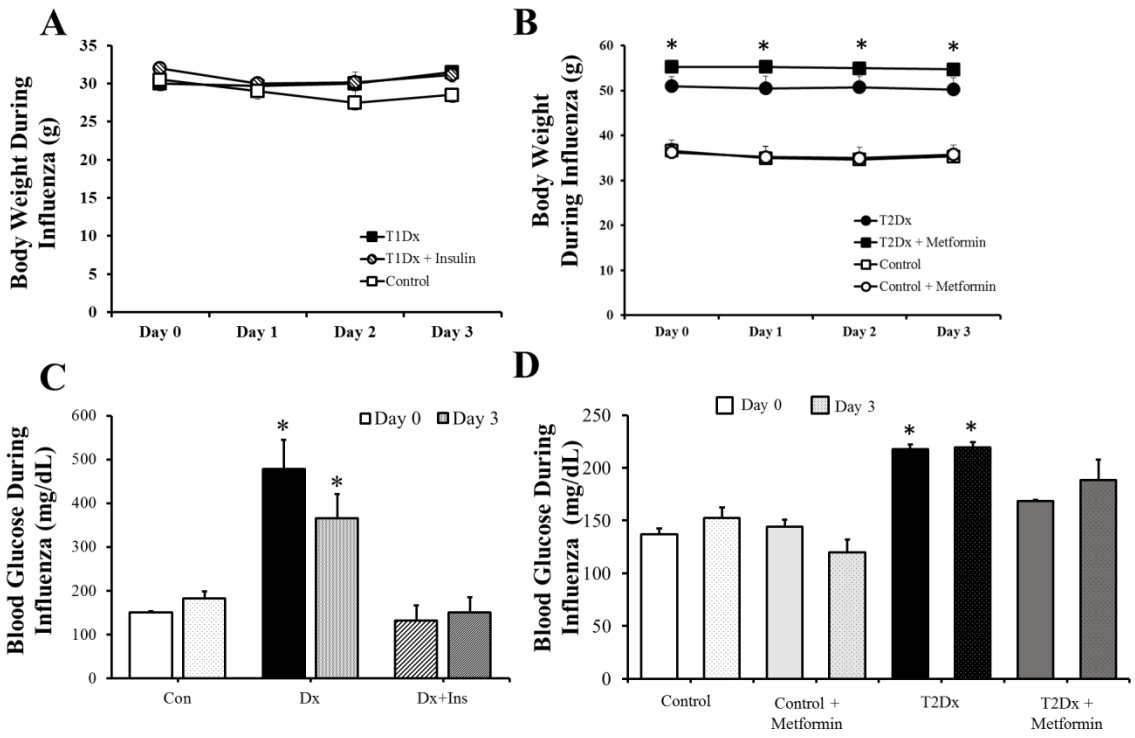

Figure 2. Body weight and blood glucose were not changed within any group during influenza infection. Mean ± SE of fasted serum blood glucose levels of **(A)** type 1 diabetic (T1Dx) and **(C)** type 2 diabetic (T2Dx) groups. T1Dx were treated with insulin (T1Dx + Ins) while T2Dx animals were treated with metformin. Mean ± SE of body weight of **(B)** type 1 diabetic (T1DX) and **(D)** type 2 diabetic (T2Dx) groups. n=9-12/group. * $p<0.05$ vs control, # $p<0.05$ vs baseline, via two-way repeat measure ANOVA.

Diabetic mice did not possess a significantly different viral titer from control mice

Viral titer was determined by qRT-PCR of the viral hemagglutinin mRNA in homogenized whole lung tissue (**Figure 3**). There was no significant different between groups in terms of viral titer when assessed by either MDCK plaque assay of BALF (not shown) or qRT-PCR of lung homogenates. While there was a large amount of variation in both type 1 diabetic (**Fig 3A**) and type 2 diabetic (**Fig 3B**) mice, control and treated groups maintained similar viral titer expressions between all animals.

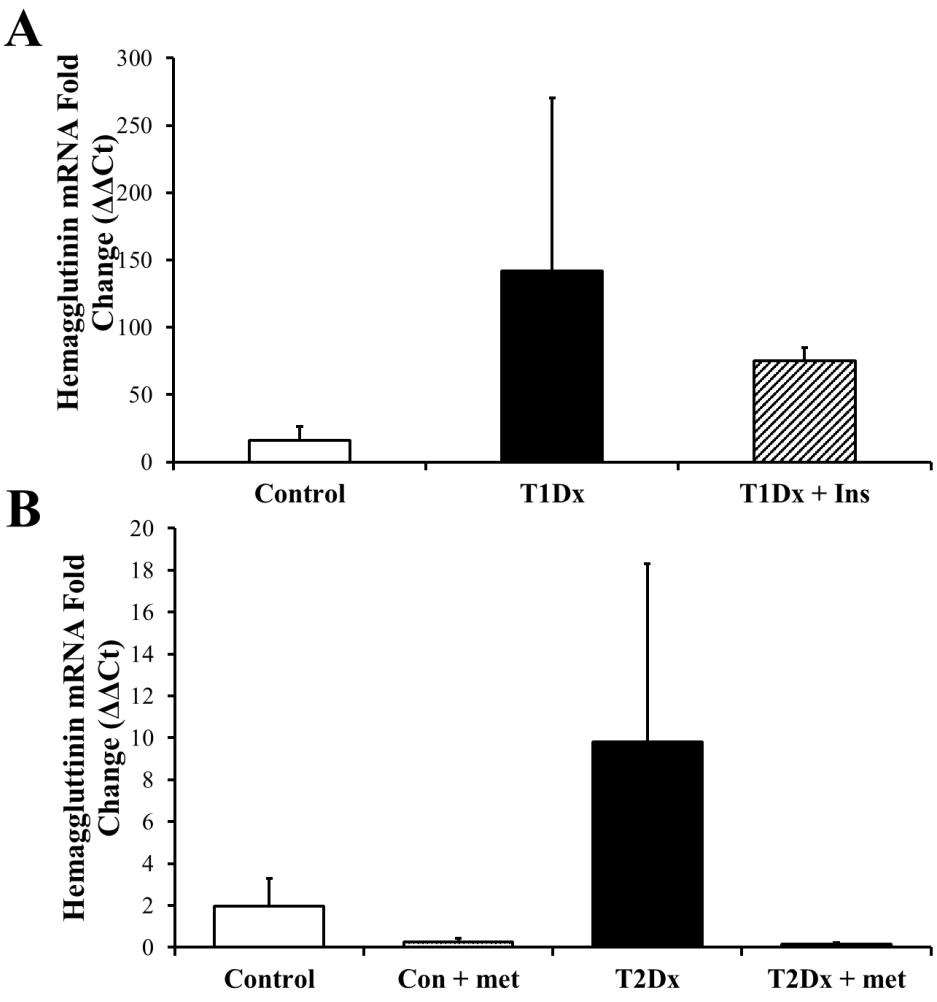

Figure 3. Diabetic mice did not possess a significantly different viral titer from control mice. Mean ± SE of relative mRNA fold change of hemagglutinin in mouse lung from **A)** type 1 diabetic (T1Dx) and **(B)** type 2 diabetic (T2Dx) groups. n=3-4/group. Ins: insulin, Met: metformin, no significance, via one-way ANOVA.

Diabetes and influenza resulted in an increase in glucose concentration in BAL fluid

BALF glucose concentration was measured via spectrophotometric assay of BALF samples collected in chilled sterile PBS (**Figure 4**). In both type 1 (**Fig 4A)** and type 2 (**Fig 4B**) diabetic models, diabetic mice possessed significantly higher concentrations of glucose in the BAL fluid versus their control counterparts ($p=0.003$ and $p=0.028$, respectively). This was rescued with insulin or metformin treatment, respectively. Interestingly, influenza alone also significantly increased BAL fluid glucose concentration, even in infected control mice versus non-infected control counterparts ($p<0.01$ vs. non-infected control). Diabetes and influenza together introduced an additive effect in increasing BAL fluid glucose concentration, and diabetic infected mice also had higher BAL fluid glucose concentration over non-infected diabetic mice. Importantly, insulin and metformin rescued these increases in infected mice down to non-infected control levels.

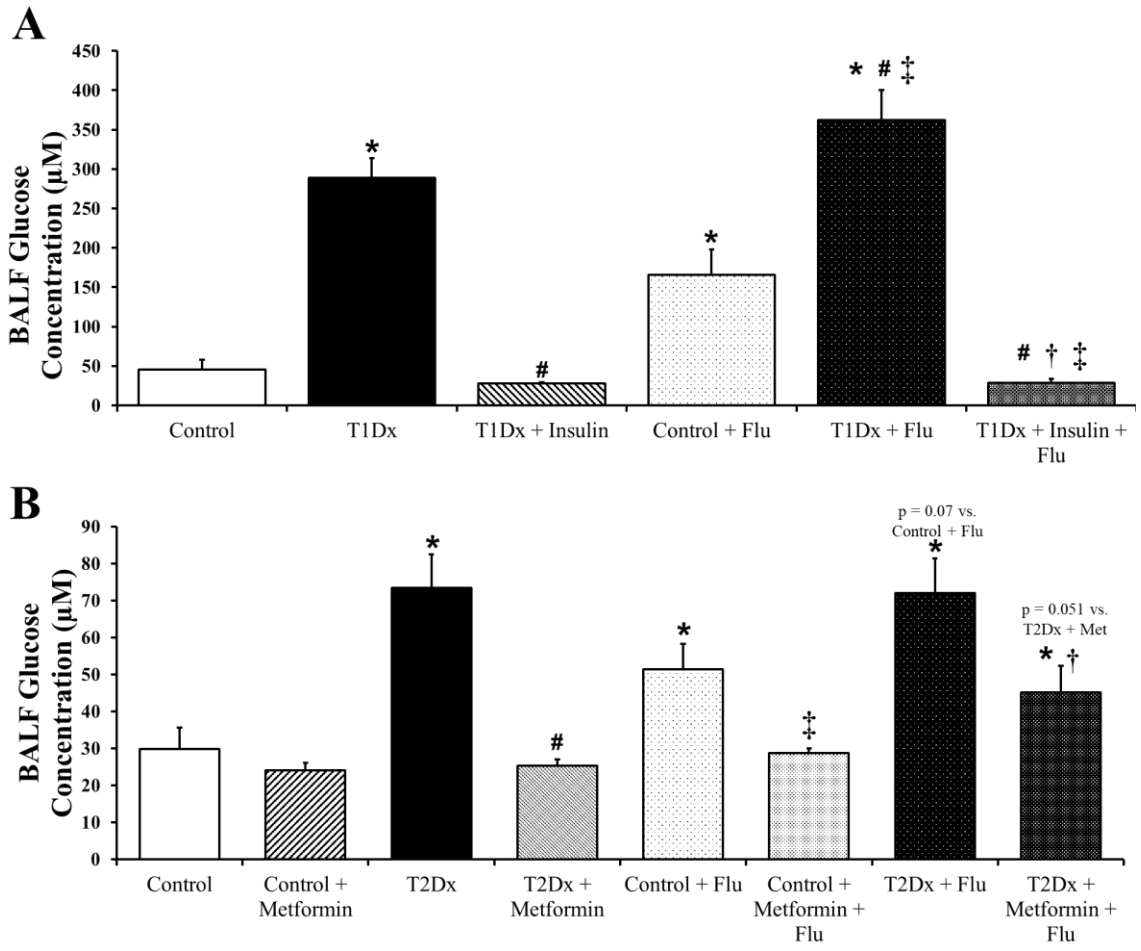

Figure 4. Both diabetic and influenza-infected animals demonstrated higher glucose concentration in the airway, which was rescued with treatment. Mean ± SE of BALF glucose concentrations of **(A)** type 1 diabetic (T1Dx) and **(B)** type 2 diabetic (T2Dx) groups. T1Dx were treated with insulin (T1Dx + Ins) while T2Dx animals were treated with metformin; n=3-6/group,***** $p<0.05$ vs. Control, # $p<0.05$ vs. Diabetic, ‡ $p<0.05$ vs. Control + Influenza (Flu), † $p<0.05$ vs. Diabetic + Flu, via two-way ANOVA.

Significant positive correlation between blood glucose and BAL fluid glucose concentrations

Final blood glucose was measured within 48 hours prior to sacrifice, and BALF glucose was measured via spectrophotometric glucose oxidase assay of BALF samples collected in chilled sterile saline. In both type 1 and type 2 diabetic models, blood glucose was significantly positively correlated with BAL fluid concentrations (**Fig 5**). This finding was consistent in both non-infected (**Fig 5A** & **5C**) and infected (**Fig 5B**) groups, but not for infected type 2 diabetic mice (**Fig 5D**).

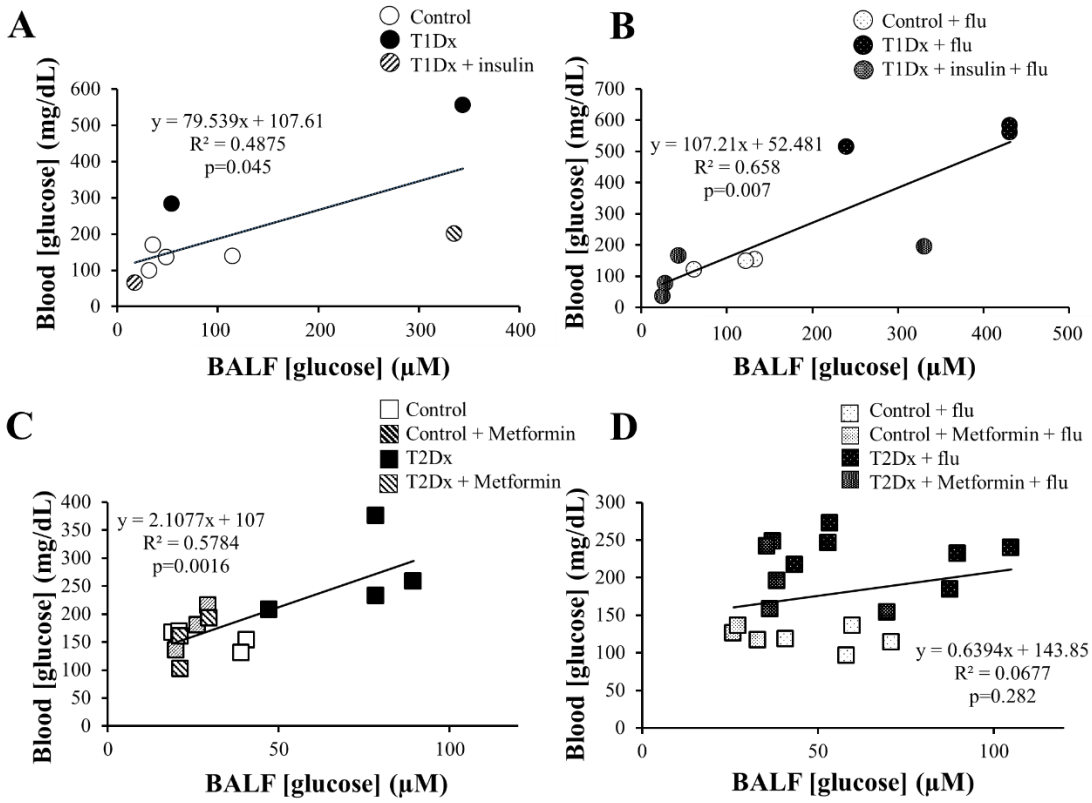

Figure 5. Blood glucose concentration and bronchoalveolar lavage (BAL) fluid glucose concentration are significantly positively correlated in non-infected and infected diabetic mice. Significant positive correlations between blood glucose and BAL fluid glucose concentrations in **(A)** type 1 diabetic (T1Dx) non-infected, **(B)** T1Dx infected, **(C)** type 2 diabetic (T2Dx) non-infected, and **(D)** T2Dx infected groups. T1Dx were treated with insulin while T2Dx animals were treated with metformin. n=3-5/group, via linear regression.

Insulin rescued the increase in lymphocytes and neutrophils in BALF of T1Dx mice

BALF of type 1 diabetic mice was collected in sterile PBS and spun down using a cytological centrifuge. Lymphocytes, macrophages, and neutrophils were counted for each animal, and used to create a total percentage of cells (**Figure 6**). T1Dx mice had a significantly increased percentage of lymphocytes in their BALF compared to control counterparts ($p=0.008$), which was rescued with insulin treatment. In line with known immunological response pathologies, both control and T1Dx mice had a substantial increase in neutrophil percentage apparent 3 days after influenza infection ($p=0.02$ and $p=0.01$ vs. non-infected counterpart, respectively). However, this increase in neutrophils in infected mice was rescued in T1Dx mice treated with insulin.

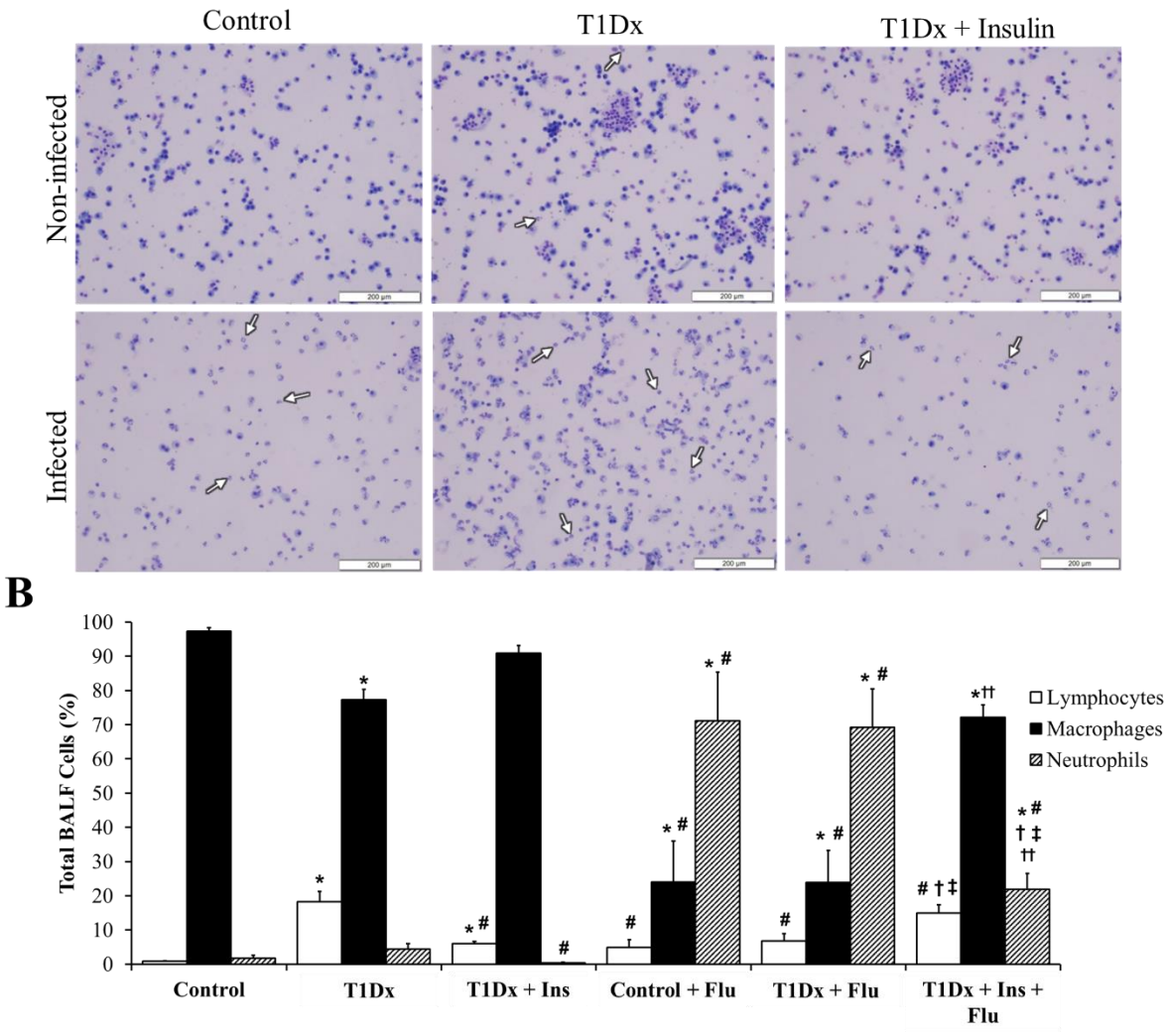

Figure 6. Hyperglycemia causes lymphocytosis in type 1 diabetic infected and non-infected mice, which is rescued with insulin treatment in non-infected mice. Neutrophilia caused by influenza infection is rescued with insulin treatment. A) Representative cytology images from bronchoalveolar lavage fluid (BALF), white arrows indicate neutrophils. **B)** Total immunological cell percentages in BALF. n=3-5/group, ***** $p<0.05$ vs. Control, **#** $p<0.05$ vs. type 1 diabetic (T1Dx), †† $p<0.05$ vs. T1Dx + Insulin (Ins), † $p<0.05$ vs. Control + Flu, ‡ $p<0.05$ vs T1Dx + Flu; via two-way ANOVA.

Metformin treatment rescued the increase in lymphocytes in BALF of T2Dx mice

BALF of type 2 diabetic mice was collected in sterile PBS and spun down using a cytological centrifuge. Lymphocytes, macrophages, and neutrophils were counted for each animal, and used to create a total percentage of cells (**Figure 7**). T2Dx mice had a significantly increased percentage of lymphocytes in their BALF compared to control counterparts ($p=0.035$), which was rescued with metformin treatment. All infected groups had a significant increase in the percentage of neutrophils over their non-infected counterparts ($p<0.05$), but there was no difference in cytological percentages between infected groups.

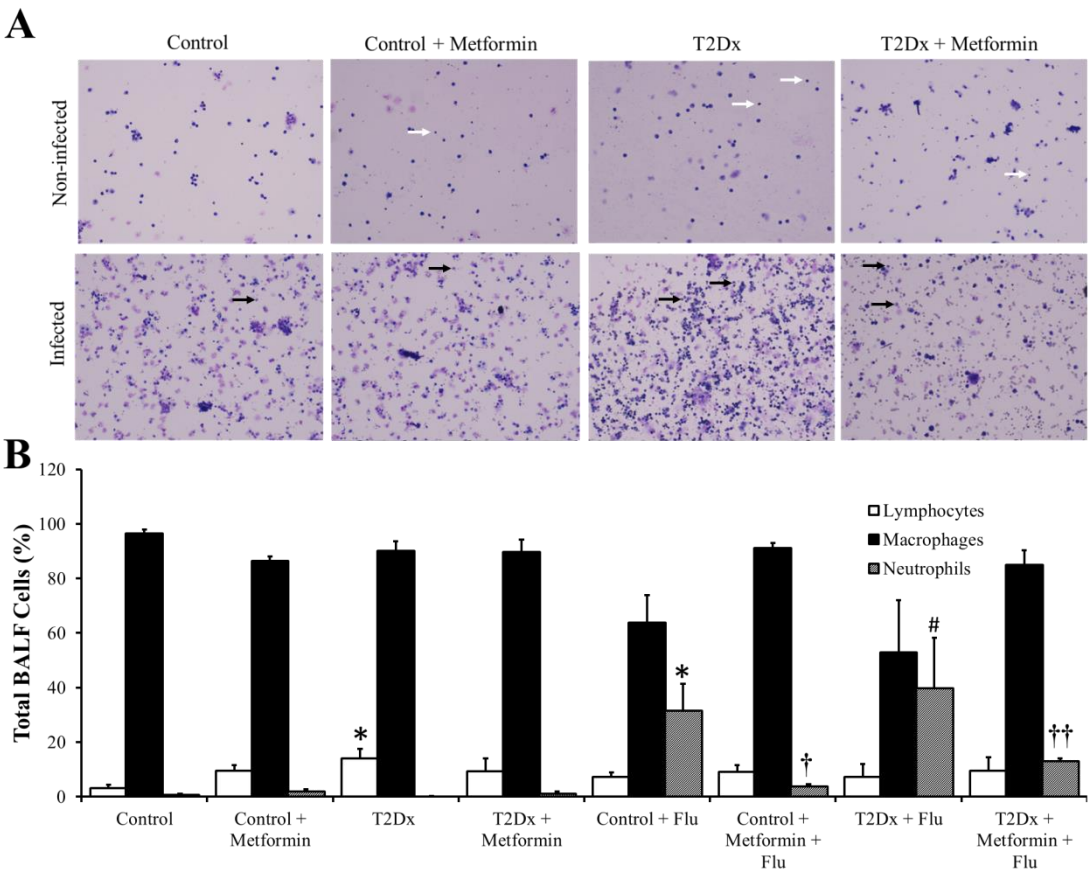

Figure 7. Lymphocytosis results from type 2 diabetes, and influenza causes neutrophilia. A) Representative cytology images from bronchoalveolar lavage fluid (BALF), white arrows indicate lymphocytes, while black arrows indicate neutrophils. **B)** Total immunological cell percentages in BALF. n=3/group, ***** $p<0.05$ vs. Control, **#** $p<0.05$ vs. type 2 diabetic (T2Dx), †† $p<0.05$ vs. T2Dx + Metformin, † $p<0.05$ vs. Control + Flu, ‡ $p<0.05$ vs T2Dx + Flu; via two-way ANOVA.

Type 1 diabetic mice demonstrated significant alteration to GLUT protein expression in the upper lung during influenza infection

The upper lung portion of adult rodent lung was analyzed for protein expression via Western blot (**Figure 8**). There were no significant differences between groups regarding GLUT1, GLUT2, or GLUT8 protein in the upper lung (**Fig 8A, 8B, & 8D**). GLUT4 total protein was significantly downregulated in the upper lung of the type 1 diabetic group of both infected and non-infected mice, compared to their relative controls ($p<0.05$, **Fig 8C**). GLUT10 total protein was significantly decreased in the upper lung of non-infected diabetic mice versus their non-infected counterparts ($p=0.032$), but this was not true for the infected mice (**Fig 8E**). Finally, GLUT12 total protein expression was significantly increased in the upper lung of both infected and non-infected type 1 diabetic compared to their control counterparts ($p<0.05$, **Fig 8F**).

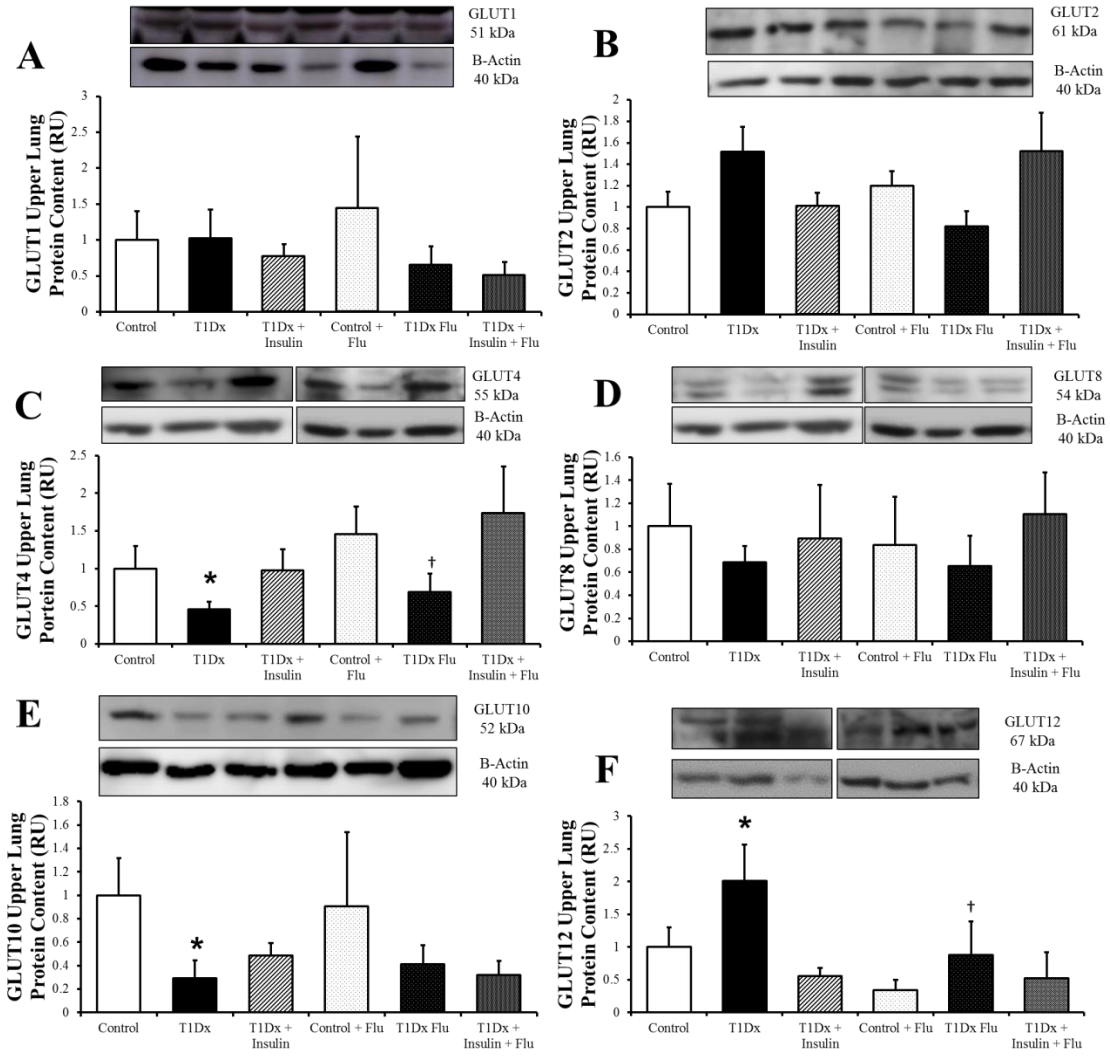

Figure 8. Type 1 diabetic mice infected with influenza possessed significant alterations of GLUT protein expression in the upper lung. Top panels, representative Western blots, bottom panels, mean ± SE of average protein quantification from the upper lung from the type 1 diabetic group. **(A)** GLUT1, **(B)** GLUT2, **(C)** GLUT4, **(D)** GLUT8, **(E)** GLUT10, **(F)** GLUT12. n=9-12/group. * $p<0.05$ vs control, † $p<0.05$ vs Control + Flu, via two-way ANOVA.

Type 1 diabetic mice demonstrated significant alteration of GLUT protein expression in the lower lung during influenza infection

The lower lung portion of adult rodent lung was analyzed for protein expression via Western blot (**Figure 9**). There were no significant differences between groups regarding GLUT2 or GLUT8 protein in the lower lung (**9B, & 9D**). GLUT1 total protein was significantly decreased in the non-infected type 1 diabetic lung compared to control ($p=0.009$), but this difference was not evident in infected mice (**Fig 9A**). GLUT4 total protein was significantly downregulated in the lower lung of the type 1 diabetic group of both infected and non-infected mice, compared to their relative controls ($p<0.001$, **Fig 9C**). There was a decrease of GLUT10 total protein in the lower lung of infected diabetic mice versus their infected control counterparts ($p=0.011$), but this was not true for the non-infected mice (**Fig 9E**). Finally, GLUT12 total protein expression was significantly increased in the lower lung of non-infected type 1 diabetic mice, while being significantly decreased in the infected type 1 diabetic mice, compared to their relative control counterparts ($p<0.05$, **Fig 9F**).

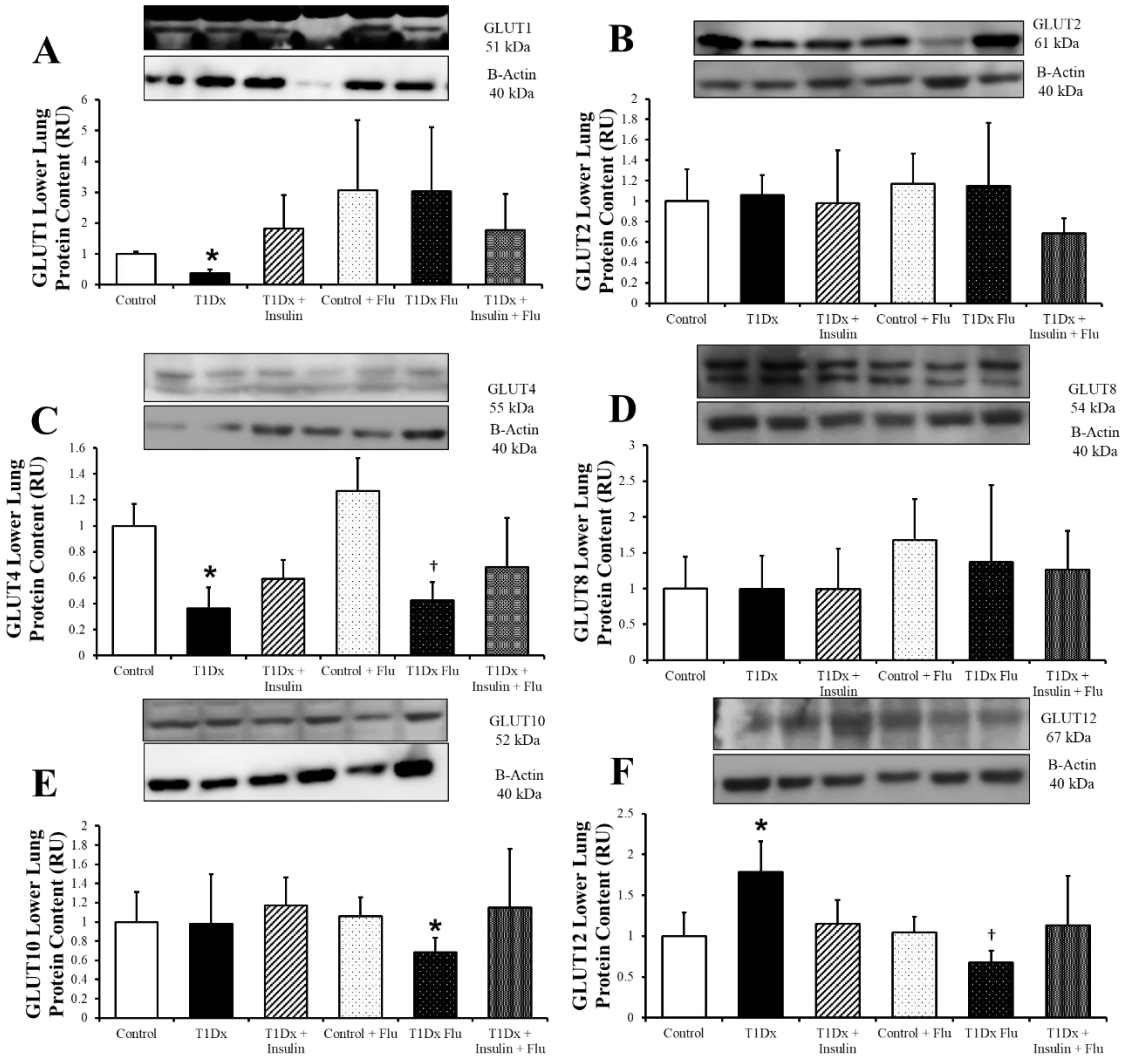

Figure 9. Type 1 diabetic mice infected with influenza possessed significant alterations to GLUT protein expression in the lower lung. Top panels, representative Western blots, bottom panels, mean ± SE of average protein quantification from the lower lung from the type 1 diabetic group. **(A)** GLUT1, **(B)** GLUT2, **(C)** GLUT4, **(D)** GLUT8, **(E)** GLUT10, **(F)** GLUT12. n=9-12/group. * $p<0.05$ vs control, † $p<0.05$ vs Control + Flu, via two-way ANOVA.

Type 2 diabetic mice demonstrated significant alteration to GLUT protein expression in the upper lung during influenza infection

The upper lung portion of adult rodent lung was analyzed for protein expression via Western blot (**Figure 10**). There were no significant differences between groups regarding GLUT1, GLUT2, or GLUT10 protein expression in the upper lung of type 2 diabetic mice (**Fig 10A, 10B, & 10D**). There was a significant downregulation of GLUT4 protein in the upper lung of both the infected and non-infected type 2 diabetic mice compared to their relevant controls ($p<0.05$, **Fig 10A**). In the type 2 diabetic upper lung, there was a trend of a decrease of GLUT10 protein in the infected control, infected diabetic, and infected treated diabetic mice compared to each of their non-infected counterparts ($p<0.1$, **Fig 10E**). GLUT12 protein expression in the upper lung was increased in both infected and non-infected type 2 diabetic mice compared to their relevant controls ($p<0.01$, **Fig 10F**).

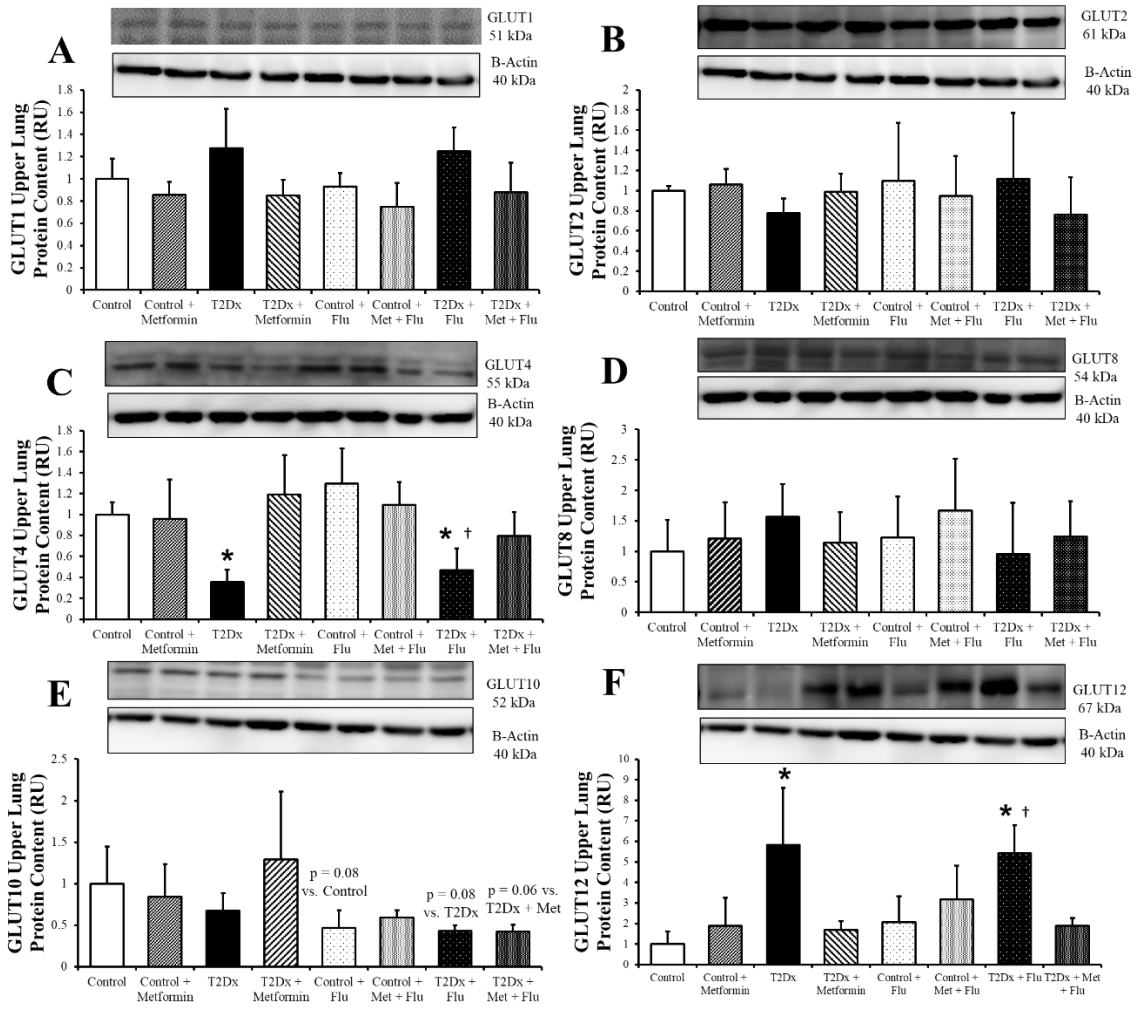

Figure 10. Type 2 diabetic mice infected with influenza possessed significant alterations to GLUT protein expression in the upper lung. Top panels, representative Western blots, bottom panels, mean ± SE of average protein quantification from the upper lung from the type 2 diabetic group. **(A)** GLUT1, **(B)** GLUT2, **(C)** GLUT4, **(D)** GLUT8, **(E)** GLUT10, **(F)** GLUT12. n=9-12/group. * $p<0.05$ vs control, † $p<0.05$ vs Control + Flu, via one-way ANOVA.

Type 2 diabetic mice demonstrated significant alteration to GLUT protein expression in the lower lung during influenza infection

The lower lung portion of adult rodent lung was analyzed for protein expression via Western blot (**Figure 11**). There were no significant differences between groups regarding GLUT2, GLUT4, GLUT8, or GLUT12 protein in the lower lung of type 2 diabetic mice (**Fig 10B, 10C, 10D & 10F**). There was a significant upregulation of GLUT1 protein in the lower lung of infected type 2 diabetic mice compared to their infected controls ($p=0.013$), but this difference was not evident in the non-infected cohort (**Fig 10A**). GLUT10 total protein expression was significantly decreased in the lower lung of non-infected type 2 diabetic mice compared to non-infected controls, and was significantly increased in the lower lung of infected control mice treated with metformin over infected control mice ($p<0.05$, **Fig 10E**).

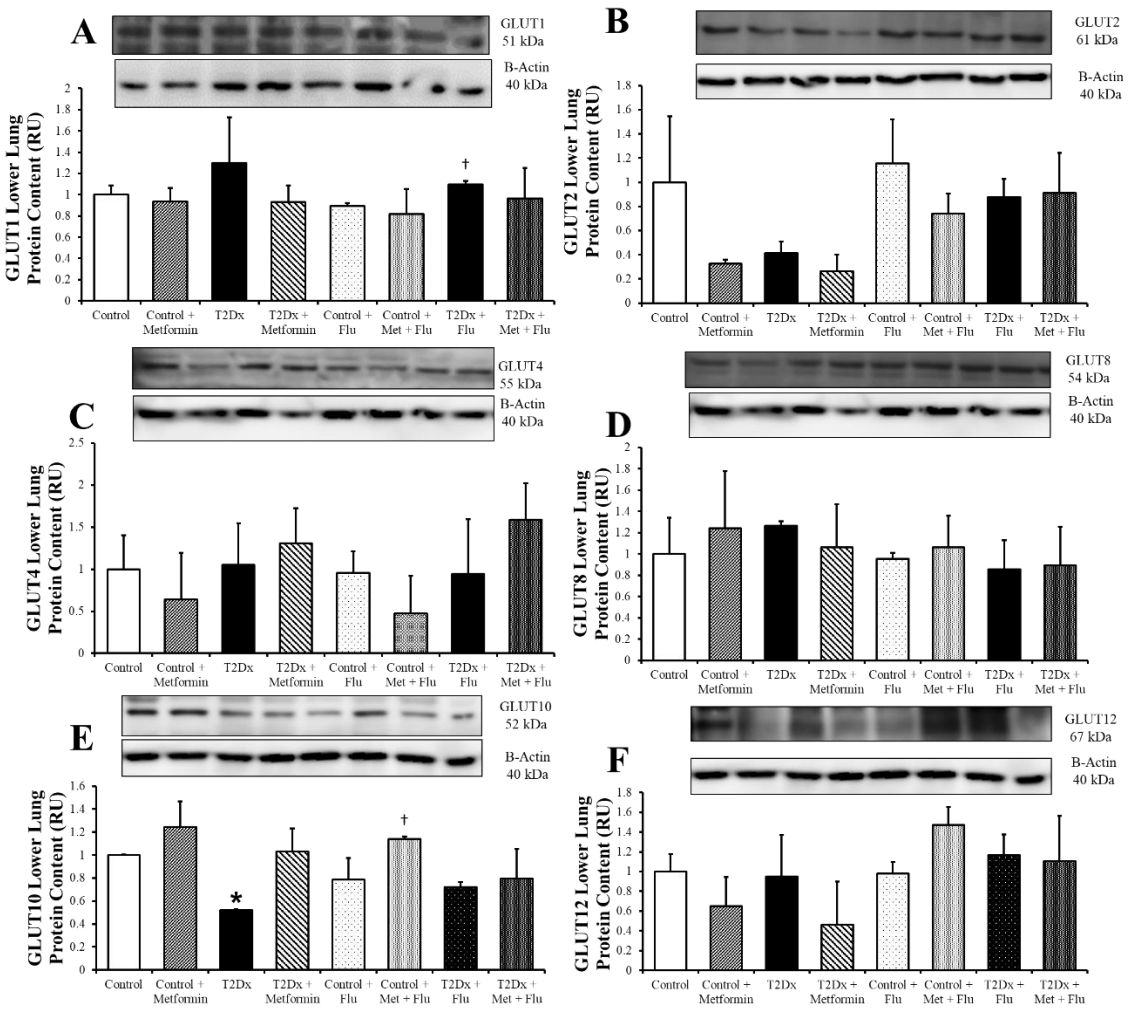

Figure 11. Type 2 diabetic mice infected with influenza possessed significant alterations to GLUT protein expression in the lower lung. Top panels, representative Western blots, bottom panels, mean ± SE of average protein quantification from the lower lung from the type 2 diabetic group. **(A)** GLUT1, **(B)** GLUT2, **(C)** GLUT4, **(D)** GLUT8, **(E)** GLUT10, **(F)** GLUT12. n=9-12/group. * $p<0.05$ vs control, † $p<0.05$ vs Control + Flu, via two-way ANOVA.

Influenza resulted a significant upregulation of cell surface GLUT4 protein expression

Whole lung from adult mice was separated into cell surface and intracellular fractions before analyzing each fraction for protein expression of GLUT4 via Western blot (**Figure 12**). Cell surface GLUT4 was significantly increased in mice infected with flu versus their non-infected counterparts. Type 1 diabetic mice possessed significantly less cell-surface GLUT4 protein versus their control counterparts, which was rescued with *in vivo* insulin treatment ($p<0.05$, **Fig 12A**). Similarly, type 2 diabetic mice possessed significantly less cell-surface GLUT4 protein versus their control counterparts, which was rescued with metformin treatment, and control infected mice possessed significantly more cell-surface GLUT4 protein than non-infected control counterparts ($p<0.05$, **Fig 12B**). For both type 1 and type 2 diabetic models, the decrease in the diabetic group versus the control group was true for the infected and non-infected cohorts.

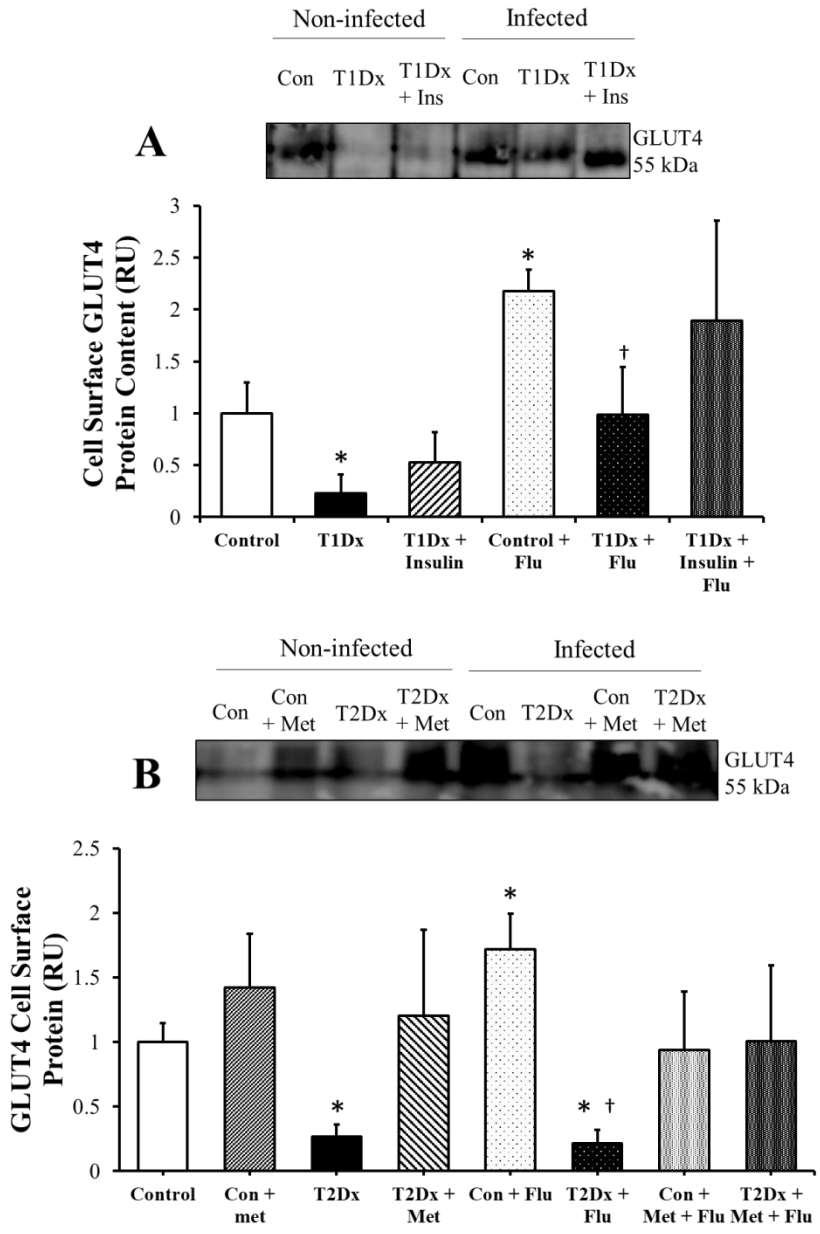

Figure 12. Influenza infection increased cell surface GLUT4 protein in control and diabetic mice, which was rescued by insulin or metformin treatment. Top panels, representative Western blots, bottom panels, mean ± SE of average GLUT4 protein quantification from the cell surface of whole lung from **(A)** the type 1 diabetic group, and **(B)** the type 2 diabetic group. n=3-4/group. * $p<0.05$ vs control, † $p<0.05$ vs Control + Flu, via two-way ANOVA.

Influenza resulted in a significant increase in hemorrhage, inflammatory cell infiltration, and vasculitis in the lung of control and type 1 diabetic mice

Whole lung from adult control, type 1 diabetic, or treated type 1 diabetic mice was perfused with paraformaldehyde upon sacrifice, and thereafter embedded in paraffin wax and sectioned into 4μm thick sections before being stained with hematoxylin and eosin (**Figure 13**). Histological scoring was completed via a blinded third party pathology specialist. Infected mice of any group demonstrated significant increases in hemorrhage, vasculitis, and inflammatory cell infiltration over their non-infected counterparts.

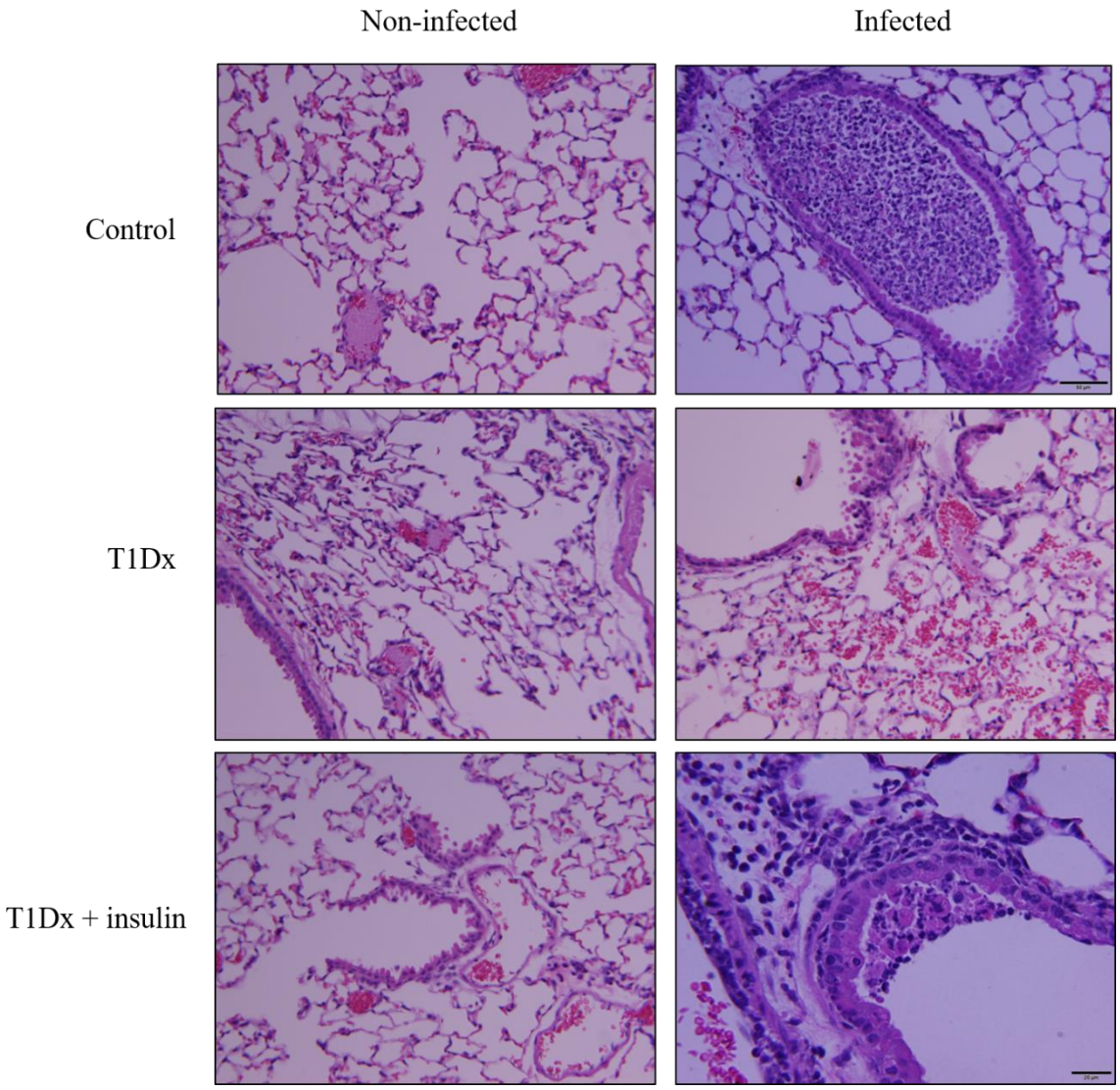

Figure 13. Influenza caused a significant increase in hemorrhage, vasculitis, and inflammatory cell infiltration in control, type 1 diabetic, and treated type 1 diabetic mice. (A) Representative images from hematoxylin & eosin stained whole left lungs from control, type 1 diabetic (T1Dx), and T1Dx mice treated with insulin. **(B)** Mean ± SE quantification of scoring of H&E-stained slides. n=4/group.

Influenza resulted in a significant increase in hemorrhage, inflammatory cell infiltration, and vasculitis in the lung of control and type 2 diabetic mice

Whole lung from adult control, control treated with metformin, type 2 diabetic, or treated type 2 diabetic mice was perfused with paraformaldehyde upon sacrifice, and thereafter embedded in paraffin wax and sectioned into 4μm thick sections before being stained with hematoxylin and eosin (**Figure 14**). Histological scoring was completed via a blinded third party pathology specialist. Infected mice of any group demonstrated significant increases in hemorrhage, vasculitis, and inflammatory cell infiltration over their non-infected counterparts.

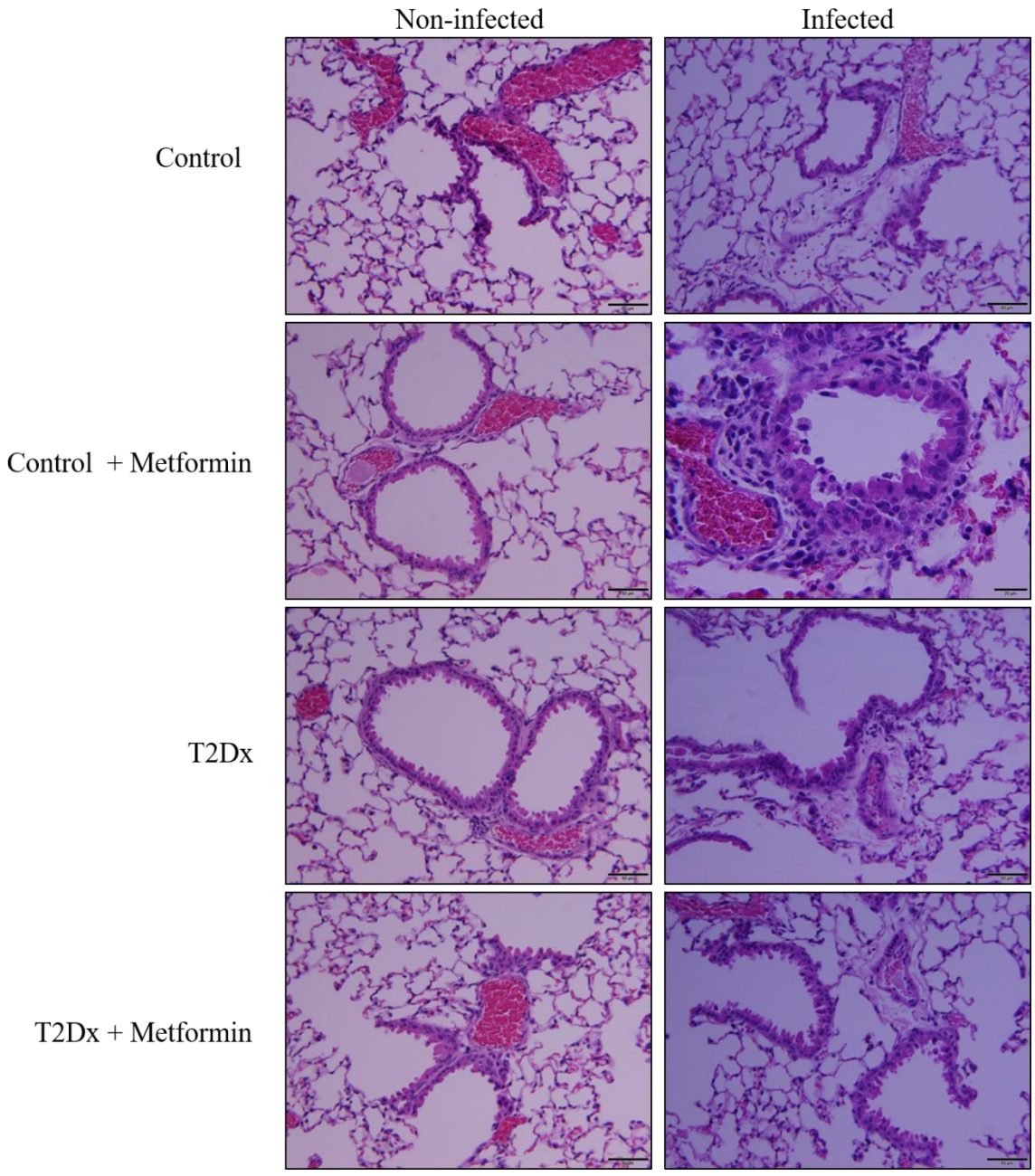

Figure 14. Influenza caused a significant increase in hemorrhage, vasculitis, and inflammatory cell infiltration in control, type 2 diabetic, and treated type 2 diabetic mice. **(A)** Representative images from hematoxylin & eosin stained whole left lungs from control, control treated with metformin, type 2 diabetic (T2Dx), and T2Dx mice treated with metformin. **(B)** Mean ± SE quantification of scoring of H&E-stained slides. n=3/group.

GLUT4 immunohistochemistry reveals an increase in GLUT4 localized to the bronchial epithelium in control and insulin-treated mice, but not in type 1 diabetic mice, during influenza

Whole lung from adult control, type 1 diabetic, or treated type 1 diabetic mice was perfused with paraformaldehyde upon sacrifice, and thereafter embedded in paraffin wax and sectioned into 4µm thick sections before being stained with primary antibodies specific to GLUT4 **(Figure 15)**. In general, GLUT4 appears to be localized to the bronchial epithelium, alveolar type II cells, and alveolar macrophages. Interestingly, an increase in GLUT4 localized to the bronchial epithelium was noted after influenza infection in control and insulin-treated mice, but not in type 1 diabetic mice.

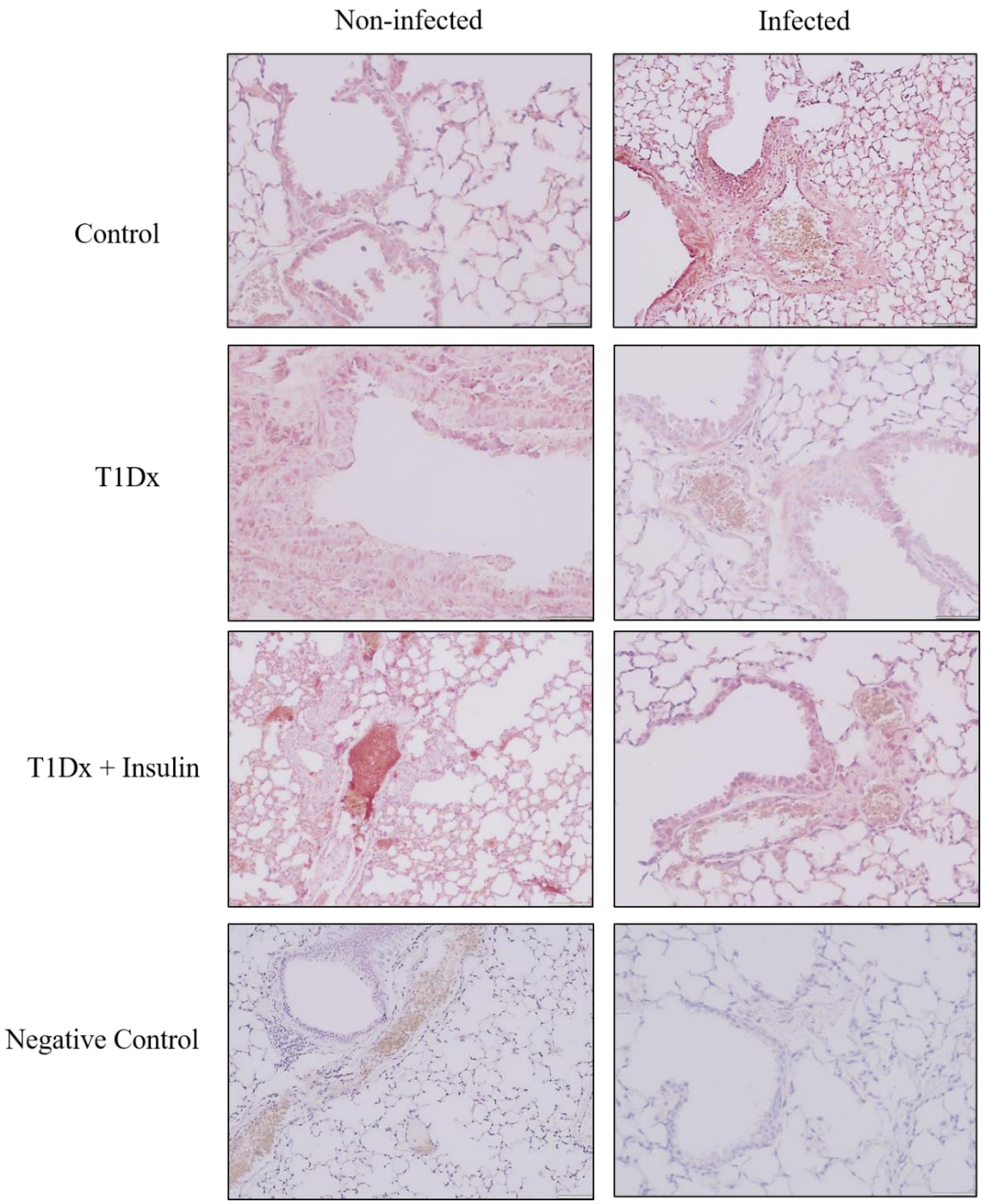

Figure 15. Influenza-infected mice possessed stronger immunohistochemical GLUT4 staining than non-infected mice in the bronchial epithelium in control and insulin-treated mice, but not in type 1 diabetic mice. Representative images from immunohistochemical GLUT 4-stained whole left lungs from control, type 1 diabetic (T1Dx), and T1Dx mice treated with insulin. Brown color indicates positive result, purple color indicates negative result. n=4/group.

GLUT4 immunohistochemistry reveals a decrease in GLUT4 localized to the bronchial epithelium in type 2 diabetic mice, which is rescued with metformin treatment, in both infected and non-infected mice.

Whole lung from adult control, treated control, type 2 diabetic, or treated type 2 diabetic mice was perfused with paraformaldehyde upon sacrifice, and thereafter embedded in paraffin wax and sectioned into 4μm thick sections before being stained with a primary antibody specific to GLUT4 **(Figure 16)**. Similar to Figure 15, GLUT4 appears to be localized to the bronchial epithelium, alveolar type II cells, and alveolar macrophages. A substantial decrease of GLUT4 staining is noted in type 2 diabetic mice in both the infected and non-infected groups, which is rescued with metformin treatment.

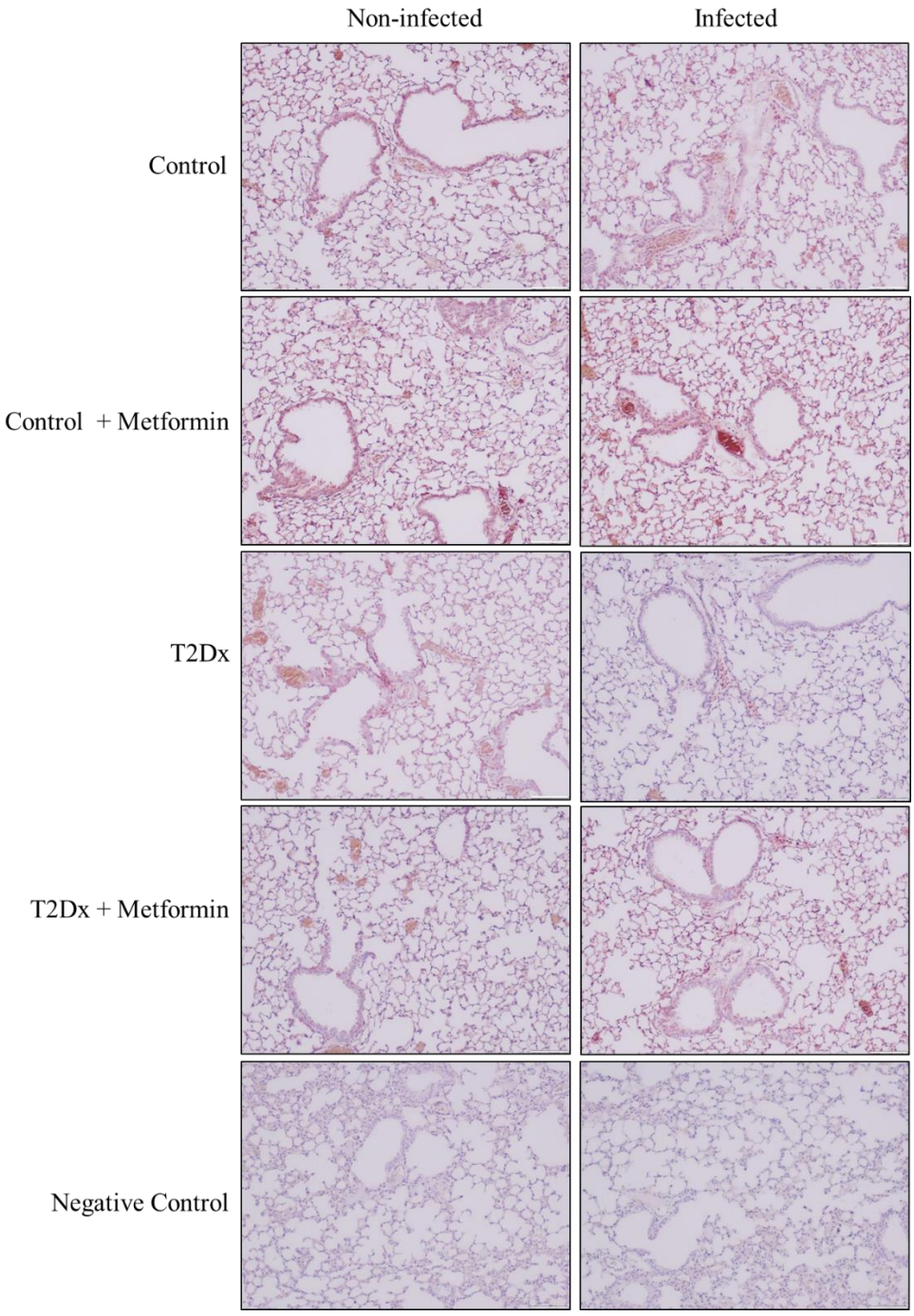

Figure 16. Type 2 diabetes causes a decrease in immunohistochemical GLUT4 staining in the bronchial epithelium, which is rescued by metformin treatment. Representative images from immunohistochemical GLUT 4-stained whole left lungs from control, control treated with metformin, type 2 diabetic (T2Dx), and T2Dx mice treated with metformin. Brown color indicates positive result, purple color indicates negative result. n=3/group.

GLUT10 immunohistochemistry reveals an increase in GLUT10 localized to the bronchial epithelium in control, type 1 diabetic, and treated type 1 diabetic mice infected with influenza

Whole lung from adult control, type 1 diabetic, or treated type 1 diabetic mice was perfused with paraformaldehyde upon sacrifice, and thereafter embedded in paraffin wax and sectioned into 4μm thick sections before being stained with a primary antibody specific to GLUT10 **(Figure 17)**. In non-infected mice, GLUT10 appears to be localized to the alveolar type I and type II cells. Conversely, 3 days post-infection with influenza, the lung from adult mice demonstrated a marked increase in expression in the alveolar cells, as well as substantial expression in the bronchial epithelium. These observations in both non-infected and infected mice were true for control, type 1 diabetic, and insulin-treated diabetic mice.

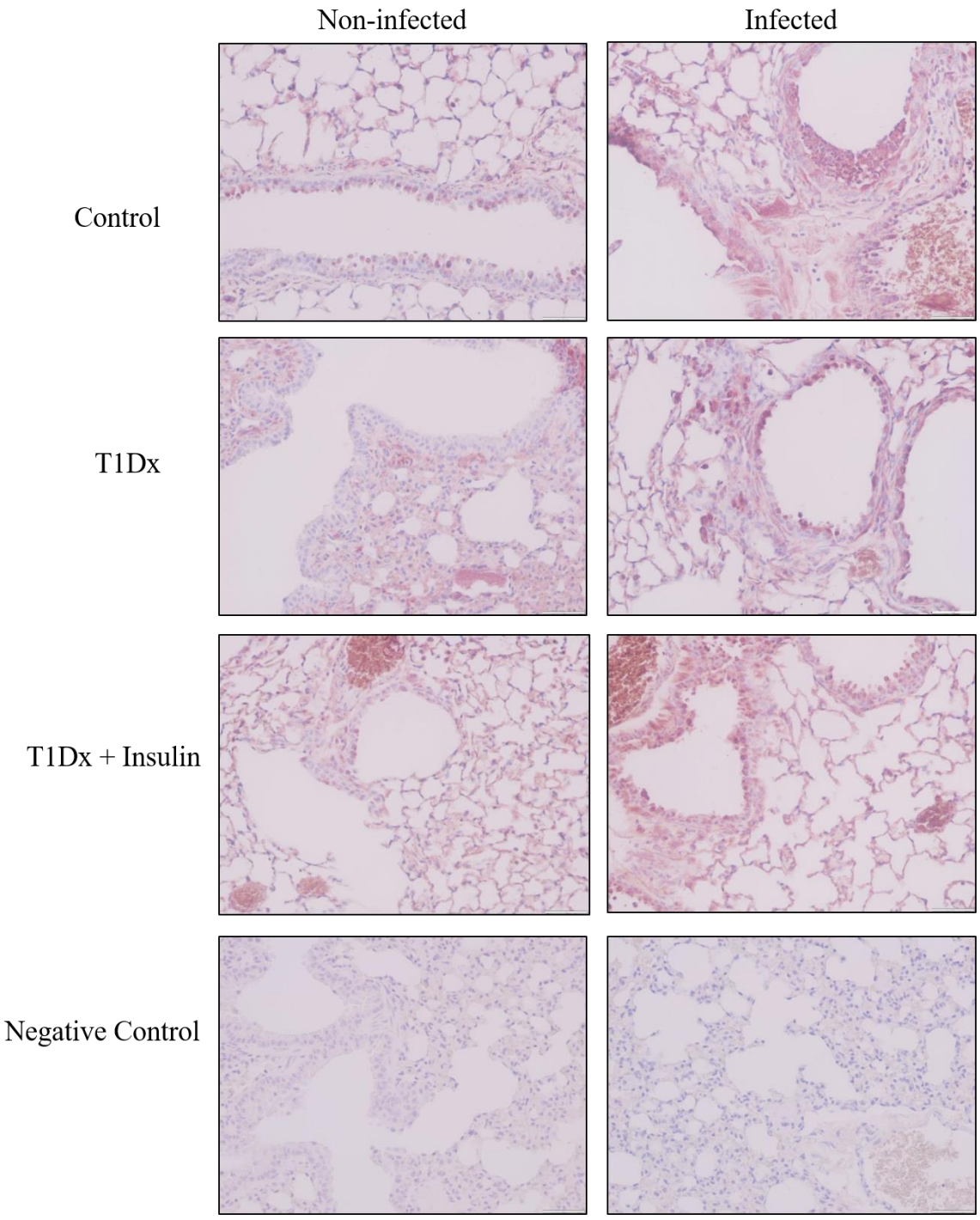

Figure 17. Influenza causes an increase in immunohistochemical GLUT10 staining in the bronchial epithelium. Representative images from immunohistochemical GLUT 10-stained whole left lungs from control, type 1 diabetic (T1Dx), and T1Dx mice treated with insulin. Brown color indicates positive result, purple color indicates negative result. n=4/group.

GLUT10 immunohistochemistry reveals an increase in GLUT10 localized to the bronchial epithelium in control, type 2 diabetic, and treated type 2 diabetic mice infected with influenza

Whole lung from adult control, treated control, type 2 diabetic, or treated type 2 diabetic mice was perfused with paraformaldehyde upon sacrifice, and thereafter embedded in paraffin wax and sectioned into 4μm thick sections before being stained with a primary antibody specific to GLUT10 **(Figure 18)**. In non-infected mice, GLUT10 appears to be localized to the alveolar type I and type II cells. Conversely, 3 days post-infection with influenza, the lung from adult mice demonstrated a marked increase in GLUT10 expression in the alveolar cells, as well as substantial expression in the bronchial epithelium. These observations in both non-infected and infected mice were true for all groups.

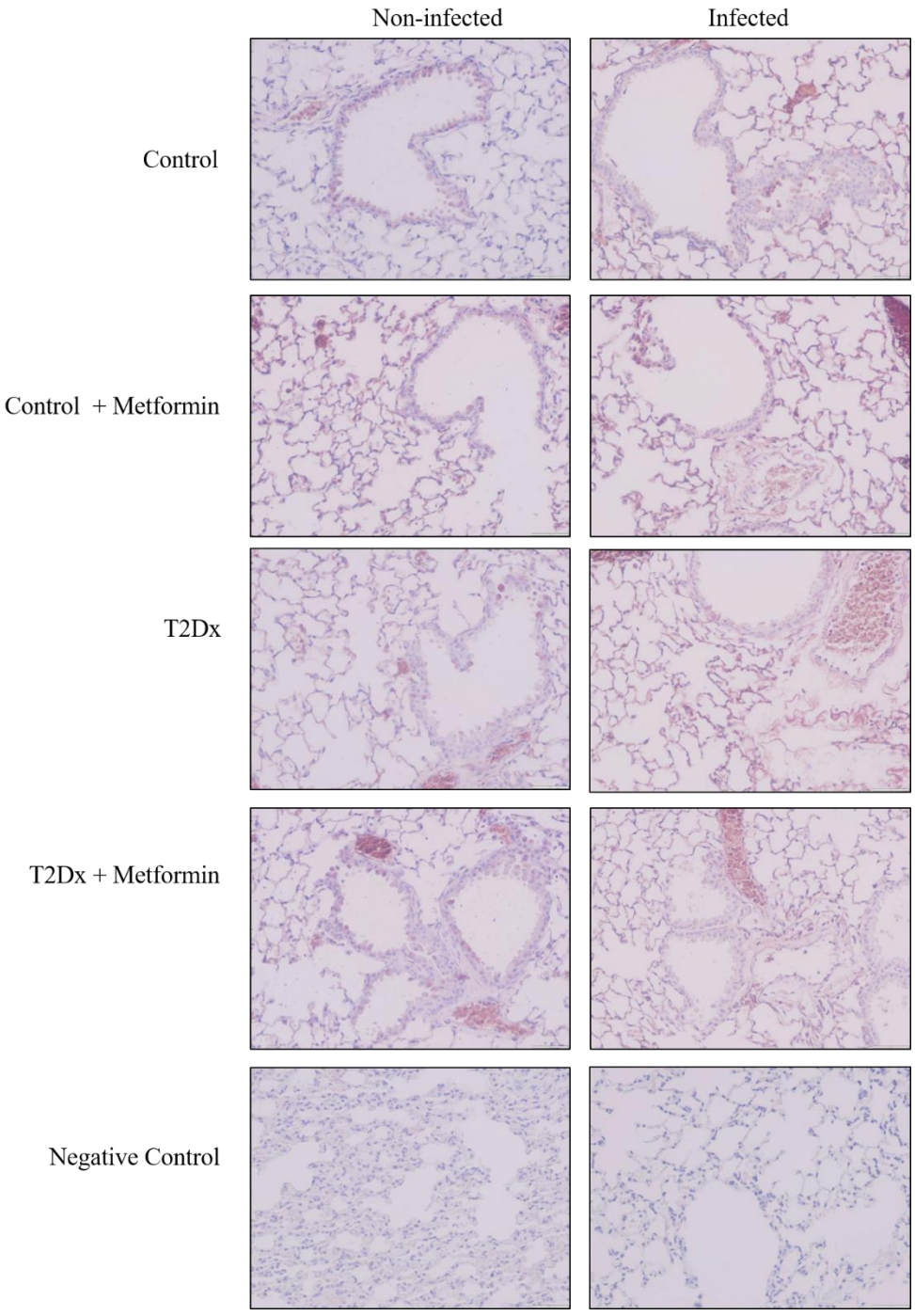

Figure 18. Influenza causes an increase in immunohistochemical GLUT10 staining in the bronchial epithelium. Representative images from immunohistochemical GLUT 10-stained whole left lungs from control, control treated with metformin, type 2 diabetic (T2Dx), and T2Dx mice treated with metformin. Brown color indicates positive result, purple color indicates negative result. n=3/group.

GLUT4 immunofluorescence confirms GLUT4 localization predominately to the bronchial epithelium

Whole lung from adult control, type 1 diabetic, or treated type 1 diabetic mice was perfused with paraformaldehyde upon sacrifice, and thereafter embedded in paraffin wax and sectioned into 4µm thick sections before being stained with a primary antibody specific to GLUT4 **(Figure 19)**. In non-infected mice GLUT4 appears to be localized to the bronchial epithelium with moderate quantities of GLUT4 staining appearing in the alveoli. 3 days post-infection with influenza, the lung from adult mice appears to increase in GLUT4 staining in the terminal bronchiole, respiratory bronchiole, and the alveoli.

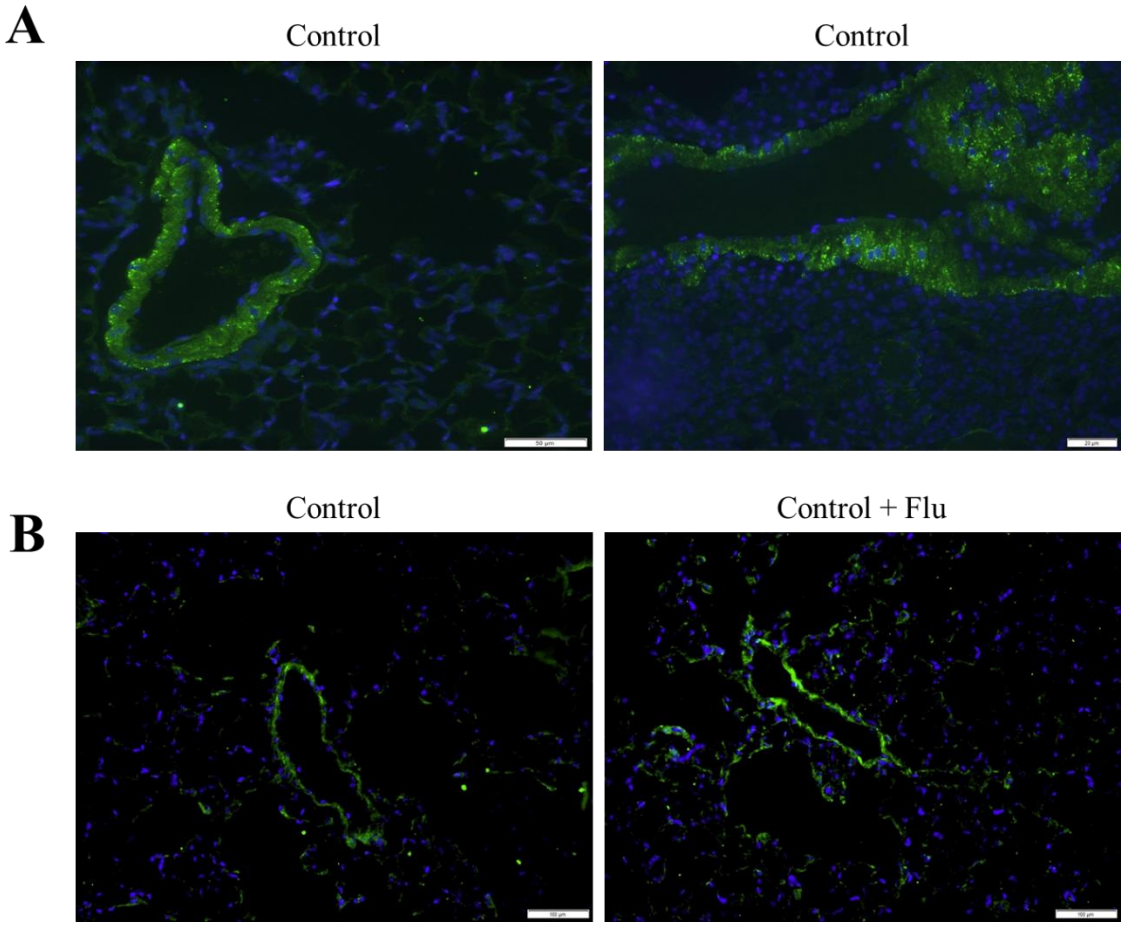

Figure 19. Immunofluorescent GLUT4 staining confirms GLUT4 localization to the bronchial epithelium in non-diabetic (control) mice. Representative images from immunohistochemical GLUT 4-stained whole left lungs in A) bronchioles from control mice and B) terminal and respiratory bronchioles and alveoli in control and infected control mice. Blue: DAPI, Green: GLUT4.

DISCUSSION

The Centers for Disease Control has recently identified that diabetic patients are at roughly a three times greater risk for complications and death from pulmonary infection than their non-diabetic counterparts.[11, 12, 288] Furthermore, recent studies indicate that obese individuals may possess a reduction in efficacy to the influenza vaccine.[313] Despite this, and the relatively active metabolic nature of the lungs, glucose homeostasis in the lung has so far remained elusive. Baker et al. has recently identified the concentration of glucose in the airway is consistently roughly 12.5 times less than that of the concentration of glucose in the blood.[295] It is presently hypothesized that glucose diffuses passively into the airway, but requires facilitated glucose transport to be taken out of the airway, and into the epithelial cells of the lung.[51] Therefore, understanding the function of glucose transporters (GLUTs) in the lung is of vital importance, especially in the context of diabetes compounded with respiratory infection. To our knowledge, no previous study has specifically examined the relationship of the GLUT isoforms in the lung during both type 1 and type 2 diabetes in an adult rodent model during influenza infection.

Type 1 diabetes is characterized by severe hyperglycemia created by a lack of insulin production, while type 2 diabetes is characterized by insulin resistance (often accompanied by obesity and inflammation) which is caused by a lack of insulin action. Of those suffering from diabetes mellitus, type 2 diabetes represents over 90% of all those afflicted in the United States[297] and in the world,[298] while the remainder suffer from type 1 diabetes. Though these two diseases share many similarities, it is critically

important to understand what alterations are due to hyperglycemia alone versus those due to hyperinsulinemia, inflammation, and obesity. In order to understand the alterations caused by hyperglycemia alone, versus those likely caused by obesity-related complications, we investigated diabetes-involved influenza by using both a type 1 diabetic and a type 2 diabetic mouse model. Along these same lines, we sought to prevent the introduction of genetic variables by not using genetically modified animals to imitate the diabetic condition. Instead, we here chose to use a highly reproducible low-dose streptozotocin protocol which induces moderate hyperglycemia (while maintaining normal body weight and insulin sensitivity) with little-to-no unintentional side effects.[68, 314] For our type 2 diabetic model, we used a 60% kilocalorie-from-fat diet, which produces extremely obese mice with hyperinsulinemia and only mild hyperglycemia.[294] These mice have been shown previously by our lab to be both glucose and insulin intolerant.[294]

In this study, we treated diabetic mice with either insulin (in the case of type 1 diabetic mice) or metformin (in the case of type 2 diabetic mice) in order determine whether any changes in GLUT protein expression, BALF glucose concentration, viral titer, or BALF cytology were reversible upon amelioration of hyperglycemia, specifically. Importantly, both of these treatments are already widely used in human patients, and thus render the results here highly applicable to human outcomes. Furthermore, the reversibility of alterations in glucose transport in the lung during type 1 diabetic mice in particular additionally lends to the idea that any alterations are due to hyperglycemia alone, and not to possible streptozotocin toxicity. Additionally, metformin did not affect the weight of

either of control or type 2 diabetic mice which were treated with it, which further enforces the probability that rescue of hyperglycemia is sufficient to amend alterations in pulmonary glucose homeostasis detected during type 2 diabetes. Finally, while we do not attempt to make any statistical comparisons between the type 1 and type 2 diabetic models, one limiting factor of this study is the differing backgrounds of our mice (type 1 diabetic mice were on an FVB/N background while type 2 diabetic mice were on a C57BL/6 background). However, as our lab has determined previously[294, 315] and has been published,[299] these two strains are decidedly comparable due to their high similarity in terms of insulin secretion from islet cells, blood glucose, and GLUT protein expression in striated muscle.

In order to examine the discreet differences between healthy and diabetic mice during influenza infection, we chose to use a low dose of influenza inoculation (250 PFU delivered intranasally). Also, based on previously published data indicating a possible increase of viral titer during diabetes at a low dose of influenza,[309] we also chose to examine the changes in viral titer between control and diabetic mice based on different days post infection. We determined here that 3 days post infection produced the highest viral titer in both control and diabetic mice compared to 5 and 7 days post infection (data not shown). This is in agreement with previously published data regarding control and diabetic influenza-infected mice of various strains of flu.[309, 316] The published data regarding influenza viral titer in diabetic mice is somewhat varied. Previous studies have separately reported an increase of viral titer in both type 1 and type 2 diabetic mice ,[309, 317] as well as no change between control and diabetic mice.[208, 309, 316] While at first glance

it may seem that the results of these differences in diabetic mice may be dependent on strain of influenza, there is variation in reports among even a single strain, such as H1N1 A/PR/8/34.[309, 317] Similarly, there is not a specific consistency between either type 1 or type 2 diabetic mice, as both have been reported to possess higher viral titer than control mice,[209, 309, 318] or to have equal viral titer to control mice.[208, 309, 316] Here, we found no significant differences in viral titer between control and diabetic groups as measured by either MDCK plaque assay of BALF (data not shown) or fold change of hemagglutinin mRNA of the lung. However, in both of our models, insulin and metformin reduced the variability in viral titer and maintained the titer to at or below control levels in all animals within those groups. This result would indicate that, while there may be other significant variables in any diabetic model which would influence severity of influenza infection, metabolic derangements resulting from diabetes alone, in combination with a low dose of viral inoculation, may not produce significant alteration to viral titer.

Glucose concentration of BALF as an estimation for glucose concentration of the airway surface liquid has recently been identified as a crucial parameter of pulmonary glucose homeostasis and pulmonary infection.[204] Non-infected control mice between our two diabetic models possessed similar BALF glucose concentrations (30-50 μM), which is in line with other reports of BALF glucose concentration in mice.[206] Interestingly, this is 10 times lower than the currently reported BALF glucose concentrations in humans.[204, 295] As has been reported in human and mouse models,[204, 295] in this study, diabetic mice displayed a substantial increase of glucose in the airway compared to control mice. This was rescued with insulin or metformin treatment. Importantly, the control mice of both of

our mouse models demonstrated a significant increase in BALF glucose concentration during influenza infection. To our knowledge, this is the first report of an increase in BALF glucose concentration in otherwise healthy model (human, rodent, or otherwise), suggesting that influenza alone increased airway surface liquid glucose concentrations. In infected type 1 diabetic mice, BALF glucose concentration was increased above the level of both non-infected type 1 diabetic mice and infected control mice, suggesting an important additive effect of this increase. In infected type 2 diabetic mice, the level of BALF glucose concentration was raised to the same level of non-infected type 2 diabetic mice. This would indicate that the severity of hyperglycemia may be an important factor in determining the level to which BALF glucose increases during influenza infection. In concert with previously published data from other groups, neither of our mouse models experienced an increase in blood glucose concentration during influenza infection over their non-infected blood glucose concentrations.[209, 319] Additionally, while there is a significant correlation between BALF glucose concentrations and blood glucose correlations in both our non-infected type 1 and type 2 diabetic models, this correlation is lost during influenza infection of the type 2 diabetic model. Thus, it would appear that an increase in blood glucose is not responsible for the increase in BALF glucose during influenza infection, and there must be some other, yet-undefined mechanism responsible. It is possible that the increase is due to hemorrhage of the airway, allowing the glucose to leak in from the blood vessels, or it could be that the cell-to-cell adhesions which allow for the passive diffusion of glucose into the airway are damaged during influenza infection, allowing for a greater quantity of glucose leakage into the airway,[204] or both. This phenomenon is certainly deserving of in-depth investigation in the future, and may

be a significant component to rescuing hyperglycemia-induced complications in diabetic patients during influenza infection.

The effects of mild dose of our influenza dose is readily apparent in several of the parameters measured here, including insignificant weight loss by day 3 and the relatively mild nature of alterations in lung histopathology determined via hematoxylin and eosin staining. Thus, any alterations demonstrated in this study are not likely the result of significant weight loss or lung injury, but instead are more likely the result of alterations to glucose homeostasis. These alterations in glucose homeostasis[316] may directly lead to alterations in viral replication or host cell response to viral infection,[202] or these alterations in glucose homeostasis may set off a chain reaction of events which impact other critical systems such as wound healing,[208] the inflammatory response,[318] and/or the homeostasis which maintains the surfactant of the alveoli.[309] Smith et al previously reported an increase in mortality and a decrease in inflammatory response in obese mice compared to their control counterparts during influenza infection.[319] Additionally, multiple investigations have demonstrated a possible link between glycemic variability and severity of influenza via the effects on pulmonary endothelial cells and the potential to increase cytokine production.[310] In this study, we reported an increase in lymphocytes in both type 1 and type 2 diabetic mice compared to their control counterparts, which is rescued with either insulin or metformin treatment, respectively. This pulmonary lymphocytosis is, to our knowledge, a parameter which is seldom reported in diabetic literature, but has previously reported in association with obese mice.[320] In diabetic patients, an upregulation of chemokines, which attract lymphocytes, has been

demonstrated in serum.[320, 321] Therefore, it is possible that the upregulation in chemokines leads to an increase in lymphocytes in the airway. We additionally found that control and diabetic mice demonstrated an increase in neutrophils during influenza infection, but that insulin or metformin treatment blunted this effect. Given similar findings in our models regarding BALF glucose concentration, it is possible that reducing BALF glucose concentration (in control or diabetic mice) directly impacts the reduction of the inflammatory response during influenza infection.

In terms of pulmonary glucose uptake, quantifying GLUT protein expression is critical. Here we quantified the protein expression of 7 different class I and class III GLUT isoforms during hyperglycemia-involved influenza infection. We did not find any evidence of GLUT3 protein in the adult rodent lung (data not shown), but we were able to quantify the protein expression of GLUT-1, -2, -4, -8, -10, and -12 in the adult rodent lung during diabetic influenza. Further, to estimate the protein expression of GLUTs in the bronchial epithelial cells versus the alveolar cells, we dissected the whole lung into upper (predominately bronchial epithelial cells) and lower (predominately alveolar cells) lung portions. To our knowledge, this is the first demonstration of specific GLUT isoforms in the alveoli of the adult mammal lung. A limitation of this study is that these lung portions are only an estimation, as neither lung portion will purely one cell type. To overcome this, we confirmed our findings of Western blot quantification data with immunohistochemical and immunofluorescence experiments. Additionally, understanding the differences between alveolar type I cells and alveolar type II cells, as they are the cells in the most direct contact with the exchange of glucose from the blood, will be critical in future investigations.

Here, we investigated the protein expression of the insulin-sensitive glucose transporters, GLUT4 and GLUT8, in the infected diabetic lung. While we did not find any alterations of total GLUT8 protein between any of our groups, we did find that GLUT4 total protein was significantly decreased in the upper and lower lung of type 1 diabetic mice, and the upper lung of type 2 diabetic mice, compared to control counterparts. Similar findings were reported in both infected and non-infected cohorts. To our knowledge, we are the first to describe GLUT4 protein in the rodent lung during diabetic influenza.[62, 205, 209] We additionally found significant reductions in GLUT4 cell surface protein from the whole lung during infected and non-infected type 1 and type 2 diabetes compared to relevant controls. However, most importantly, we determined there were significant upregulations in cell-surface GLUT4 protein in infected control mice over non-infected control mice. Accordingly, the human cytomegalovirus has been described to increase GLUT4 in human fibroblasts.[322] Our findings were consistent with our results from the immunohistochemistry and immunofluorescence experiments in which GLUT4, while found in the alveoli, seems to localize predominately to the bronchial epithelial cells. Further, GLUT4 staining demonstrated an increase of GLUT4 protein expression in the bronchial epithelium during influenza infection in control and treated diabetic mice, and a decrease of GLUT4 protein expression in infected and non-infected diabetic mice. The lung has not been previously described as an insulin-sensitive organ and we have previously demonstrated that the lung does not seem to be stimulated by insulin *ex vivo*. However, our results here, combined with the rescue of these alterations via *in vivo* insulin or metformin treatment, indicate that the lung may be sensitive to insulin-mediated glucose transport relevant to whole-body glucose homeostasis.

We also quantified total protein expression of non-insulin-sensitive glucose transporters, GLUT-1, -2, -10, and -12. While GLUT2 has previously been reported as a potentially important GLUT isoform in the lung,[205] we did not find a difference of GLUT2 protein expression between any of our groups. GLUT1 protein expression was decreased in the lower lung of non-infected type 1 diabetic mice compared to control counterparts, but this was not consistent for infected mice, for the upper lung, or for type 2 diabetic mice. In type 2 diabetic mice, we found an upregulation of GLUT1 protein in the lower lung of infected mice versus infected control counterparts. Thus, there may be specific alterations to GLUT protein expression during diabetic influenza that are uniquely different from the alterations observed during non-infected diabetes. GLUT10 total protein was significantly decreased in the upper lung of non-infected (but not infected) type 1 diabetic mice and in the lower lung of non-infected type 2 diabetic mice. There was a trend towards a decrease of GLUT10 total protein expression in the lower type 1 infected diabetic lung and the upper type 2 diabetic lung compared to control counterparts. Interestingly, while the alteration of total GLUT protein expression may have been too slight to quantify via Western blotting of the upper lung as we have dissected it here, there appears to be a stronger localization of GLUT10 protein to the bronchial epithelium during infection versus non-infected mice, as revealed by immunohistochemical staining. Finally, we determined that there was a significant upregulation of GLUT12 total protein in the upper and lower lung of non-infected type 1 diabetic mice, and in the upper lung of non-infected type 2 diabetic mice compared to non-infected control counterparts. This was again true in the upper lung of infected type 1 diabetic mice and the upper lung of infected type 2 diabetic mice. However, there was an opposite effect in the lower lung of

infected type 1 diabetic mice, which possessed a significant decrease of GLUT12 protein expression compared to infected controls. We have previously reported an upregulation of GLUT12 in the heart during diabetes,[156] and as other groups have demonstrated that in the lack of major isoforms such as GLUT4,[74] some GLUT isoforms may be upregulated in order to compensate for the downregulation of others. Together, these data indicate a significant alteration of pulmonary GLUT protein expression during both infected and non-infected type 1 and type 2 diabetes. There are some discrepancies of these alterations between type 1 and type 2 diabetes, and between infected and non-infected diabetic mice. This would indicate that a) hyperglycemia caused by a lack of insulin action produces different alterations than hyperglycemia caused by a lack of insulin production, b) influenza may cause unique metabolic derangements which affect glucose transport and GLUT isoform productivity, and c) these alterations are rescued when whole-body glucose homeostasis is restored via *in vivo* insulin or metformin treatment.

In conclusion, we have demonstrated here that there are major alterations to pulmonary glucose metabolism during hyperglycemia-involved influenza infection. We determined that, while there may be other factors involved in determining the severity of respiratory infection, such as inflammatory response and surfactant homeostasis, many of the alterations found here appeared to be incrementally in line with the severity of hyperglycemia. Further, these changes were rescued with insulin or metformin treatment. This would suggest that maintaining normal blood glucose levels in diabetic patients is critically important in reducing the risk and mortality resulting from influenza infection.

CHAPTER VII

CONCLUSIONS

The two goals of this study were to investigate the metabolic derangements underlying complications associated with diabetes, specifically regarding multi-organ dysfunction and vascular dysregulation. To investigate these things, we here focused on the potential involvement of cardiac muscle, skeletal muscle, and lamellar tissue during insulin-induced laminitis, and the involvement of influenza infection of the lung during diabetes.

To investigate multi-organ dysfunction associated with metabolic disease, our first hypothesis was, "*Insulin-induced laminitis will cause significant alterations of the insulin signaling and glucose transport pathways, as well as additional novel cellular pathways."* To that end, the insulin signaling pathway of the cardiac, skeletal and lamellar tissues during hyperinsulinemia-induced laminitis were investigated. Further, a proteomic investigation from these same animals was undertaken in order to determine yet-uninvestigated proteins which may underlie endocrinopathic laminitis, and which may constitute novel therapeutic targets for the treatment of this debilitating disease. The findings from this study indicate that 1) endocrinopathic laminitis is not dependent on insulin resistance to manifest, 2) responses to insulin are tissue-specific in the horse, and 3) there were substantial alterations of focal adhesions, cell-to-cell matrices, integrins,

and heat shock proteins in the lamellae of laminitic horses compared to controls, indicating potentially significant vascular dysfunction during endocrinopathic laminitis. These findings are in agreement with our initial hypothesis.

Our initial second hypothesis regarding the investigation of metabolic multi-organ dysfunction was that, "*Impaired glucose metabolism during diabetes will alter the glucose transporter expression in the lung and increase viral replication, thereby increasing the severity and mortality of diabetes-involved influenza infection."* In order to investigate the mechanisms underlying hyperglycemia-involved influenza infections, the regulation of glucose transport was investigated in the lung of adult mice. The findings from this study indicate that 1) GLUT-1, -2, -4, -8, 10, and -12 protein is present in the adult rodent lung, and there are significant alterations of GLUT protein expression in the lung during infected and non-infected type 1 and type 2 diabetes, 2) cell-surface insulin-sensitive GLUT protein (GLUT4 and GLUT8) are significantly downregulated in the lung during diabetes, 3) insulin or metformin treatment rescues the alterations of these GLUT isoforms in the lung, 4) discrepancies in total GLUT protein and cell surface GLUT protein indicate potentially important trafficking mechanisms, 5) both influenza and diabetes caused significant increases to glucose in the airway, 6) both influenza and diabetes cause significant increases to lymphocytes in the airway, and 7) cell surface GLUT4 protein expression was significantly upregulated in infected mice over their non-infected counterparts. Collectively, our data indicate that, while we found no evidence of a significant increase in viral titer during diabetes, there are major alterations to glucose homeostasis in the lung during influenza and during diabetic influenza. Thus, these findings are only partially consistent with our hypothesis.

Pointedly, based on the current findings, influenza alone appears to directly affect the glucose metabolism of the lung. This is evidenced by the substantial upregulation of both the glucose concentration in BALF and cell surface GLUT4 protein expression in control and diabetic mice during influenza infection. It is possible that mechanisms responsible for the upregulation of glucose in the airway, such as the degradation of cell-to-cell tight junctions of the respiratory epithelium, are also responsible for the leakage of insulin into the airway, which would account for the upregulation of GLUT4 trafficking during influenza infection. This hypothesis is bolstered by the fact that infected diabetic mice possessed less cell surface GLUT4 than control or treated diabetic infected mice, which would be consistent with either insulin resistance or a lack of circulating insulin during diabetes. As infected diabetic mice had the greatest concentration of glucose in the airway of any group, it would then stand to reason that the depressed GLUT4 trafficking evidenced in diabetic mice even during influenza infection is then not sufficient to clear the airway of increased glucose. However, it remains to be proven that the lung epithelium is sensitive to insulin. Further investigations into this and into insulin concentrations in the airway during health, influenza, diabetes, and diabetic influenza would be prudent. Alternatively, other factors which can drive GLUT4 trafficking may be at play in the lung during influenza infection, including calcium signaling, neuregulin signaling, and AMPK activation.[67, 323, 324] Based on the results here, all of these mechanisms are deserving of attention in the infected lung epithelium.

The mechanisms which may be responsible for increased viral replication during diabetes due to an increased amount of intracellular glucose are outlined in Figure 1 of this chapter. However, the alternative hypotheses regarding increased morbidity and

mortality during diabetes should not be discounted. For instance, in terms of excess extracellular glucose, it has been hypothesized that collectin-mediated host response is compromised by increased glucose in the lung during diabetes, even at low doses of influenza inoculation.[309] Additionally, excess extracellular glucose, in addition to comorbidities from obesity, may impair wound healing in obese mice infected with high doses of influenza, leading to higher mortality.[208] Similarly, high inoculations of influenza have been shown to lead to a greater quantity and severity of lung lesions in type 1 diabetic mice versus control mice.[209] Intracellularly, as we hypothesize here and in conjunction with the results from Kohio et al.'s findings in 2013, increased glucose within the diabetic cell (made possible by the upregulation of basal GLUTs in respiratory cells during diabetes) may be used by the vacuolar ATPase pump required for viral unencapsulating within the host cell.[202] It is also possible that the influenza virus is harnessing excess glucose carbon by diverting it away from the TCA cycle, as has been shown in other viruses.[325] Along these lines, the influenza virus may be altering the host cell metabolism, stimulating glycolysis and higher metabolite pools for glycolytic intermediates, as has been demonstrated during human cytomegalovirus infection[326] and several other viral families.[327] However, while influenza has been shown to increase glycolysis alongside an increase in apoptosis, most other viral families have not been shown to produce a similar apoptotic increase.[328] Interestingly, these metabolic studies conclude that for influenza specifically, viral replication itself does not cause a major impact on metabolism, but rather the onset of apoptosis causes metabolic imbalance.[328] However, investigations in this area are few, and our work here clearly points to an

intracellular component of influenza infection acting on host cell metabolism, both during health and during diabetes. Thus, further studies in this area are required.

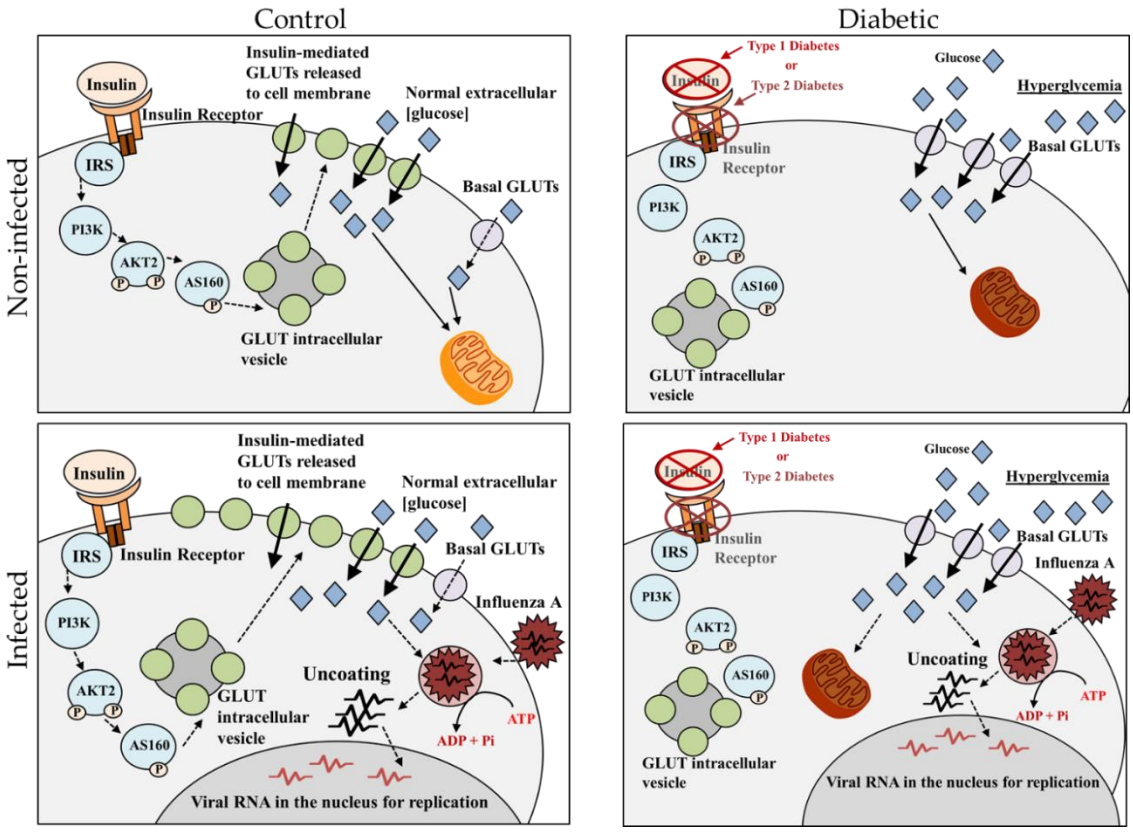

Figure 1: Potential mechanism for hyperglycemia leading to increased viral replication in the respiratory epithelium involving the activity of insulin-mediated and basal glucose transporters. In the control non-infected lung, the insulin signaling and basal GLUTs are both functional. In the diabetic non-infected lung, the insulin-mediated GLUTs are not functional at the cell surface, while the basal GLUTs are upregulated, allowing for an increased amount of glucose to enter the cell from the airway. In the infected control lung, the insulin-mediated GLUTs are upregulated, without an upregulation of basal GLUTs, with a normal (low) amount of glucose in the airway. In the infected diabetic lung, while the insulin-mediated GLUTs are not present at the cell surface, the basal GLUTs are upregulated, allowing for an increased amount of glucose to be transported into cell due to the increased amount of glucose available in the airway. Excess glucose may be used by the vacuolar ATPase pump which is necessary for the uncoating of the virion once inside the host cell.

Importantly, in this investigation we elected to use a low dose of influenza to discern the subtle differences of glucose transport in the lung between control, diabetic, and treated diabetic animals during infection. Thus, while we here found no alterations of viral titer or lung injury between groups during influenza infection, it is possible that a higher inoculation dose would provide more significant differences in these areas.[209, 309] Additionally, we found evidence of bacterial involvement in our hematoxylin & eosin stained slides, but when BALF was plated on blood agar plates, cultures were negative. However, previous investigations have shown that only very high level of pulmonary bacterial infection produces positive bacterial culture after plating.[329,330] Regardless, it has recently been established that hyperglycemia leads to a substantial increase in bacterial colonization of the lung.[331] Thus, it is highly likely that a significant cause of increased mortality from hyperglycemic influenza infection in human population is dual infection between viral and bacterial pathogens.[332] This is particularly true following our findings that influenza alone causes a substantial increase of glucose in the airway, and this effect appears to be additively worse when combined with the increase of glucose in the airway from diabetes. Therefore, a likely progression of severe hyperglycemia-involved respiratory infection would involve the development of type 1 or type 2 diabetes leading to an upregulation of glucose in the airway, followed by viral respiratory infection which further increases airway glucose concentrations, followed by opportunistic bacterial infection which uses the glucose as a substrate. As we and others have shown, airway glucose concentration in diabetic animals can be restored to normal by utilizing readily available pharmaceutical interventions aimed at lowering whole-body glucose homeostasis.[331] This would indicate a potential therapeutic target for diabetic

patients with uncontrolled blood glucose at the time of infection. Furthermore, intranasal insulin therapy could constitute a particularly direct and effective route for reduction of pulmonary glucose levels during infection, but this remains to be investigated.

Overall, the results from this study indicated that insulin resistance is not required in the development of endocrinopathic laminitis, and that both diabetes and influenza cause significant alterations to glucose transport in the lung. Better understanding of both of these disease outcomes may lead to the discovery of novel therapeutic targets for treatment of either endocrinopathic laminitis associated with equine metabolic syndrome, or hyperglycemia-involved respiratory infections in human patients.

REFERENCES

[1] Lacombe, V. A. (2014) Expression and regulation of facilitative glucose transporters in equine insulin-sensitive tissue: from physiology to pathology, ISRN veterinary science 2014.

[2] National Diabetes Statistics Report, 2017. Centers for Disease Control. Accessed at https://www.cdc.gov/diabetes/pdfs/data/statistics/national-diabetes-statistics-report.pdf on January 4, 2019.

[3] Global Report on Diabetes, 2016. World Health Organization. Accessed at http://apps.who.int/iris/bitstream/handle/10665/204871/9789241565257_eng.pdf;jsessionid=1D0CBAF67A00D299DD278773BAC55D1D?sequence=1 on January 4th, 2019.

[4] Bommer, C., Sagalova, V., Heesemann, E., Manne-Goehler, J., Atun, R., Barnighausen, T., Davies, J., and Vollmer, S. (2018) Global Economic Burden of Diabetes in Adults: Projections From 2015 to 2030, Diabetes Care 41, 963-970.

[5] Kipperman, B. S., and German, A. J. (2018) The Responsibility of Veterinarians to Address Companion Animal Obesity, Animals (Basel) 8.

[6] Danaei, G., Finucane, M. M., Lu, Y., Singh, G. M., Cowan, M. J., Paciorek, C. J., Lin, J. K., Farzadfar, F., Khang, Y. H., Stevens, G. A., Rao, M., Ali, M. K., Riley, L. M., Robinson, C. A., Ezzati, M., and Global Burden of Metabolic Risk Factors of Chronic Diseases Collaborating, G. (2011) National, regional, and global trends in fasting plasma glucose and diabetes prevalence since 1980: systematic analysis of health examination surveys and epidemiological studies with 370 country-years and 2.7 million participants, Lancet 378, 31-40.

[7] CDC Leading Causes of Death (2016). Accessed at https://www.cdc.gov/nchs/fastats/leading-causes-of-death.htm June 24, 2019.

[8] World Health Organization Leading Causes of Death (2016). Accessed at https://www.who.int/news-room/fact-sheets/detail/the-top-10-causes-of-death June 24, 2019.

[9] CDC National Diabetes Statistics Report (2017). Accessed at https://www.cdc.gov/diabetes/pdfs/data/statistics/national-diabetes-statistics-report.pdf June 24, 2019.

[10] Cho, N. H., Shaw, J. E., Karuranga, S., Huang, Y., da Rocha Fernandes, J. D., Ohlrogge, A. W., and Malanda, B. (2018) IDF Diabetes Atlas: Global estimates of diabetes prevalence for 2017 and projections for 2045, Diabetes Res Clin Pract 138, 271-281.

[11] Kornum, J. B., Thomsen, R. W., Riis, A., Lervang, H. H., Schonheyder, H. C., and Sorensen, H. T. (2008) Diabetes, glycemic control, and risk of hospitalization with pneumonia: a population-based case-control study, Diabetes Care 31, 1541-1545.

[12] Leegaard, A., Riis, A., Kornum, J. B., Prahl, J. B., Thomsen, V. O., Sorensen, H. T., Horsburgh, C. R., and Thomsen, R. W. (2011) Diabetes, glycemic control, and risk of tuberculosis: a population-based case-control study, Diabetes Care 34, 2530-2535.

[13] Muller, L. M. A. J., Gorter, K. J., Hak, E., Goudzwaard, W. L., Schellevis, F. G., Hoepelman, A. I. M., and Rutten, G. E. H. M. (2005) Increased Risk of Common Infections in Patients with Type 1 and Type 2 Diabetes Mellitus, Clinical Infectious Diseases 41, 281-288.

[14] Emerging Risk Factors, C., Sarwar, N., Gao, P., Seshasai, S. R., Gobin, R., Kaptoge, S., Di Angelantonio, E., Ingelsson, E., Lawlor, D. A., Selvin, E., Stampfer, M., Stehouwer, C. D., Lewington, S., Pennells, L., Thompson, A., Sattar, N., White, I. R., Ray, K. K., and Danesh, J. (2010) Diabetes mellitus, fasting blood glucose concentration, and risk of vascular disease: a collaborative meta-analysis of 102 prospective studies, Lancet 375, 2215-2222.

[15] Gilbert, R. E., and Krum, H. (2015) Heart failure in diabetes: effects of anti-hyperglycaemic drug therapy, Lancet 385, 2107-2117.

[16] Maria, Z., Campolo, A. R., Scherlag, B. J., Ritchey, J. W., and Lacombe, V. A. (2017) Dysregulation of insulin-sensitive glucose transporters during insulin resistance-induced atrial fibrillation, Biochim Biophys Acta.

[17] Creager, M. A., Luscher, T. F., Cosentino, F., and Beckman, J. A. (2003) Diabetes and vascular disease: pathophysiology, clinical consequences, and medical therapy: Part I, Circulation 108, 1527-1532.

[18] Tesfamariam, B., Brown, M. L., and Cohen, R. A. (1991) Elevated glucose impairs endothelium-dependent relaxation by activating protein kinase C, J Clin Invest 87, 1643-1648.

[19] Williams, S. B., Goldfine, A. B., Timimi, F. K., Ting, H. H., Roddy, M. A., Simonson, D. C., and Creager, M. A. (1998) Acute hyperglycemia attenuates endothelium-dependent vasodilation in humans in vivo, Circulation 97, 1695-1701.

[20] Beckman, J. A., Goldfine, A. B., Gordon, M. B., and Creager, M. A. (2001) Ascorbate restores endothelium-dependent vasodilation impaired by acute hyperglycemia in humans, Circulation 103, 1618-1623.

[21] De Vriese, A. S., Verbeuren, T. J., Van de Voorde, J., Lameire, N. H., and Vanhoutte, P. M. (2000) Endothelial dysfunction in diabetes, Br J Pharmacol 130, 963-974.

[22] Cosentino, F., Eto, M., De Paolis, P., van der Loo, B., Bachschmid, M., Ullrich, V., Kouroedov, A., Delli Gatti, C., Joch, H., Volpe, M., and Luscher, T. F. (2003) High glucose causes upregulation of cyclooxygenase-2 and alters prostanoid profile in human endothelial cells: role of protein kinase C and reactive oxygen species, Circulation 107, 1017-1023.

[23] Notkins, A. L., and Lernmark, A. (2001) Autoimmune type 1 diabetes: resolved and unresolved issues, J Clin Invest 108, 1247-1252.

[24] Katsarou, A., Gudbjörnsdottir, S., Rawshani, A., Dabelea, D., Bonifacio, E., Anderson, B. J., Jacobsen, L. M., Schatz, D. A., and Lernmark, Å. (2017) Type 1 diabetes mellitus, Nature Reviews Disease Primers 3, 17016.

[25] Knip, M., Veijola, R., Virtanen, S. M., Hyoty, H., Vaarala, O., and Akerblom, H. K. (2005) Environmental triggers and determinants of type 1 diabetes, Diabetes 54 Suppl 2, S125-136.

[26] Atkinson, M. A., Bluestone, J. A., Eisenbarth, G. S., Hebrok, M., Herold, K. C., Accili, D., Pietropaolo, M., Arvan, P. R., Von Herrath, M., Markel, D. S., and Rhodes, C. J. (2011) How Does Type 1 Diabetes Develop?, The Notion of Homicide or β-Cell Suicide Revisited 60, 1370-1379.

[27] Donath, M. Y., and Shoelson, S. E. (2011) Type 2 diabetes as an inflammatory disease, Nature Reviews Immunology 11, 98.

[28] Robertson, R. P., Harmon, J., Tran, P. O., Tanaka, Y., and Takahashi, H. (2003) Glucose toxicity in beta-cells: type 2 diabetes, good radicals gone bad, and the glutathione connection, Diabetes 52, 581-587.

[29] Unger, R. H. (1995) Lipotoxicity in the pathogenesis of obesity-dependent NIDDM. Genetic and clinical implications, Diabetes 44, 863-870.

[30] Maedler, K., Oberholzer, J., Bucher, P., Spinas, G. A., and Donath, M. Y. (2003) Monounsaturated fatty acids prevent the deleterious effects of palmitate and high glucose on human pancreatic beta-cell turnover and function, Diabetes 52, 726-733.

[31] Maedler, K., Spinas, G. A., Dyntar, D., Moritz, W., Kaiser, N., and Donath, M. Y. (2001) Distinct effects of saturated and monounsaturated fatty acids on beta-cell turnover and function, Diabetes 50, 69-76.

[32] Araki, E., Oyadomari, S., and Mori, M. (2003) Impact of endoplasmic reticulum stress pathway on pancreatic beta-cells and diabetes mellitus, Exp Biol Med (Maywood) 228, 1213-1217.

[33] Spijker, H. S., Song, H., Ellenbroek, J. H., Roefs, M. M., Engelse, M. A., Bos, E., Koster, A. J., Rabelink, T. J., Hansen, B. C., Clark, A., Carlotti, F., and de Koning, E. J. P. (2015) Loss of β-Cell Identity Occurs in Type 2 Diabetes and Is Associated With Islet Amyloid Deposits, 64, 2928-2938.

[34] Douard, V., and Ferraris, R. P. (2008) Regulation of the fructose transporter GLUT5 in health and disease, Am J Physiol Endocrinol Metab 295, E227-237.

[35] Byrne, F. L., Olzomer, E. M., Brink, R., and Hoehn, K. L. (2018) Knockout of glucose transporter GLUT6 has minimal effects on whole body metabolic physiology in mice, Am J Physiol Endocrinol Metab 315, E286-E293.

[36] Li, Q., Manolescu, A., Ritzel, M., Yao, S., Slugoski, M., Young, J. D., Chen, X. Z., and Cheeseman, C. I. (2004) Cloning and functional characterization of the human GLUT7 isoform SLC2A7 from the small intestine, Am J Physiol Gastrointest Liver Physiol 287, G236-242.

[37] Preitner, F., Bonny, O., Laverriere, A., Rotman, S., Firsov, D., Da Costa, A., Metref, S., and Thorens, B. (2009) Glut9 is a major regulator of urate homeostasis and its genetic inactivation induces hyperuricosuria and urate nephropathy, Proc Natl Acad Sci U S A 106, 15501-15506.

[38] Di Daniel, E., Mok, M. H., Mead, E., Mutinelli, C., Zambello, E., Caberlotto, L. L., Pell, T. J., Langmead, C. J., Shah, A. J., Duddy, G., Kew, J. N., and Maycox, P. R. (2009) Evaluation of expression and function of the H+/myo-inositol transporter HMIT, BMC Cell Biol 10, 54.

[39] Doege, H., Bocianski, A., Scheepers, A., Axer, H., Eckel, J., Joost, H. G., and Schurmann, A. (2001) Characterization of human glucose transporter (GLUT) 11

(encoded by SLC2A11), a novel sugar-transport facilitator specifically expressed in heart and skeletal muscle, Biochem J 359, 443-449.

[40] Mueckler, M., and Thorens, B. (2013) The SLC2 (GLUT) family of membrane transporters, Molecular Aspects of Medicine 34, 121-138.

[41] Mueckler, M., Caruso, C., Baldwin, S. A., Panico, M., Blench, I., Morris, H. R., Allard, W. J., Lienhard, G. E., and Lodish, H. F. (1985) Sequence and structure of a human glucose transporter, Science 229, 941-945.

[42] Koranyi, L., Bourey, R. E., James, D., Mueckler, M., Fiedorek, F. T., Jr., and Permutt, M. A. (1991) Glucose transporter gene expression in rat brain: Pretranslational changes associated with chronic insulin-induced hypoglycemia, fasting, and diabetes, Mol Cell Neurosci 2, 244-252.

[43] Pellerin, L., Bonvento, G., Chatton, J. Y., Pierre, K., and Magistretti, P. J. (2002) Role of neuron-glia interaction in the regulation of brain glucose utilization, Diabetes Nutr Metab 15, 268-273; discussion 273.

[44] de Laat, M., Clement, C., Sillence, M., McGowan, C., Pollitt, C., and Lacombe, V. (2015) The impact of prolonged hyperinsulinaemia on glucose transport in equine skeletal muscle and digital lamellae, Equine veterinary journal 47, 494-501.

[45] de Laat, M., Gruntmeir, K., Pollitt, C., McGowan, C., Sillence, M., and Lacombe, V. (2014) Hyperinsulinaemia down-regulates TLR4 expression in the mammalian heart, Frontiers in endocrinology 5.

[46] Hyun, C. K., Kim, E. D., Flowers, M. T., Liu, X., Kim, E., Strable, M., and Ntambi, J. M. (2010) Adipose-specific deletion of stearoyl-CoA desaturase 1 up-regulates the glucose transporter GLUT1 in adipose tissue, Biochem Biophys Res Commun 399, 480-486.

[47] De Vivo, D. C., Leary, L., and Wang, D. (2002) Glucose transporter 1 deficiency syndrome and other glycolytic defects, J Child Neurol 17 Suppl 3, 3S15-23; discussion 13S24-15.

[48] Heilig, C. W., Saunders, T., Brosius, F. C., 3rd, Moley, K., Heilig, K., Baggs, R., Guo, L., and Conner, D. (2003) Glucose transporter-1-deficient mice exhibit impaired development and deformities that are similar to diabetic embryopathy, Proc Natl Acad Sci U S A 100, 15613-15618.

[49] Fidler, T. P., Campbell, R. A., Funari, T., Dunne, N., Balderas Angeles, E., Middleton, E. A., Chaudhuri, D., Weyrch, A. S., and Abel, E. D. (2017) Deletion of

GLUT1 and GLUT3 Reveals Multiple Roles for Glucose Metabolism in Platelet and Megakaryocyte Function, Cell Rep 20, 2277.

[50] Thorens, B. (2015) GLUT2, glucose sensing and glucose homeostasis, Diabetologia 58, 221-232.

[51] Garnett, J. P., Baker, E. H., and Baines, D. L. (2012) Sweet talk: insights into the nature and importance of glucose transport in lung epithelium, Eur Respir J 40, 1269-1276.

[52] Olson, A. L., and Pessin, J. E. (1996) Structure, function, and regulation of the mammalian facilitative glucose transporter gene family, Annu Rev Nutr 16, 235-256.

[53] Augustin, R. (2010) The protein family of glucose transport facilitators: It's not only about glucose after all, IUBMB Life 62, 315-333.

[54] Stumpel, F., Burcelin, R., Jungermann, K., and Thorens, B. (2001) Normal kinetics of intestinal glucose absorption in the absence of GLUT2: evidence for a transport pathway requiring glucose phosphorylation and transfer into the endoplasmic reticulum, Proc Natl Acad Sci U S A 98, 11330-11335.

[55] Tarussio, D., Metref, S., Seyer, P., Mounien, L., Vallois, D., Magnan, C., Foretz, M., and Thorens, B. (2014) Nervous glucose sensing regulates postnatal beta cell proliferation and glucose homeostasis, J Clin Invest 124, 413-424.

[56] Guillam, M. T., Hummler, E., Schaerer, E., Yeh, J. I., Birnbaum, M. J., Beermann, F., Schmidt, A., Deriaz, N., and Thorens, B. (1997) Early diabetes and abnormal postnatal pancreatic islet development in mice lacking Glut-2, Nat Genet 17, 327-330.

[57] Guillam, M. T., Burcelin, R., and Thorens, B. (1998) Normal hepatic glucose production in the absence of GLUT2 reveals an alternative pathway for glucose release from hepatocytes, Proc Natl Acad Sci U S A 95, 12317-12321.

[58] Al-Haggar, M. (2012) Fanconi-Bickel syndrome as an example of marked allelic heterogeneity, World J Nephrol 1, 63-68.

[59] Welch, K. C., Jr., Allalou, A., Sehgal, P., Cheng, J., and Ashok, A. (2013) Glucose transporter expression in an avian nectarivore: the ruby-throated hummingbird (Archilochus colubris), PLoS One 8, e77003.

[60] Carayannopoulos, M. O., Xiong, F., Jensen, P., Rios-Galdamez, Y., Huang, H., Lin, S., and Devaskar, S. U. (2014) GLUT3 gene expression is critical for embryonic growth, brain development and survival, Mol Genet Metab 111, 477-483.

[61] Reno, C. M., Puente, E. C., Sheng, Z., Daphna-Iken, D., Bree, A. J., Routh, V. H., Kahn, B. B., and Fisher, S. J. (2017) Brain GLUT4 Knockout Mice Have Impaired Glucose Tolerance, Decreased Insulin Sensitivity, and Impaired Hypoglycemic Counterregulation, Diabetes 66, 587-597.

[62] Molina, S. A., Moriarty, H. K., Infield, D. T., Imhoff, B. R., Vance, R. J., Kim, A. H., Hansen, J. M., Hunt, W. R., Koval, M., and McCarty, N. A. (2017) Insulin signaling via the PI3-kinase/Akt pathway regulates airway glucose uptake and barrier function in a CFTR-dependent manner, Am J Physiol Lung Cell Mol Physiol 312, L688-L702.

[63] Diaz, M., Antonescu, C. N., Capilla, E., Klip, A., and Planas, J. V. (2007) Fish glucose transporter (GLUT)-4 differs from rat GLUT4 in its traffic characteristics but can translocate to the cell surface in response to insulin in skeletal muscle cells, Endocrinology 148, 5248-5257.

[64] Pessin, J. E., and Bell, G. I. (1992) Mammalian facilitative glucose transporter family: structure and molecular regulation, Annu Rev Physiol 54, 911-930.

[65] Sano, H., Roach, W. G., Peck, G. R., Fukuda, M., and Lienhard, G. E. (2008) Rab10 in insulin-stimulated GLUT4 translocation, Biochem J 411, 89-95.

[66] Ojuka, E. O. (2004) Role of calcium and AMP kinase in the regulation of mitochondrial biogenesis and GLUT4 levels in muscle, Proc Nutr Soc 63, 275-278.

[67] Shoop, S., Maria, Z., Campolo, A., Rashdan, N., Martin, D., Lovern, P., and Lacombe, V. A. (2019) Glial Growth Factor 2 Regulates Glucose Transport in Healthy Cardiac Myocytes and During Myocardial Infarction via an Akt-Dependent Pathway, Front Physiol 10, 189.

[68] Maria, Z., Campolo, A. R., and Lacombe, V. A. (2015) Diabetes Alters the Expression and Translocation of the Insulin-Sensitive Glucose Transporters 4 and 8 in the Atria, PLoS One 10, e0146033.

[69] Waller, A. P., Burns, T. A., Mudge, M. C., Belknap, J. K., and Lacombe, V. A. (2011) Insulin resistance selectively alters cell-surface glucose transporters but not their total protein expression in equine skeletal muscle, J Vet Intern Med 25, 315-321.

[70] Waller, A. P., Kohler, K., Burns, T. A., Mudge, M. C., Belknap, J. K., and Lacombe, V. A. (2011) Naturally occurring compensated insulin resistance selectively alters glucose transporters in visceral and subcutaneous adipose tissues without change in AS160 activation, Biochim Biophys Acta 1812, 1098-1103.

[71] Gaster, M., Staehr, P., Beck-Nielsen, H., Schrøder, H. D., and Handberg, A. (2001) GLUT4 Is Reduced in Slow Muscle Fibers of Type 2 Diabetic Patients, Is Insulin Resistance in Type 2 Diabetes a Slow, Type 1 Fiber Disease? 50, 1324-1329.

[72] Vannucci, S. J., Koehler-Stec, E. M., Li, K., Reynolds, T. H., Clark, R., and Simpson, I. A. (1998) GLUT4 glucose transporter expression in rodent brain: effect of diabetes, Brain Res 797, 1-11.

[73] Kennedy, J. W., Hirshman, M. F., Gervino, E. V., Ocel, J. V., Forse, R. A., Hoenig, S. J., Aronson, D., Goodyear, L. J., and Horton, E. S. (1999) Acute exercise induces GLUT4 translocation in skeletal muscle of normal human subjects and subjects with type 2 diabetes, Diabetes 48, 1192-1197.

[74] Kadowaki, T. (2000) Insights into insulin resistance and type 2 diabetes from knockout mouse models, The Journal of Clinical Investigation 106, 459-465.

[75] Ebert, K., Ludwig, M., Geillinger, K. E., Schoberth, G. C., Essenwanger, J., Stolz, J., Daniel, H., and Witt, H. (2017) Reassessment of GLUT7 and GLUT9 as Putative Fructose and Glucose Transporters, J Membr Biol 250, 171-182.

[76] Navale, A. M., and Paranjape, A. N. (2016) Glucose transporters: physiological and pathological roles, Biophys Rev 8, 5-9.

[77] Lisinski, I., Schurmann, A., Joost, H. G., Cushman, S. W., and Al-Hasani, H. (2001) Targeting of GLUT6 (formerly GLUT9) and GLUT8 in rat adipose cells, Biochem J 358, 517-522.

[78] Doege, H., Bocianski, A., Joost, H. G., and Schurmann, A. (2000) Activity and genomic organization of human glucose transporter 9 (GLUT9), a novel member of the family of sugar-transport facilitators predominantly expressed in brain and leucocytes, Biochem J 350 Pt 3, 771-776.

[79] Baker, W., Paquette, C., Byrne, F. L., Atkins, K. A., Shupnik, M., Modesitt, S. C., Hoehn, K. L., and Slack-Davis, J. K. (2016) Postmenopausal endometrial cancer patients have significantly higher expression of GLUT6 in the endometrium, Gynecologic Oncology 141, 175-176.

[80] The UniProt, C. (2017) UniProt: the universal protein knowledgebase, Nucleic Acids Res 45, D158-D169.

[81] Pyla, R., Poulose, N., Jun, J. Y., and Segar, L. (2013) Expression of conventional and novel glucose transporters, GLUT1, -9, -10, and -12, in vascular smooth muscle cells, Am J Physiol Cell Physiol 304, C574-589.

[82] Ostrowska, M. et al. (2015). Glucose transporters in cattle - a review. Animal Science Papers and Reports vol. 33 no. 3, 191-212.

[83] Dalmolin, C., Almeida, D. V., Figueiredo, M. A., and Marins, L. F. (2018) Expression profile of glucose transport-related genes under chronic and acute exposure to growth hormone in zebrafish, Comparative Biochemistry and Physiology Part A: Molecular & Integrative Physiology 221, 1-6.

[84] Byrne, F. L., Olzomer, E. M., Brink, R., and Hoehn, K. L. (2018) Knockout of glucose transporter GLUT6 has minimal effects on whole-body metabolic physiology in mice, Am J Physiol Endocrinol Metab.

[85] Schlosser, H. A., Drebber, U., Urbanski, A., Haase, S., Baltin, C., Berlth, F., Neiss, S., von Bergwelt-Baildon, M., Fetzner, U. K., Warnecke-Eberz, U., Bollschweiler, E., Holscher, A. H., Monig, S. P., and Alakus, H. (2017) Glucose transporters 1, 3, 6, and 10 are expressed in gastric cancer and glucose transporter 3 is associated with UICC stage and survival, Gastric Cancer 20, 83-91.

[86] Dattani, N. et al (2018). The significance of glucose transporters in the pathogenesis of abdominal aortic aneurysms. Graduate thesis. Accessed August 7, 2018. Available at http://hdl.handle.net/2381/42531.

[87] Piroli, G. G., Grillo, C. A., Charron, M. J., McEwen, B. S., and Reagan, L. P. (2004) Biphasic effects of stress upon GLUT8 glucose transporter expression and trafficking in the diabetic rat hippocampus, Brain Res 1006, 28-35.

[88] Schurmann, A., Axer, H., Scheepers, A., Doege, H., and Joost, H. G. (2002) The glucose transport facilitator GLUT8 is predominantly associated with the acrosomal region of mature spermatozoa, Cell Tissue Res 307, 237-242.

[89] Stanirowski, P. J., Szukiewicz, D., Pazura-Turowska, M., Sawicki, W., and Cendrowski, K. (2018) Placental Expression of Glucose Transporter Proteins in Pregnancies Complicated by Gestational and Pregestational Diabetes Mellitus, Can J Diabetes 42, 209-217.

[90] DeBosch, B., Sambandam, N., Weinheimer, C., Courtois, M., and Muslin, A. J. (2006) Akt2 regulates cardiac metabolism and cardiomyocyte survival, J Biol Chem 281.

[91] Schiffer, M., Susztak, K., Ranalletta, M., Raff, A. C., Bottinger, E. P., and Charron, M. J. (2005) Localization of the GLUT8 glucose transporter in murine kidney and regulation in vivo in nondiabetic and diabetic conditions, Am J Physiol Renal Physiol 289, F186-193.

[92] Romero, A., Gomez, O., Terrado, J., and Mesonero, J. E. (2009) Expression of GLUT8 in mouse intestine: identification of alternative spliced variants, J Cell Biochem 106, 1068-1078.

[93] Doege, H., Schurmann, A., Bahrenberg, G., Brauers, A., and Joost, H. G. (2000) GLUT8, a novel member of the sugar transport facilitator family with glucose transport activity, J Biol Chem 275, 16275-16280.

[94] Aerni-Flessner, L., Abi-Jaoude, M., Koenig, A., Payne, M., and Hruz, P. W. (2012) GLUT4, GLUT1, and GLUT8 are the dominant GLUT transcripts expressed in the murine left ventricle, Cardiovasc Diabetol 11, 63.

[95] CAMPOLO, A., MARIA, Z., HINSDALE, M., LIU, L., and LACOMBE, V. (2018) Insulin Rescues Diabetes-Induced Pulmonary Complications, Diabetes 67.

[96] Fan, J., Chaturvedi, V., and Shen, S. H. (2002) Identification and phylogenetic analysis of a glucose transporter gene family from the human pathogenic yeast Candida albicans, J Mol Evol 55, 336-346.

[97] DeBosch, B. J., Chi, M., and Moley, K. H. (2012) Glucose transporter 8 (GLUT8) regulates enterocyte fructose transport and global mammalian fructose utilization, Endocrinology 153, 4181-4191.

[98] Seki, Y., Sato, K., Kono, T., Abe, H., and Akiba, Y. (2003) Broiler chickens (Ross strain) lack insulin-responsive glucose transporter GLUT4 and have GLUT8 cDNA, Gen Comp Endocrinol 133, 80-87.

[99] de Laat, M. A., Robinson, M. A., Gruntmeir, K. J., Liu, Y., Soma, L. R., and Lacombe, V. A. (2015) AICAR administration affects glucose metabolism by upregulating the novel glucose transporter, GLUT8, in equine skeletal muscle, The Veterinary Journal 205, 381-386.

[100] Zhao, F. Q., Miller, P. J., Wall, E. H., Zheng, Y. C., Dong, B., Neville, M. C., and McFadden, T. B. (2004) Bovine glucose transporter GLUT8: cloning, expression, and developmental regulation in mammary gland, Biochim Biophys Acta 1680, 103-113.

[101] Xi, H., Zhang, Z., Ji, R., Shen, H., Fan, X., Li, Q., Bai, X., Cheng, Z., and He, J. (2017) Expression of glucose transporter 8 (GLUT8) in spermatogenesis of adult boar testes, Acta Histochem 119, 632-637.

[102] Augustin, R., Riley, J., and Moley, K. H. (2005) GLUT8 contains a [DE]XXXL[LI] sorting motif and localizes to a late endosomal/lysosomal compartment, Traffic 6, 1196-1212.

[103] Miinea, C. P., Sano, H., Kane, S., Sano, E., Fukuda, M., Peranen, J., Lane, W. S., and Lienhard, G. E. (2005) AS160, the Akt substrate regulating GLUT4 translocation, has a functional Rab GTPase-activating protein domain, Biochem J 391, 87-93.

[104] Piroli, G. G., Grillo, C. A., Hoskin, E. K., Znamensky, V., Katz, E. B., Milner, T. A., McEwen, B. S., Charron, M. J., and Reagan, L. P. (2002) Peripheral glucose administration stimulates the translocation of GLUT8 glucose transporter to the endoplasmic reticulum in the rat hippocampus, J Comp Neurol 452, 103-114.

[105] Widmer, M., Uldry, M., and Thorens, B. (2005) GLUT8 subcellular localization and absence of translocation to the plasma membrane in PC12 cells and hippocampal neurons, Endocrinology 146, 4727-4736.

[106] Martinez, E., Maria, Z., Periasamy, M., and Lacombe, V. (2014) Abstract 15940: Calcium and Insulin Regulate the Novel Glucose Transporter 8 (GLUT8) in the Healthy and Diabetic Myocardium, Circulation 130, A15940-A15940.

[107] Membrez, M., Hummler, E., Beermann, F., Haefliger, J. A., Savioz, R., Pedrazzini, T., and Thorens, B. (2006) GLUT8 is dispensable for embryonic development but influences hippocampal neurogenesis and heart function, Mol Cell Biol 26, 4268-4276.

[108] Debosch, B. J., Chen, Z., Saben, J. L., Finck, B. N., and Moley, K. H. (2014) Glucose transporter 8 (GLUT8) mediates fructose-induced de novo lipogenesis and macrosteatosis, J Biol Chem 289, 10989-10998.

[109] Gandhi, G. R., Jothi, G., Antony, P. J., Balakrishna, K., Paulraj, M. G., Ignacimuthu, S., Stalin, A., and Al-Dhabi, N. A. (2014) Gallic acid attenuates high-fat diet fed-streptozotocin-induced insulin resistance via partial agonism of PPARgamma in experimental type 2 diabetic rats and enhances glucose uptake through translocation and activation of GLUT4 in PI3K/p-Akt signaling pathway, Eur J Pharmacol 745, 201-216.

[110] Gulbranson, D. R., Davis, E. M., Demmitt, B. A., Ouyang, Y., Ye, Y., Yu, H., and Shen, J. (2017) RABIF/MSS4 is a Rab-stabilizing holdase chaperone required for GLUT4 exocytosis, Proc Natl Acad Sci U S A 114, E8224-E8233.

[111] Waller, A. P., Kalyanasundaram, A., Hayes, S., Periasamy, M., and Lacombe, V. A. (2015) Sarcoplasmic reticulum Ca2+ ATPase pump is a major regulator of glucose transport in the healthy and diabetic heart, Biochim Biophys Acta 1852, 873-881.

[112] Dehghan, F., Hajiaghaalipour, F., Yusof, A., Muniandy, S., Hosseini, S. A., Heydari, S., Salim, L. Z., and Azarbayjani, M. A. (2016) Saffron with resistance exercise improves diabetic parameters through the GLUT4/AMPK pathway in-vitro and in-vivo, Sci Rep 6, 25139.

[113] Buller, C. L., Loberg, R. D., Fan, M. H., Zhu, Q., Park, J. L., Vesely, E., Inoki, K., Guan, K. L., and Brosius, F. C., 3rd. (2008) A GSK-3/TSC2/mTOR pathway regulates glucose uptake and GLUT1 glucose transporter expression, Am J Physiol Cell Physiol 295, C836-843.

[114] Yang, J., Hamid, S., Cai, J., Liu, Q., Xu, S., and Zhang, Z. (2017) Selenium deficiency-induced thioredoxin suppression and thioredoxin knock down disbalanced insulin responsiveness in chicken cardiomyocytes through PI3K/Akt pathway inhibition, Cell Signal 38, 192-200.

[115] Schmidt, U., Briese, S., Leicht, K., Schurmann, A., Joost, H. G., and Al-Hasani, H. (2006) Endocytosis of the glucose transporter GLUT8 is mediated by interaction of a dileucine motif with the beta2-adaptin subunit of the AP-2 adaptor complex, J Cell Sci 119, 2321-2331.

[116] Gomez, O., Ballester-Lurbe, B., Mesonero, J. E., and Terrado, J. (2011) Glucose transporters GLUT4 and GLUT8 are upregulated after facial nerve axotomy in adult mice, J Anat 219, 525-530.

[117] Gomez, O., Romero, A., Terrado, J., and Mesonero, J. E. (2006) Differential expression of glucose transporter GLUT8 during mouse spermatogenesis, Reproduction 131, 63-70.

[118] Schmidt, S., Gawlik, V., Holter, S. M., Augustin, R., Scheepers, A., Behrens, M., Wurst, W., Gailus-Durner, V., Fuchs, H., Hrabe de Angelis, M., Kluge, R., Joost, H. G., and Schurmann, A. (2008) Deletion of glucose transporter GLUT8 in mice increases locomotor activity, Behav Genet 38, 396-406.

[119] DeBosch, B. J., Chen, Z., Finck, B. N., Chi, M., and Moley, K. H. (2013) Glucose transporter-8 (GLUT8) mediates glucose intolerance and dyslipidemia in high-fructose diet-fed male mice, Mol Endocrinol 27, 1887-1896.

[120] Schmidt, S., Joost, H. G., and Schurmann, A. (2009) GLUT8, the enigmatic intracellular hexose transporter, Am J Physiol Endocrinol Metab 296, E614-618.

[121] La Vignera, S., Condorelli, R. A., Di Mauro, M., Lo Presti, D., Mongioi, L. M., Russo, G., and Calogero, A. E. (2015) Reproductive function in male patients with type 1 diabetes mellitus, Andrology 3, 1082-1087.

[122] Gawlik, V., Schmidt, S., Scheepers, A., Wennemuth, G., Augustin, R., Aumuller, G., Moser, M., Al-Hasani, H., Kluge, R., Joost, H. G., and Schurmann, A. (2008) Targeted disruption of Slc2a8 (GLUT8) reduces motility and mitochondrial potential of spermatozoa, Mol Membr Biol 25, 224-235.

[123] Kurth-Kraczek, E. J., Hirshman, M. F., Goodyear, L. J., and Winder, W. W. (1999) 5' AMP-activated protein kinase activation causes GLUT4 translocation in skeletal muscle, Diabetes 48, 1667-1671.

[124] Seki, Y. (2004). Alteration in Expression of GLUT4, GLUT8, and GLUT12 in Human Skeletal Muscle 305 after Prolonged Exercise. American Diabetes Association 64th Scientific Session. (Abstract).

[125] Mayer, A. L., Higgins, C. B., Heitmeier, M. R., Kraft, T. E., Qian, X., Crowley, J. R., Hyrc, K. L., Beatty, W. L., Yarasheski, K. E., Hruz, P. W., and DeBosch, B. J. (2016) SLC2A8 (GLUT8) is a mammalian trehalose transporter required for trehalose-induced autophagy, Sci Rep 6, 38586.

[126] Sarkar, S., Davies, J. E., Huang, Z., Tunnacliffe, A., and Rubinsztein, D. C. (2007) Trehalose, a novel mTOR-independent autophagy enhancer, accelerates the clearance of mutant huntingtin and alpha-synuclein, J Biol Chem 282, 5641-5652.

[127] Huang, S., and Czech, M. P. (2007) The GLUT4 glucose transporter, Cell Metab 5, 237-252.

[128] Katz, E. B., Stenbit, A. E., Hatton, K., DePinho, R., and Charron, M. J. (1995) Cardiac and adipose tissue abnormalities but not diabetes in mice deficient in GLUT4, Nature 377, 151-155.

[129] Solini, A., Rossi, C., Mazzanti, C. M., Proietti, A., Koepsell, H., and Ferrannini, E. (2017) Sodium-glucose co-transporter (SGLT)2 and SGLT1 renal expression in patients with type 2 diabetes, Diabetes Obes Metab 19, 1289-1294.

[130] Campolo, A., de Laat, M. A., Keith, L., Gruntmeir, K. J., and Lacombe, V. A. (2015) Prolonged hyperinsulinemia affects metabolic signal transduction markers in a tissue specific manner, Domest Anim Endocrinol 55, 41-45.

[131] Gomez, O., Ballester, B., Romero, A., Arnal, E., Almansa, I., Miranda, M., Mesonero, J. E., and Terrado, J. (2009) Expression and regulation of insulin and the glucose transporter GLUT8 in the testes of diabetic rats, Horm Metab Res 41, 343-349.

[132] Jiang, Z. Y., Chawla, A., Bose, A., Way, M., and Czech, M. P. (2002) A phosphatidylinositol 3-kinase-independent insulin signaling pathway to N-WASP/Arp2/3/F-actin required for GLUT4 glucose transporter recycling, J Biol Chem 277, 509-515.

[133] Shao, Y., Wellman, T. L., Lounsbury, K. M., and Zhao, F. Q. (2014) Differential regulation of GLUT1 and GLUT8 expression by hypoxia in mammary epithelial cells, Am J Physiol Regul Integr Comp Physiol 307, R237-247.

[134] Wood, I. S., Hunter, L., and Trayhurn, P. (2003) Expression of Class III facilitative glucose transporter genes (GLUT-10 and GLUT-12) in mouse and human adipose tissues, Biochem Biophys Res Commun 308, 43-49.

[135] Macheda, M. L., Rogers, S., and Best, J. D. (2005) Molecular and cellular regulation of glucose transporter (GLUT) proteins in cancer, J Cell Physiol 202, 654-662.

[136] Chen, B., Wang, Y., Geng, M., Lin, X., and Tang, W. (2018) Localization of Glucose Transporter 10 to Hair Cells' Cuticular Plate in the Mouse Inner Ear, Biomed Res Int 2018, 7817453.

[137] Dawson, P. A., Mychaleckyj, J. C., Fossey, S. C., Mihic, S. J., Craddock, A. L., and Bowden, D. W. (2001) Sequence and functional analysis of GLUT10: a glucose transporter in the Type 2 diabetes-linked region of chromosome 20q12-13.1, Mol Genet Metab 74, 186-199.

[138] McMillin, S. L., Schmidt, D. L., Kahn, B. B., and Witczak, C. A. (2017) Glucose Transporter 4 (GLUT4) is Not Necessary for Overload-Induced Glucose Uptake or Hypertrophic Growth in Mouse Skeletal Muscle, Diabetes.

[139] Chiarelli, N., Ritelli, M., Zoppi, N., Benini, A., Borsani, G., Barlati, S., and Colombi, M. (2011) Characterization and expression pattern analysis of the facilitative glucose transporter 10 gene (slc2a10) in Danio rerio, Int J Dev Biol 55, 229-236.

[140] Ciampi, R., Vivaldi, A., Romei, C., Del Guerra, A., Salvadori, P., Cosci, B., Pinchera, A., and Elisei, R. (2008) Expression analysis of facilitative glucose transporters (GLUTs) in human thyroid carcinoma cell lines and primary tumors, Mol Cell Endocrinol 291, 57-62.

[141] McVie-Wylie, A. J., Lamson, D. R., and Chen, Y. T. (2001) Molecular cloning of a novel member of the GLUT family of transporters, SLC2a10 (GLUT10), localized on chromosome 20q13.1: a candidate gene for NIDDM susceptibility, Genomics 72, 113-117.

[142] Love-Gregory, L. D., Wasson, J., Ma, J., Jin, C. H., Glaser, B., Suarez, B. K., and Permutt, M. A. (2004) A common polymorphism in the upstream promoter region of the hepatocyte nuclear factor-4 alpha gene on chromosome 20q is associated with type 2 diabetes and appears to contribute to the evidence for linkage in an ashkenazi jewish population, Diabetes 53, 1134-1140.

[143] Lee, Y. C., Huang, H. Y., Chang, C. J., Cheng, C. H., and Chen, Y. T. (2010) Mitochondrial GLUT10 facilitates dehydroascorbic acid import and protects cells against oxidative stress: mechanistic insight into arterial tortuosity syndrome, Hum Mol Genet 19, 3721-3733.

[144] Willaert, A., Khatri, S., Callewaert, B. L., Coucke, P. J., Crosby, S. D., Lee, J. G., Davis, E. C., Shiva, S., Tsang, M., De Paepe, A., and Urban, Z. (2012) GLUT10 is required for the development of the cardiovascular system and the notochord and connects mitochondrial function to TGFbeta signaling, Hum Mol Genet 21, 1248-1259.

[145] Pezzulo, A. A., Gutierrez, J., Duschner, K. S., McConnell, K. S., Taft, P. J., Ernst, S. E., Yahr, T. L., Rahmouni, K., Klesney-Tait, J., Stoltz, D. A., and Zabner, J. (2011) Glucose depletion in the airway surface liquid is essential for sterility of the airways, PLoS One 6, e16166.

[146] Garnett, J. P., Braun, D., McCarthy, A. J., Farrant, M. R., Baker, E. H., Lindsay, J. A., and Baines, D. L. (2014) Fructose transport-deficient Staphylococcus aureus reveals important role of epithelial glucose transporters in limiting sugar-driven bacterial growth in airway surface liquid, Cell Mol Life Sci 71, 4665-4673.

[147] Gamberucci, A., Marcolongo, P., Nemeth, C. E., Zoppi, N., Szarka, A., Chiarelli, N., Hegedus, T., Ritelli, M., Carini, G., Willaert, A., Callewaert, B. L., Coucke, P. J., Benedetti, A., Margittai, E., Fulceri, R., Banhegyi, G., and Colombi, M. (2017) GLUT10-Lacking in Arterial Tortuosity Syndrome-Is Localized to the Endoplasmic Reticulum of Human Fibroblasts, Int J Mol Sci 18.

[148] Loeys, B. L., Chen, J., Neptune, E. R., Judge, D. P., Podowski, M., Holm, T., Meyers, J., Leitch, C. C., Katsanis, N., Sharifi, N., Xu, F. L., Myers, L. A., Spevak, P. J., Cameron, D. E., De Backer, J., Hellemans, J., Chen, Y., Davis, E. C., Webb, C. L., Kress, W., Coucke, P., Rifkin, D. B., De Paepe, A. M., and Dietz, H. C. (2005) A syndrome of altered cardiovascular, craniofacial, neurocognitive and skeletal development caused by mutations in TGFBR1 or TGFBR2, Nat Genet 37, 275-281.

[149] Coucke, P. J., Willaert, A., Wessels, M. W., Callewaert, B., Zoppi, N., De Backer, J., Fox, J. E., Mancini, G. M., Kambouris, M., Gardella, R., Facchetti, F., Willems, P. J., Forsyth, R., Dietz, H. C., Barlati, S., Colombi, M., Loeys, B., and De Paepe, A. (2006) Mutations in the facilitative glucose transporter GLUT10 alter angiogenesis and cause arterial tortuosity syndrome, Nat Genet 38, 452-457.

[150] Rogers, S., Macheda, M. L., Docherty, S. E., Carty, M. D., Henderson, M. A., Soeller, W. C., Gibbs, E. M., James, D. E., and Best, J. D. (2002) Identification of a novel glucose transporter-like protein—GLUT-12, 282, E733-E738.

[151] Scheepers, A., Joost, H. G., and Schurmann, A. (2004) The glucose transporter families SGLT and GLUT: molecular basis of normal and aberrant function, JPEN J Parenter Enteral Nutr 28, 364-371.

[152] Pujol-Gimenez, J., Perez, A., Reyes, A. M., Loo, D. D., and Lostao, M. P. (2015) Functional characterization of the human facilitative glucose transporter 12 (GLUT12) by electrophysiological methods, Am J Physiol Cell Physiol 308, C1008-1022.

[153] Rogers, S., Docherty, S. E., Slavin, J. L., Henderson, M. A., and Best, J. D. (2003) Differential expression of GLUT12 in breast cancer and normal breast tissue, Cancer Lett 193, 225-233.

[154] Zhou, Y., Kaye, P. L., and Pantaleon, M. (2004) Identification of the facilitative glucose transporter 12 gene Glut12 in mouse preimplantation embryos, Gene Expr Patterns 4, 621-631.

[155] Stuart, C. A., Yin, D., Howell, M. E., Dykes, R. J., Laffan, J. J., and Ferrando, A. A. (2006) Hexose transporter mRNAs for GLUT4, GLUT5, and GLUT12 predominate in human muscle, Am J Physiol Endocrinol Metab 291, E1067-1073.

[156] Waller, A. P., George, M., Kalyanasundaram, A., Kang, C., Periasamy, M., Hu, K., and Lacombe, V. A. (2013) GLUT12 functions as a basal and insulin-independent glucose transporter in the heart, Biochim Biophys Acta 1832, 121-127.

[157] Purcell, S. H., Aerni-Flessner, L. B., Willcockson, A. R., Diggs-Andrews, K. A., Fisher, S. J., and Moley, K. H. (2011) Improved insulin sensitivity by GLUT12 overexpression in mice, Diabetes 60, 1478-1482.

[158] Chandler, J. D., Williams, E. D., Slavin, J. L., Best, J. D., and Rogers, S. (2003) Expression and localization of GLUT1 and GLUT12 in prostate carcinoma, Cancer 97, 2035-2042.

[159] Lacombe, V. A. (2014) Expression and regulation of facilitative glucose transporters in equine insulin-sensitive tissue: from physiology to pathology, ISRN Vet Sci 2014, 409547.

[160] Deng, D., and Yan, N. (2016) GLUT, SGLT, and SWEET: Structural and mechanistic investigations of the glucose transporters, Protein Sci 25, 546-558.

[161] Gude, N. M., Stevenson, J. L., Murthi, P., Rogers, S., Best, J. D., Kalionis, B., and King, R. G. (2005) Expression of GLUT12 in the fetal membranes of the human placenta, Placenta 26, 67-72.

[162] Flessner, L. B., and Moley, K. H. (2009) Similar [DE]XXXL[LI] motifs differentially target GLUT8 and GLUT12 in Chinese hamster ovary cells, Traffic 10, 324-333.

[163] NCBI Resource Coordinators Database resources of the National Center for Biotechnology Information. Nucleic Acids Res. 2016. 44: D7-D19.

[164] Byers, M. S., Howard, C., and Wang, X. (2017) Avian and Mammalian Facilitative Glucose Transporters, Microarrays (Basel) 6.

[165] Piper, R. C., Tai, C., Kulesza, P., Pang, S., Warnock, D., Baenziger, J., Slot, J. W., Geuze, H. J., Puri, C., and James, D. E. (1993) GLUT-4 NH2 terminus contains a phenylalanine-based targeting motif that regulates intracellular sequestration, J Cell Biol 121, 1221-1232.

[166] Verhey, K. J., and Birnbaum, M. J. (1994) A Leu-Leu sequence is essential for COOH-terminal targeting signal of GLUT4 glucose transporter in fibroblasts, J Biol Chem 269, 2353-2356.

[167] Robinson, M. S., and Bonifacino, J. S. (2001) Adaptor-related proteins, Curr Opin Cell Biol 13, 444-453.

[168] Bonifacino, J. S., and Traub, L. M. (2003) Signals for sorting of transmembrane proteins to endosomes and lysosomes, Annu Rev Biochem 72, 395-447.

[169] Stuart, C. A., Howell, M. E., Zhang, Y., and Yin, D. (2009) Insulin-stimulated translocation of glucose transporter (GLUT) 12 parallels that of GLUT4 in normal muscle, J Clin Endocrinol Metab 94, 3535-3542.

[170] Macheda, M. L., Williams, E. D., Best, J. D., Wlodek, M. E., and Rogers, S. (2003) Expression and localisation of GLUT1 and GLUT12 glucose transporters in the pregnant and lactating rat mammary gland, Cell Tissue Res 311, 91-97.

[171] Gude, N. M., Stevenson, J. L., Rogers, S., Best, J. D., Kalionis, B., Huisman, M. A., Erwich, J. J., Timmer, A., and King, R. G. (2003) GLUT12 expression in human placenta in first trimester and term, Placenta 24, 566-570.

[172] Ware, B., Bevier, M., Nishijima, Y., Rogers, S., Carnes, C. A., and Lacombe, V. A. (2011) Chronic heart failure selectively induces regional heterogeneity of insulin-responsive glucose transporters, Am J Physiol Regul Integr Comp Physiol 301, R1300-1306.

[173] Pujol-Gimenez, J., de Heredia, F. P., Idoate, M. A., Airley, R., Lostao, M. P., and Evans, A. R. (2015) Could GLUT12 be a Potential Therapeutic Target in Cancer Treatment? A Preliminary Report, J Cancer 6, 139-143.

[174] Jimenez-Amilburu, V., Jong-Raadsen, S., Bakkers, J., Spaink, H. P., and Marin-Juez, R. (2015) GLUT12 deficiency during early development results in heart failure and a diabetic phenotype in zebrafish, J Endocrinol 224, 1-15.

[175] Pujol-Gimenez, J., Martisova, E., Perez-Mediavilla, A., Lostao, M. P., and Ramirez, M. J. (2014) Expression of the glucose transporter GLUT12 in Alzheimer's disease patients, J Alzheimers Dis 42, 97-101.

[176] Linden, K. C., DeHaan, C. L., Zhang, Y., Glowacka, S., Cox, A. J., Kelly, D. J., and Rogers, S. (2006) Renal expression and localization of the facilitative glucose transporters GLUT1 and GLUT12 in animal models of hypertension and diabetic nephropathy, Am J Physiol Renal Physiol 290, F205-213.

[177] Uldry, M., Ibberson, M., Horisberger, J. D., Chatton, J. Y., Riederer, B. M., and Thorens, B. (2001) Identification of a mammalian H(+)-myo-inositol symporter expressed predominantly in the brain, EMBO J 20, 4467-4477.

[178] Uldry, M., Steiner, P., Zurich, M. G., Beguin, P., Hirling, H., Dolci, W., and Thorens, B. (2004) Regulated exocytosis of an H+/myo-inositol symporter at synapses and growth cones, EMBO J 23, 531-540.

[179] Boucher, J., Kleinridders, A., and Kahn, C. R. (2014) Insulin receptor signaling in normal and insulin-resistant states, Cold Spring Harb Perspect Biol 6.

[180] Luiken, J. J., Ouwens, D. M., Habets, D. D., van der Zon, G. C., Coumans, W. A., Schwenk, R. W., Bonen, A., and Glatz, J. F. (2009) Permissive action of protein kinase C-zeta in insulin-induced CD36- and GLUT4 translocation in cardiac myocytes, J Endocrinol 201, 199-209.

[181] Gumà, A., Martínez-Redondo, V., López-Soldado, I., Cantó, C., and Zorzano, A. (2009) Emerging role of neuregulin as a modulator of muscle metabolism, Vol. 298.

[182] Frank, N., Geor, R. J., Bailey, S. R., Durham, A. E., Johnson, P. J., and American College of Veterinary Internal, M. (2010) Equine metabolic syndrome, J Vet Intern Med 24, 467-475.

[183] Johnson, P. J. (2002) The equine metabolic syndrome peripheral Cushing's syndrome, Vet Clin North Am Equine Pract 18, 271-293.

[184] Morgan, R., Keen, J., and McGowan, C. (2015) Equine metabolic syndrome, Vet Rec 177, 173-179.

[185] Thatcher, C. D., Pleasant, R. S., Geor, R. J., Elvinger, F., Negrin, K. A., Franklin, J., Gay, L., and Werre, S. R. (2008) Prevalence of obesity in mature horses: an equine body condition study, Journal of Animal Physiology and Animal Nutrition 92, 222-222.

[186] Wylie, C. E., Collins, S. N., Verheyen, K. L., and Richard Newton, J. (2011) Frequency of equine laminitis: a systematic review with quality appraisal of published evidence, Vet J 189, 248-256.

[187] Leise, B. S., Watts, M. R., Roy, S., Yilmaz, A. S., Alder, H., and Belknap, J. K. (2015) Use of laser capture microdissection for the assessment of equine lamellar basal epithelial cell signalling in the early stages of laminitis, Equine Vet J 47, 478-488.

[188] Wang, L., Pawlak, E. A., Johnson, P. J., Belknap, J. K., Eades, S., Stack, S., Cousin, H., and Black, S. J. (2013) Impact of Laminitis on the Canonical Wnt Signaling Pathway in Basal Epithelial Cells of the Equine Digital Laminae, PLoS ONE 8, e56025.

[189] de Laat, M. A., Kyaw-Tanner, M. T., Nourian, A. R., McGowan, C. M., Sillence, M. N., and Pollitt, C. C. (2011) The developmental and acute phases of insulin-induced laminitis involve minimal metalloproteinase activity, Vet Immunol Immunopathol 140, 275-281.

[190] Menzies-Gow, N. (2018) Diagnosing and treating laminitis in horses, Vet Rec 183, 505-506.

[191] Johnson, P. J., Wiedmeyer, C. E., LaCarrubba, A., Ganjam, V. K., and Messer, N. T. t. (2010) Laminitis and the equine metabolic syndrome, Vet Clin North Am Equine Pract 26, 239-255.

[192] McGowan, C. M. (2010) Endocrinopathic laminitis, Vet Clin North Am Equine Pract 26, 233-237.

[193] Meier, A., Reiche, D., de Laat, M., Pollitt, C., Walsh, D., and Sillence, M. (2018) The sodium-glucose co-transporter 2 inhibitor velagliflozin reduces hyperinsulinemia and prevents laminitis in insulin-dysregulated ponies, PLoS One 13, e0203655.

[194] Morgan, R. A., Keen, J. A., Walker, B. R., and Hadoke, P. W. (2016) Vascular Dysfunction in Horses with Endocrinopathic Laminitis, PLoS One 11, e0163815.

[195] Asplin, K. E., Patterson-Kane, J. C., Sillence, M. N., Pollitt, C. C., and Mc Gowan, C. M. (2010) Histopathology of insulin-induced laminitis in ponies, Equine Vet J 42, 700-706.

[196] Treiber, K., Carter, R., Gay, L., Williams, C., and Geor, R. (2009) Inflammatory and redox status of ponies with a history of pasture-associated laminitis, Vet Immunol Immunopathol 129, 216-220.

[197] Belknap, J. K., Giguere, S., Pettigrew, A., Cochran, A. M., Van Eps, A. W., and Pollitt, C. C. (2007) Lamellar pro-inflammatory cytokine expression patterns in laminitis at the developmental stage and at the onset of lameness: innate vs. adaptive immune response, Equine Vet J 39, 42-47.

[198] de Laat, M. A., McGowan, C. M., Sillence, M. N., and Pollitt, C. C. (2010) Equine laminitis: Induced by 48 h hyperinsulinaemia in Standardbred horses, Equine Veterinary Journal 42, 129-135.

[199] Asplin, K. E., McGowan, C. M., Pollitt, C. C., Curlewis, J., and Sillence, M. N. (2007) Role of insulin in glucose uptake in the equine hoof, Journal of Veterinary Internal Medicine 21, 668-668.

[200] Baker, E. H., Wood, D. M., Brennan, A. L., Clark, N., Baines, D. L., and Philips, B. J. (2006) Hyperglycaemia and pulmonary infection, Proc Nutr Soc 65, 227-235.

[201] Valdez, R., Narayan, K. M., Geiss, L. S., and Engelgau, M. M. (1999) Impact of diabetes mellitus on mortality associated with pneumonia and influenza among non-Hispanic black and white US adults, Am J Public Health 89, 1715-1721.

[202] Kohio, H. P., and Adamson, A. L. (2013) Glycolytic control of vacuolar-type ATPase activity: a mechanism to regulate influenza viral infection, Virology 444, 301-309.

[203] Fisher, A. B. (1984) Intermediary metabolism of the lung, Environ Health Perspect 55, 149-158.

[204] Baker, E. H., and Baines, D. L. (2018) Airway Glucose Homeostasis: A New Target in the Prevention and Treatment of Pulmonary Infection, Chest 153, 507-514.

[205] Baines, D. L., and Baker, E. H. (2017) Chapter 3 - Glucose Transport and Homeostasis in Lung Epithelia, In Lung Epithelial Biology in the Pathogenesis of Pulmonary Disease (Sidhaye, V. K., and Koval, M., Eds.), pp 33-57, Academic Press, Boston.

[206] Gill, S. K., Hui, K., Farne, H., Garnett, J. P., Baines, D. L., Moore, L. S., Holmes, A. H., Filloux, A., and Tregoning, J. S. (2016) Increased airway glucose increases airway bacterial load in hyperglycaemia, Sci Rep 6, 27636.

[207] Astrand, A., Wingren, C., Benjamin, A., Tregoning, J. S., Garnett, J. P., Groves, H., Gill, S., Orogo-Wenn, M., Lundqvist, A. J., Walters, D., Smith, D. M., Taylor, J. D., Baker, E. H., and Baines, D. L. (2017) Dapagliflozin-lowered blood glucose reduces respiratory Pseudomonas aeruginosa infection in diabetic mice, Br J Pharmacol 174, 836-847.

[208] O'Brien, K. B., Vogel, P., Duan, S., Govorkova, E. A., Webby, R. J., McCullers, J. A., and Schultz-Cherry, S. (2012) Impaired wound healing predisposes obese mice to severe influenza virus infection, J Infect Dis 205, 252-261.

[209] Huo, C., Zhang, S., Zhang, S., Wang, M., Qi, P., Xiao, J., Hu, Y., and Dong, H. (2017) Mice with type 1 diabetes exhibit increased susceptibility to influenza A virus, Microb Pathog 113, 233-241.

[210] CDC Leading Causes of Death. (2016). Accessed at https://www.cdc.gov/nchs/fastats/leading-causes-of-death.htm June 22, 2019.

[211] Taubenberger, J. K., and Morens, D. M. (2008) The pathology of influenza virus infections, Annu Rev Pathol 3, 499-522.

[212] Putri, W., Muscatello, D. J., Stockwell, M. S., and Newall, A. T. (2018) Economic burden of seasonal influenza in the United States, Vaccine 36, 3960-3966.

[213] CDC 2017-2018 Flu Season Burden Estimates (2018). Accessed at https://www.cdc.gov/flu/about/burden/2017-2018.htm on June 22, 2019.

[214] Ludwig, S., Pleschka, S., and Wolff, T. (1999) A fatal relationship--influenza virus interactions with the host cell, Viral Immunol 12, 175-196.

[215] Adamson, A. L., Chohan, K., Swenson, J., and LaJeunesse, D. (2011) A Drosophila model for genetic analysis of influenza viral/host interactions, Genetics 189, 495-506.

[216] Marjuki, H., Gornitzky, A., Marathe, B. M., Ilyushina, N. A., Aldridge, J. R., Desai, G., Webby, R. J., and Webster, R. G. (2011) Influenza A virus-induced early activation of ERK and PI3K mediates V-ATPase-dependent intracellular pH change required for fusion, Cell Microbiol 13, 587-601.

[217] Parra, K. J., and Kane, P. M. (1998) Reversible association between the V1 and V0 domains of yeast vacuolar H+-ATPase is an unconventional glucose-induced effect, Mol Cell Biol 18, 7064-7074.

[218] Frank, N., and Tadros, E. M. (2014) Insulin dysregulation, Equine Veterinary Journal 46, 103-112.

[219] Rask-Madsen, C., and Kahn, C. R. (2012) Tissue-specific insulin signaling, metabolic syndrome, and cardiovascular disease, Arterioscler Thromb Vasc Biol 32, 2052-2059.

[220] McCutcheon, L. J., Geor, R. J., Pratt, S. E., Martineau, E., and Ho, K. (2006) Effects of prior exercise on components of insulin signalling in equine skeletal muscle, Equine veterinary journal. Supplement, 330-334.

[221] Waller, A. P., Kohler, K., Burns, T. A., Mudge, M. C., Belknap, J. K., and Lacombe, V. A. (2011) Naturally occurring compensated insulin resistance selectively alters glucose transporters in visceral and subcutaneous adipose tissues without change in AS160 activation, Biochimica Et Biophysica Acta-Molecular Basis of Disease 1812, 1098-1103.

[222] Pollitt, C. C. (2008) Equine Laminitis: Current Concepts, (RIRDC, Ed.), Rural Industries Research and Development Corporation, Horse RD&E Plan Barton ACT.

[223] Muniyappa, R., Montagnani, M., Koh, K. K., and Quon, M. J. (2007) Cardiovascular actions of insulin, Endocrine Reviews 28, 463-491.

[224] Entingh-Pearsall, A., and Kahn, C. R. (2004) Differential roles of the insulin and insulin-like growth factor-I (IGF-I) receptors in response to insulin and IGF-I, The Journal of biological chemistry 279, 38016-38024.

[225] Frasca, F., Pandini, G., Sciacca, L., Pezzino, V., Squatrito, S., Belfiore, A., and Vigneri, R. (2008) The role of insulin receptors and IGF-I receptors in cancer and other diseases, Archives of physiology and biochemistry 114, 23-37.

[226] White, M. F., and Kahn, C. R. (1994) The insulin signaling system, The Journal of biological chemistry 269, 1-4.

[227] Madonna, R., and De Caterina, R. (2009) Prolonged exposure to high insulin impairs the endothelial PI3-kinase/Akt/nitric oxide signalling, Thrombosis and Haemostasis 101, 345-350.

[228] Avruch, J. (1998) Insulin signal transduction through protein kinase cascades, Molecular and Cellular Biochemistry 182, 31-48.

[229] Cobb, M. H. (1999) MAP kinase pathways, Progress in Biophysics and Molecular Biology 71, 479-500.

[230] Patel, S., Doble, B. W., MacAulay, K., Sinclair, E. M., Drucker, D. J., and Woodgett, J. R. (2008) Tissue-specific role of glycogen synthase kinase 3beta in glucose homeostasis and insulin action, Mol Cell Biol 28, 6314-6328.

[231] Schmittgen, T. D., and Livak, K. J. (2008) Analyzing real-time PCR data by the comparative C-T method, Nature Protocols 3, 1101-1108.

[232] de Laat, M. A., Pollitt, C. C., Kyaw-Tanner, M. T., McGowan, C. M., and Sillence, M. N. (2013) A potential role for lamellar insulin-like growth factor-1 receptor in the pathogenesis of hyperinsulinaemic laminitis, Veterinary Journal 197, 302-306.

[233] de Laat, M. A., Kyaw-Tanner, M. T., Patterson-Kane, J. C., Sillence, M. N., McGowan, C. M., and Pollitt, C. C. (2011) Insulin and the insulin-like growth factor system: a novel theory for hyperinsulinaemic laminitis pathogenesis Journal of Equine Veterinary Science 31, 581-582.

[234] Wattle, O., and Pollitt, C. C. (2004) Lamellar metabolism, Clinical Techniques in Equine Practice 3, 22-33.

[235] Burns, T. A., Watts, M. R., Weber, P. S., McCutcheon, L. J., Geor, R. J., and Belknap, J. K. (2013) Distribution of insulin receptor and insulin-like growth factor-1 receptor in the digital laminae of mixed-breed ponies: An immunohistochemical study, Equine Vet J 45, 326-332.

[236] Kullmann, A., Weber, P. S., Bishop, J. B., Roux, T. M., Norby, B., Burns, T. A., McCutcheon, L. J., Belknap, J. K., and Geor, R. J. (2015) Equine insulin receptor and insulin-like growth factor-1 receptor expression in digital lamellar tissue and insulin target tissues, Equine Veterinary Journal, n/a-n/a.

[237] Bertrand, L., Horman, S., Beauloye, C., and Vanoverschelde, J. L. (2008) Insulin signalling in the heart, Cardiovasc Res 79, 238-248.

[238] DeBosch, B., Sambandam, N., Weinheimer, C., Courtois, M., and Muslin, A. J. (2006) Akt2 regulates cardiac metabolism and cardiomyocyte survival, The Journal of biological chemistry 281, 32841-32851.

[239] Ciaraldi, T. P., Oh, D. K., Christiansen, L., Nikoulina, S. E., Kong, A. P., Baxi, S., Mudaliar, S., and Henry, R. R. (2006) Tissue-specific expression and regulation of GSK-3 in human skeletal muscle and adipose tissue, American journal of physiology. Endocrinology and metabolism 291, E891-898.

[240] Waller, A. P., Burns, T. A., Mudge, M. C., Belknap, J. K., and Lacombe, V. A. (2011) Insulin resistance selectively alters cell-surface glucose transporters but not their total protein expression in equine skeletal muscle, Journal of Veterinary Internal Medicine 25, 315-321.

[241] Bertacca, A., Ciccarone, A., Cecchetti, P., Vianello, B., Laurenza, I., Maffei, M., Chiellini, C., Del Prato, S., and Benzi, L. (2005) Continually high insulin levels impair

Akt phosphorylation and glucose transport in human myoblasts, Metabolism-Clinical and Experimental 54, 1687-1693.

[242] Pollitt, C. C. (2004) Anatomy and physiology of the inner hoof wall, Clinical Techniques in Equine Practice 3, 3-21.

[243] de Laat, M. A., Kyaw-Tanner, M. T., Sillence, M. N., McGowan, C. M., and Pollitt, C. C. (2012) Advanced glycation endproducts in horses with insulin-induced laminitis, Veterinary Immunology and Immunopathology 145, 395-401.

[244] Roustit, M., Loader, J., Deusenbery, C., Baltzis, D., and Veves, A. (2016) Endothelial Dysfunction as a Link Between Cardiovascular Risk Factors and Peripheral Neuropathy in Diabetes, J Clin Endocrinol Metab 101, 3401-3408.

[245] De Laat, M. A., McGowan, C. M., Sillence, M. N., and Pollitt, C. C. (2010) Equine laminitis: Induced by 48 h hyperinsulinaemia in Standardbred horses, Equine Veterinary Journal 42, 129-135.

[246] Tyanova, S., Temu, T., Sinitcyn, P., Carlson, A., Hein, M. Y., Geiger, T., Mann, M., and Cox, J. (2016) The Perseus computational platform for comprehensive analysis of (prote)omics data, Nat Methods 13, 731-740.

[247] Schmittgen, T. D., and Livak, K. J. (2008) Analyzing real-time PCR data by the comparative C(T) method, Nat Protoc 3, 1101-1108.

[248] Karikoski, N. P., Horn, I., McGowan, T. W., and McGowan, C. M. (2011) The prevalence of endocrinopathic laminitis among horses presented for laminitis at a first-opinion/referral equine hospital, Domest Anim Endocrinol 41, 111-117.

[249] Karikoski, N. P., McGowan, C. M., Singer, E. R., Asplin, K. E., Tulamo, R. M., and Patterson-Kane, J. C. (2015) Pathology of Natural Cases of Equine Endocrinopathic Laminitis Associated With Hyperinsulinemia, Vet Pathol 52, 945-956.

[250] Ceciliani, F., Eckersall, D., Burchmore, R., and Lecchi, C. (2014) Proteomics in veterinary medicine: applications and trends in disease pathogenesis and diagnostics, Vet Pathol 51, 351-362.

[251] Smits, A. H., and Vermeulen, M. (2016) Characterizing Protein-Protein Interactions Using Mass Spectrometry: Challenges and Opportunities, Trends Biotechnol 34, 825-834.

[252] de Laat, M. A., McGowan, C. M., Sillence, M. N., and Pollitt, C. C. (2010) Equine laminitis: induced by 48 h hyperinsulinaemia in Standardbred horses, Equine Vet J 42, 129-135.

[253] de Laat, M. A., Clement, C. K., McGowan, C. M., Sillence, M. N., Pollitt, C. C., and Lacombe, V. A. (2014) Toll-like receptor and pro-inflammatory cytokine expression during prolonged hyperinsulinaemia in horses: implications for laminitis, Vet Immunol Immunopathol 157, 78-86.

[254] Waller, A. P., Huettner, L., Kohler, K., and Lacombe, V. A. (2012) Novel link between inflammation and impaired glucose transport during equine insulin resistance, Vet Immunol Immunopathol 149, 208-215.

[255] de Laat, M. A., Clement, C. K., Sillence, M. N., McGowan, C. M., Pollitt, C. C., and Lacombe, V. A. (2015) The impact of prolonged hyperinsulinaemia on glucose transport in equine skeletal muscle and digital lamellae, Equine Veterinary Journal 47, 494-501.

[256] de Laat, M. A., Gruntmeir, K. J., Pollitt, C. C., McGowan, C. M., Sillence, M. N., and Lacombe, V. A. (2014) Hyperinsulinemia Down-Regulates TLR4 Expression in the Mammalian Heart, Frontiers in Endocrinology 5, 120.

[257] Campolo, A., de Laat, M. A., Keith, L., Gruntmeir, K. J., and Lacombe, V. A. (2016) Prolonged hyperinsulinemia affects metabolic signal transduction markers in a tissue specific manner, Domest Anim Endocrinol 55, 41-45.

[258] von Essen, M., Rahikainen, R., Oksala, N., Raitoharju, E., Seppala, I., Mennander, A., Sioris, T., Kholova, I., Klopp, N., Illig, T., Karhunen, P. J., Kahonen, M., Lehtimaki, T., and Hytonen, V. P. (2016) Talin and vinculin are downregulated in atherosclerotic plaque; Tampere Vascular Study, Atherosclerosis 255, 43-53.

[259] Corada, M., Mariotti, M., Thurston, G., Smith, K., Kunkel, R., Brockhaus, M., Lampugnani, M. G., Martin-Padura, I., Stoppacciaro, A., Ruco, L., McDonald, D. M., Ward, P. A., and Dejana, E. (1999) Vascular endothelial-cadherin is an important determinant of microvascular integrity in vivo, Proc Natl Acad Sci U S A 96, 9815-9820.

[260] Beauvais, D. M., and Rapraeger, A. C. (2010) Syndecan-1 couples the insulin-like growth factor-1 receptor to inside-out integrin activation, J Cell Sci 123, 3796-3807.

[261] de Laat, M. A., Pollitt, C. C., Kyaw-Tanner, M. T., McGowan, C. M., and Sillence, M. N. (2013) A potential role for lamellar insulin-like growth factor-1 receptor in the pathogenesis of hyperinsulinaemic laminitis, Vet J 197, 302-306.

[262] Das Evcimen, N., and King, G. L. (2007) The role of protein kinase C activation and the vascular complications of diabetes, Pharmacol Res 55, 498-510.

[263] Philippova, M., Joshi, M. B., Pfaff, D., Kyriakakis, E., Maslova, K., Erne, P., and Resink, T. J. (2012) T-cadherin attenuates insulin-dependent signalling, eNOS activation, and angiogenesis in vascular endothelial cells, Cardiovasc Res 93, 498-507.

[264] Chung, C. M., Lin, T. H., Chen, J. W., Leu, H. B., Yang, H. C., Ho, H. Y., Ting, C. T., Sheu, S. H., Tsai, W. C., Chen, J. H., Lin, S. J., Chen, Y. T., and Pan, W. H. (2011) A genome-wide association study reveals a quantitative trait locus of adiponectin on CDH13 that predicts cardiometabolic outcomes, Diabetes 60, 2417-2423.

[265] Kern, P. A., Di Gregorio, G. B., Lu, T., Rassouli, N., and Ranganathan, G. (2003) Adiponectin expression from human adipose tissue: relation to obesity, insulin resistance, and tumor necrosis factor-alpha expression, Diabetes 52, 1779-1785.

[266] Menzies-Gow, N. J., Harris, P. A., and Elliott, J. (2017) Prospective cohort study evaluating risk factors for the development of pasture-associated laminitis in the United Kingdom, Equine Vet J 49, 300-306.

[267] Takeuchi, T., Adachi, Y., Ohtsuki, Y., and Furihata, M. (2007) Adiponectin receptors, with special focus on the role of the third receptor, T-cadherin, in vascular disease, Med Mol Morphol 40, 115-120.

[268] Frismantiene, A., Pfaff, D., Frachet, A., Coen, M., Joshi, M. B., Maslova, K., Bochaton-Piallat, M. L., Erne, P., Resink, T. J., and Philippova, M. (2014) Regulation of contractile signaling and matrix remodeling by T-cadherin in vascular smooth muscle cells: constitutive and insulin-dependent effects, Cell Signal 26, 1897-1908.

[269] Tyrberg, B., Miles, P., Azizian, K. T., Denzel, M. S., Nieves, M. L., Monosov, E. Z., Levine, F., and Ranscht, B. (2011) T-cadherin (Cdh13) in association with pancreatic beta-cell granules contributes to second phase insulin secretion, Islets 3, 327-337.

[270] Takada, Y., Takada, Y. K., and Fujita, M. (2017) Crosstalk between insulin-like growth factor (IGF) receptor and integrins through direct integrin binding to IGF1, Cytokine Growth Factor Rev 34, 67-72.

[271] Alam, N., Goel, H. L., Zarif, M. J., Butterfield, J. E., Perkins, H. M., Sansoucy, B. G., Sawyer, T. K., and Languino, L. R. (2007) The integrin-growth factor receptor duet, J Cell Physiol 213, 649-653.

[272] Stolla, M. C., Li, D., Lu, L., and Woulfe, D. S. (2013) Enhanced platelet activity and thrombosis in a murine model of type I diabetes are partially insulin-like growth factor 1-dependent and phosphoinositide 3-kinase-dependent, J Thromb Haemost 11, 919-929.

[273] Midwood, K. S., Williams, L. V., and Schwarzbauer, J. E. (2004) Tissue repair and the dynamics of the extracellular matrix, Int J Biochem Cell Biol 36, 1031-1037.

[274] Halper, J., and Kjaer, M. (2014) Basic components of connective tissues and extracellular matrix: elastin, fibrillin, fibulins, fibrinogen, fibronectin, laminin, tenascins and thrombospondins, Adv Exp Med Biol 802, 31-47.

[275] Black, S. J. (2009) Extracellular matrix, leukocyte migration and laminitis, Vet Immunol Immunopathol 129, 161-163.

[276] Patterson-Kane, J. C., Karikoski, N. P., and McGowan, C. M. (2018) Paradigm shifts in understanding equine laminitis, Vet J 231, 33-40.

[277] Wang, L., Pawlak, E. A., Johnson, P. J., Belknap, J. K., Alfandari, D., and Black, S. J. (2014) Expression and activity of collagenases in the digital laminae of horses with carbohydrate overload-induced acute laminitis, J Vet Intern Med 28, 215-222.

[278] Parsons, C. S., Orsini, J. A., Krafty, R., Capewell, L., and Boston, R. (2007) Risk factors for development of acute laminitis in horses during hospitalization: 73 cases (1997-2004), J Am Vet Med Assoc 230, 885-889.

[279] Kannel, W. B., D'Agostino, R. B., Wilson, P. W., Belanger, A. J., and Gagnon, D. R. (1990) Diabetes, fibrinogen, and risk of cardiovascular disease: the Framingham experience, Am Heart J 120, 672-676.

[280] Weiss, D. J., Evanson, O. A., McClenahan, D., Fagliari, J. J., and Jenkins, K. (1997) Evaluation of platelet activation and platelet-neutrophil aggregates in ponies with alimentary laminitis, Am J Vet Res 58, 1376-1380.

[281] James, K., Merriman, J., Gray, R. S., Duncan, L. J., and Herd, R. (1980) Serum alpha 2-macroglobulin levels in diabetes, J Clin Pathol 33, 163-166.

[282] Carr, M. E. (2001) Diabetes mellitus: a hypercoagulable state, J Diabetes Complications 15, 44-54.

[283] Kurucz, I., Morva, A., Vaag, A., Eriksson, K. F., Huang, X., Groop, L., and Koranyi, L. (2002) Decreased expression of heat shock protein 72 in skeletal muscle of patients with type 2 diabetes correlates with insulin resistance, Diabetes 51, 1102-1109.

[284] Venojarvi, M., Korkmaz, A., Aunola, S., Hallsten, K., Virtanen, K., Marniemi, J., Halonen, J. P., Hanninen, O., Nuutila, P., and Atalay, M. (2014) Decreased thioredoxin-1 and increased HSP90 expression in skeletal muscle in subjects with type 2 diabetes or impaired glucose tolerance, Biomed Res Int 2014, 386351.

[285] Lazaro, I., Oguiza, A., Recio, C., Mallavia, B., Madrigal-Matute, J., Blanco, J., Egido, J., Martin-Ventura, J. L., and Gomez-Guerrero, C. (2015) Targeting HSP90 Ameliorates Nephropathy and Atherosclerosis Through Suppression of NF-kappaB and STAT Signaling Pathways in Diabetic Mice, Diabetes 64, 3600-3613.

[286] Lazaro, I., Oguiza, A., Recio, C., Lopez-Sanz, L., Bernal, S., Egido, J., and Gomez-Guerrero, C. (2017) Interplay between HSP90 and Nrf2 pathways in diabetes-associated atherosclerosis, Clin Investig Arterioscler 29, 51-59.

[287] Riebold, M., Kozany, C., Freiburger, L., Sattler, M., Buchfelder, M., Hausch, F., Stalla, G. K., and Paez-Pereda, M. (2015) A C-terminal HSP90 inhibitor restores glucocorticoid sensitivity and relieves a mouse allograft model of Cushing disease, Nat Med 21, 276-280.

[288] Casqueiro, J., Casqueiro, J., and Alves, C. (2012) Infections in patients with diabetes mellitus: A review of pathogenesis, Indian J Endocrinol Metab 16 Suppl 1, S27-36.

[289] Colquhoun, A. J., Nicholson, K. G., Botha, J. L., and Raymond, N. T. (1997) Effectiveness of influenza vaccine in reducing hospital admissions in people with diabetes, Epidemiol Infect 119, 335-341.

[290] Vrhovac, I., Balen Eror, D., Klessen, D., Burger, C., Breljak, D., Kraus, O., Radovic, N., Jadrijevic, S., Aleksic, I., Walles, T., Sauvant, C., Sabolic, I., and Koepsell, H. (2015) Localizations of Na(+)-D-glucose cotransporters SGLT1 and SGLT2 in human kidney and of SGLT1 in human small intestine, liver, lung, and heart, Pflugers Arch 467, 1881-1898.

[291] Kraegen, E. W., James, D. E., Jenkins, A. B., and Chisholm, D. J. (1985) Dose-response curves for in vivo insulin sensitivity in individual tissues in rats, Am J Physiol 248, E353-362.

[292] Maria, Z., and Lacombe, V. A. (2018) Quantification of Cell-Surface Glucose Transporters in the Heart Using a Biotinylated Photolabeling Assay, Methods Mol Biol 1713, 229-240.

[293] Maria, Z., Campolo, A. R., Scherlag, B. J., Ritchey, J. W., and Lacombe, V. A. (2018) Dysregulation of insulin-sensitive glucose transporters during insulin resistance-induced atrial fibrillation, Biochim Biophys Acta 1864, 987-996.

[294] Maria, Z., Campolo, A. R., Scherlag, B. J., Ritchey, J. W., and Lacombe, V. A. (2018) Dysregulation of insulin-sensitive glucose transporters during insulin resistance-induced atrial fibrillation, Biochim Biophys Acta Mol Basis Dis 1864, 987-996.

[295] Baker, E. H., Clark, N., Brennan, A. L., Fisher, D. A., Gyi, K. M., Hodson, M. E., Philips, B. J., Baines, D. L., and Wood, D. M. (2007) Hyperglycemia and cystic fibrosis alter respiratory fluid glucose concentrations estimated by breath condensate analysis, J Appl Physiol (1985) 102, 1969-1975.

[296] Damasceno, D. C., Netto, A. O., Iessi, I. L., Gallego, F. Q., Corvino, S. B., Dallaqua, B., Sinzato, Y. K., Bueno, A., Calderon, I. M., and Rudge, M. V. (2014) Streptozotocin-induced diabetes models: pathophysiological mechanisms and fetal outcomes, Biomed Res Int 2014, 819065.

[297] Xu, G., Liu, B., Sun, Y., Du, Y., Snetselaar, L. G., Hu, F. B., and Bao, W. (2018) Prevalence of diagnosed type 1 and type 2 diabetes among US adults in 2016 and 2017: population based study, BMJ 362, k1497.

[298] Zimmet, P., Alberti, K. G., and Shaw, J. (2001) Global and societal implications of the diabetes epidemic, Nature 414, 782-787.

[299] Berglund, E. D., Li, C. Y., Poffenberger, G., Ayala, J. E., Fueger, P. T., Willis, S. E., Jewell, M. M., Powers, A. C., and Wasserman, D. H. (2008) Glucose metabolism in vivo in four commonly used inbred mouse strains, Diabetes 57, 1790-1799.

[300] Sajan, M. P., Bandyopadhyay, G., Miura, A., Standaert, M. L., Nimal, S., Longnus, S. L., Van Obberghen, E., Hainault, I., Foufelle, F., Kahn, R., Braun, U., Leitges, M., and Farese, R. V. (2010) AICAR and metformin, but not exercise, increase muscle glucose transport through AMPK-, ERK-, and PDK1-dependent activation of atypical PKC, Am J Physiol Endocrinol Metab 298, E179-192.

[301] Grisouard, J., Timper, K., Radimerski, T. M., Frey, D. M., Peterli, R., Kola, B., Korbonits, M., Herrmann, P., Krahenbuhl, S., Zulewski, H., Keller, U., Muller, B., and Christ-Crain, M. (2010) Mechanisms of metformin action on glucose transport and metabolism in human adipocytes, Biochem Pharmacol 80, 1736-1745.

[302] Storozhuk, Y., Hopmans, S. N., Sanli, T., Barron, C., Tsiani, E., Cutz, J. C., Pond, G., Wright, J., Singh, G., and Tsakiridis, T. (2013) Metformin inhibits growth and enhances radiation response of non-small cell lung cancer (NSCLC) through ATM and AMPK, Br J Cancer 108, 2021-2032.

[303] Memmott, R. M., Mercado, J. R., Maier, C. R., Kawabata, S., Fox, S. D., and Dennis, P. A. (2010) Metformin prevents tobacco carcinogen--induced lung tumorigenesis, Cancer Prev Res (Phila) 3, 1066-1076.

[304] Lin, J. J., Gallagher, E. J., Sigel, K., Mhango, G., Galsky, M. D., Smith, C. B., LeRoith, D., and Wisnivesky, J. P. (2015) Survival of patients with stage IV lung cancer with diabetes treated with metformin, Am J Respir Crit Care Med 191, 448-454.

[305] Wu, K., Tian, R., Huang, J., Yang, Y., Dai, J., Jiang, R., and Zhang, L. (2018) Metformin alleviated endotoxemia-induced acute lung injury via restoring AMPK-dependent suppression of mTOR, Chem Biol Interact 291, 1-6.

[306] Miceli, D. D., Vidal, P. N., Batter, M. F. C., Pignataro, O., and Castillo, V. A. (2018) Metformin reduces insulin resistance and the tendency toward hyperglycaemia and dyslipidaemia in dogs with hyperadrenocorticism, Open Vet J 8, 193-199.

[307] Freitas, H. S., D'Agord Schaan, B., da Silva, R. S., Okamoto, M. M., Oliveira-Souza, M., and Machado, U. F. (2007) Insulin but not phlorizin treatment induces a transient increase in GLUT2 gene expression in the kidney of diabetic rats, Nephron Physiol 105, p42-51.

[308] Philips, B. J., Meguer, J. X., Redman, J., and Baker, E. H. (2003) Factors determining the appearance of glucose in upper and lower respiratory tract secretions, Intensive Care Med 29, 2204-2210.

[309] Reading, P. C., Allison, J., Crouch, E. C., and Anders, E. M. (1998) Increased susceptibility of diabetic mice to influenza virus infection: compromise of collectin-mediated host defense of the lung by glucose?, J Virol 72, 6884-6887.

[310] Hulme, K. D., Gallo, L. A., and Short, K. R. (2017) Influenza Virus and Glycemic Variability in Diabetes: A Killer Combination?, Front Microbiol 8, 861.

[311] Bullard, K. M., Cowie, C. C., Lessem, S. E., Saydah, S. H., Menke, A., Geiss, L. S., Orchard, T. J., Rolka, D. B., and Imperatore, G. (2018) Prevalence of Diagnosed Diabetes in Adults by Diabetes Type - United States, 2016, MMWR Morb Mortal Wkly Rep 67, 359-361.

[312] Forouhi, N. G., and Wareham, N. J. (2014) Epidemiology of diabetes, Medicine (Abingdon) 42, 698-702.

[313] Cho, W. J., Lee, D. K., Lee, S. Y., Sohn, S. H., Park, H. L., Park, Y. W., Kim, H., and Nam, J. H. (2016) Diet-induced obesity reduces the production of influenza vaccine-induced antibodies via impaired macrophage function, Acta Virol 60, 298-306.

[314] Deeds, M. C., Anderson, J. M., Armstrong, A. S., Gastineau, D. A., Hiddinga, H. J., Jahangir, A., Eberhardt, N. L., and Kudva, Y. C. (2011) Single dose streptozotocin-induced diabetes: considerations for study design in islet transplantation models, Lab Anim 45, 131-140.

[315] Maria, Z., Campolo, A., Scherlag, A., Ritchey, J., Lacombe, V. (2019). Insulin Deficiency is a Major Contributor to Atrial Fibrillation. Scientific Reports. In press.

[316] Milner, J. J., Rebeles, J., Dhungana, S., Stewart, D. A., Sumner, S. C., Meyers, M. H., Mancuso, P., and Beck, M. A. (2015) Obesity Increases Mortality and Modulates the Lung Metabolome during Pandemic H1N1 Influenza Virus Infection in Mice, J Immunol 194, 4846-4859.

[317] Karlsson, E. A., Sheridan, P. A., and Beck, M. A. (2010) Diet-induced obesity impairs the T cell memory response to influenza virus infection, J Immunol 184, 3127-3133.

[318] Karlsson, E. A., Sheridan, P. A., and Beck, M. A. (2010) Diet-induced obesity in mice reduces the maintenance of influenza-specific CD8+ memory T cells, J Nutr 140, 1691-1697.

[319] Smith, A. G., Sheridan, P. A., Harp, J. B., and Beck, M. A. (2007) Diet-induced obese mice have increased mortality and altered immune responses when infected with influenza virus, J Nutr 137, 1236-1243.

[320] Manicone, A. M., Gong, K., Johnston, L. K., and Giannandrea, M. (2016) Diet-induced obesity alters myeloid cell populations in naive and injured lung, Respir Res 17, 24.

[321] Nomura, S., Shouzu, A., Omoto, S., Nishikawa, M., and Fukuhara, S. (2000) Significance of chemokines and activated platelets in patients with diabetes, Clin Exp Immunol 121, 437-443.

[322] Yu, Y., Maguire, T. G., and Alwine, J. C. (2011) Human cytomegalovirus activates glucose transporter 4 expression to increase glucose uptake during infection, J Virol 85, 1573-1580.

[323] Lee, J. O., Lee, S. K., Kim, J. H., Kim, N., You, G. Y., Moon, J. W., Kim, S. J., Park, S. H., and Kim, H. S. (2012) Metformin regulates glucose transporter 4 (GLUT4) translocation through AMP-activated protein kinase (AMPK)-mediated Cbl/CAP signaling in 3T3-L1 preadipocyte cells, J Biol Chem 287, 44121-44129.

[324] Angin, Y., Schwenk, R. W., Nergiz-Unal, R., Hoebers, N., Heemskerk, J. W., Kuijpers, M. J., Coumans, W. A., van Zandvoort, M. A., Bonen, A., Neumann, D., Glatz, J. F., and Luiken, J. J. (2014) Calcium signaling recruits substrate transporters GLUT4 and CD36 to the sarcolemma without increasing cardiac substrate uptake, Am J Physiol Endocrinol Metab 307, E225-236.

[325] Fontaine, K. A., Sanchez, E. L., Camarda, R., and Lagunoff, M. (2015) Dengue virus induces and requires glycolysis for optimal replication, J Virol 89, 2358-2366.

[326] Munger, J., Bajad, S. U., Coller, H. A., Shenk, T., and Rabinowitz, J. D. (2006) Dynamics of the cellular metabolome during human cytomegalovirus infection, PLoS Pathog 2, e132.

[327] Sanchez, E. L., and Lagunoff, M. (2015) Viral activation of cellular metabolism, Virology 479-480, 609-618.

[328] Ritter, J. B., Wahl, A. S., Freund, S., Genzel, Y., and Reichl, U. (2010) Metabolic effects of influenza virus infection in cultured animal cells: Intra- and extracellular metabolite profiling, BMC Syst Biol 4, 61.

[329] Nuzum, J. W., Pilot, I., Stangl, F. H., and Bonar, B. E. (1976) 1918 pandemic influenza and pneumonia in a large civil hospital, IMJ Ill Med J 150, 612-616.

[330] Rudd, Jennifer. (2018) Neutrophil characterization for the development of novel combination therapy in a murine model of influenza pneumonia with secondary pneumococcal coinfection. PhD diss., Oklahoma State University.

[331] Patkee, W. R., Carr, G., Baker, E. H., Baines, D. L., and Garnett, J. P. (2016) Metformin prevents the effects of Pseudomonas aeruginosa on airway epithelial tight junctions and restricts hyperglycaemia-induced bacterial growth, J Cell Mol Med 20, 758-764.

[332] Rudd, J. M., Ashar, H. K., Chow, V. T., and Teluguakula, N. (2016) Lethal Synergism between Influenza and Streptococcus pneumoniae, J Infect Pulm Dis 2.

APPENDIX A

ABBREVIATIONS

AMPK AMP (5’ Adenosine Mono Phosphate) Activated Protein Kinase

AS160 Akt Substrate of 160kDa

BALF Bronchoalveolar Lavage Fluid

GLUT Glucose Transporter

GSK3β Glycogen Synthase Kinase Beta

IRS-1 Insulin Receptor Substrate 1

L Labeled (cell surface)

PI3-K Phosphoinositide 3-Kinase

STZ Streptozotocin

T1Dx Type 1 Diabetes

T2Dx Type 2 Diabetes

UL Unlabeled (intracellular)

VITA

Allison Renee Campolo

Candidate for the Degree of

Doctor of Philosophy

Dissertation: MECHANISMS UNDERLYING VASCULAR AND RESPIRATORY COMPLICATIONS ASSOCIATED WITH DIABETES

Major Field: Veterinary Biomedical Science

Biographical:

Education:

Completed the requirements for the Doctor of Philosophy in Veterinary Biomedical Science at Oklahoma State University, Stillwater, Oklahoma in July, 2019.

Completed the requirements for the Master of Science in International Agriculture at Oklahoma State University, Stillwater, Oklahoma in 2016.

Completed the requirements for the Bachelor of Arts in Biology at University of Texas at Dallas, Richardson, Texas in 2012.

Experience:

Graduate Teaching Associate, Department of Physiological Sciences, Oklahoma State University, Stillwater, OK

Graduate Research Associate, Department of Physiological Sciences, Oklahoma State University, Stillwater, OK

Professional Memberships:

American Heart Association (AHA)
American Diabetes Association (ADA)
Harold Hamm Diabetes Research Center (HHDRC)
American Physiological Society (APS)